

Hydrogen and Fuel Cells Program
2020 Annual Progress Report



ElectroCat (Electrocatalysis Consortium)

Piotr Zelenay

Los Alamos National Laboratory
Los Alamos, New Mexico 87545



Deborah Myers

Argonne National Laboratory
Lemont, Illinois 60439



Project ID: FC160

Overview

Timeline

- **Start date** (launch): Feb 1, 2016
- **End date:** Sep 30, 2020

Budget

- **FY19 funding total:** \$4,646k
- **FY20 funding total:** \$3,900k

Barriers

- **A. Cost** (catalyst)
- **D. Activity** (catalyst; MEA)
- **B. Durability** (catalyst; MEA)
- **C. Power density** (MEA)

Partner – PI

Los Alamos National Laboratory



– Piotr Zelenay

Argonne National Laboratory



– Deborah Myers

National Renewable Energy Laboratory



– K. C. Neyerlin

Oak Ridge National Laboratory



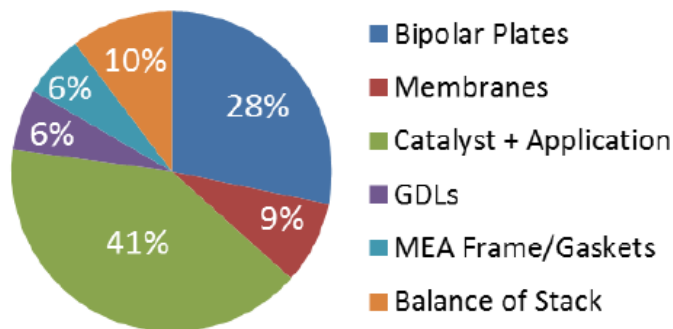
– David Cullen

Relevance: Fuel Cell Stack Cost Challenge

Fuel cell system targets set to be competitive with ICEVs

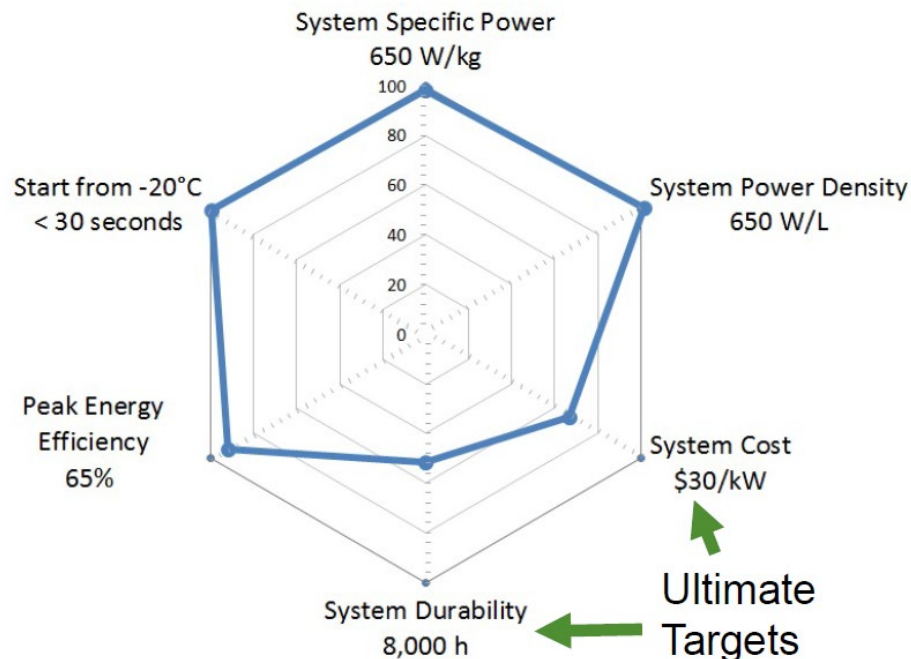
Durability and cost are the primary challenges to fuel cell commercialization and must be met concurrently

PGM Stack Cost Breakdown (500,000 systems/year)



DOE Hydrogen and Fuel Cells Program Record # 1707, September 2017

PGM-based System Automotive Stack Status



D. Papageorgopoulos, DEO-EERE-FCTO, 2019 DOE Annual Merit Review, www.hydrogen.energy.gov/pdfs/review19/plenary_fuel_cell_papageorgopoulos_2019.pdf

ElectroCat created as part of



Energy Materials Network in February 2016

U.S. Department of Energy

Mission: Develop and implement PGM-free catalysts and electrodes by streamlining access to unique synthesis and characterization tools across national labs, developing missing strategic capabilities, and curating a public database of information.

Approach: FY19 ElectroCat Milestone and FY20 GPRA QPMs

FY19

Date	ElectroCat Annual Milestone	Status
September 2019 (FY19 Q4)	Achieve PGM-free cathode MEA performance in an H ₂ -O ₂ fuel cell of 29 mA cm ⁻² at 0.90 V (<i>iR</i> -corrected) at 1.0 bar partial pressure of O ₂ and cell temperature 80 °C; define performance-limiting catalyst and electrode properties to guide the synthesis of PGM-free catalysts and fabrication of electrodes/MEAs (LANL, ANL, ORNL, NREL).	Completed (see slide 7)

FY20

Date	GPRA Quarterly Progress Measures	Status
December 2019 (FY20 Q1) *	Automated electrode deposition: Demonstrate catalyst-coated membrane fabricated by automated deposition of PGM-free catalyst-ionomer inks with reproducibility of hydrogen-air fuel cell current density within 95% and 10% current density improvement at <0.7 V versus the standard fabrication technique.	Completed (see slide 18)
March 2020 (FY20 Q2) *,**	MEA and RDE protocol validation: Complete round robin of MEA and RDE protocol validation at three national laboratories with the ElectroCat core team PGM-free catalyst. Agreement of data taken at the three labs of > 95% in MEA H ₂ -air performance and >95% in mass-normalized current at 0.80 V in oxygen-saturated electrolyte in RDE testing.	Completed (see slide 21)
June 2020 (FY20 Q3) *,**	Hydrogen-air fuel cell performance durability: Accomplish 15 mV improvement in voltage loss versus baseline (H ₂ -air fuel cell at 200 mA/cm ²) after application of ElectroCat durability protocol (difference between voltage at end of durability protocol and voltage immediately after conditioning). Baseline durability determined in FY20 Q2 protocol validation milestone.	Completed (see slides 36, 38, 60)

* ANL and NREL QPM; ** LANL QPM

Approach: FY Q1 LANL QPM, FY20 ORNL QPMs, FY20 ElectroCat Milestone

Date	LANL Quarterly Progress Measures	Status
December 2019 (FY20 Q1)	Durability descriptor calculations: Complete methodology from Task 5 and apply to M-N ₄ -C bulk-C-hosted sites (M = Mn, Fe, Co) with and without OH ligand. Upload and store input calculations on Data Hub along with stability plots.	Completed (see slides 28-30)

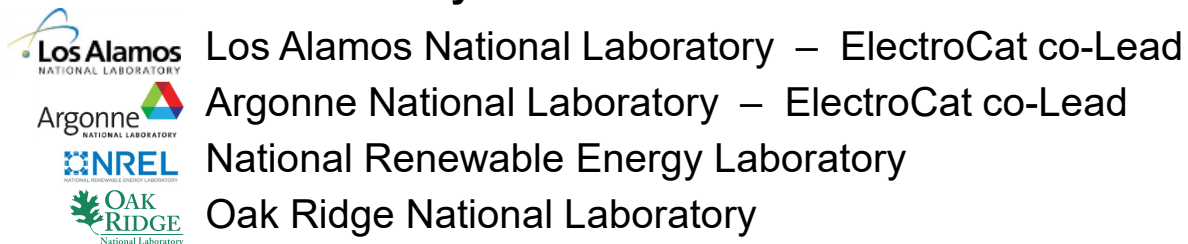
Date	ORNL Quarterly Progress Measures	Status
December 2019 (FY20 Q1)	Coordinate automated electrode deposition at ANL with characterization at ORNL: Automated electrode deposition: Demonstrate catalyst-coated membrane fabricated by automated deposition of PGM-free catalyst-ionomer inks with reproducibility of hydrogen-air fuel cell current density within 95% and 10% current density improvement at < 0.7 V versus the standard fabrication technique. ORNL to conduct preliminary characterization of CCMs produced by automated deposition at ANL to assess electrode structural/compositional characteristics.	Completed (see slide 18)
March 2020 (FY20 Q2)	Establish methodology for measuring Fe loss/migration for selected PGM-free MEAs after fuel cell operation/testing using STEM/EELS/EDS and XPS. Coordinate microscopy measurements with MEA fabrication method and testing protocols at NREL, LANL, and ANL.	Completed
June 2020 (FY20 Q3)	Publish results of in situ microscopy heating experiments conducted in coordination with high-throughput efforts at ANL. Experiments will be designed to assess microstructural and compositional evolution of at least two PGM-free catalyst systems (extent of graphitization, loss of catalytic sites, clustering, etc.)	On track

Date	ElectroCat Annual Milestone	Status
September 2020 (FY20 Q4) ***	Hydrogen-oxygen performance: Achieve PGM-free cathode MEA performance in an H ₂ -O ₂ fuel cell of 32 mA cm ⁻² at 0.90 V (<i>iR</i> -corrected) at 1.0 bar partial pressure of O ₂ and cell temperature 80 °C.	On track

*** LANL, ANL, NREL, ORNL QPM

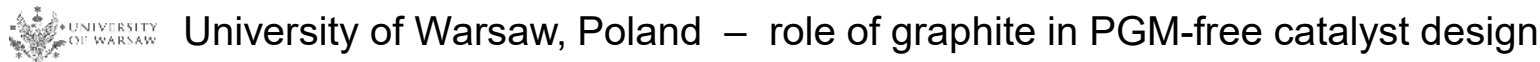
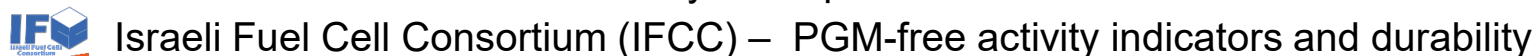
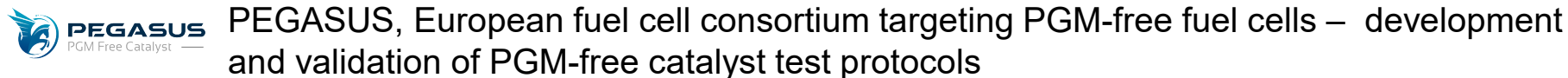
Collaboration and Coordination: Summary

- **Four national laboratory core ElectroCat members:**



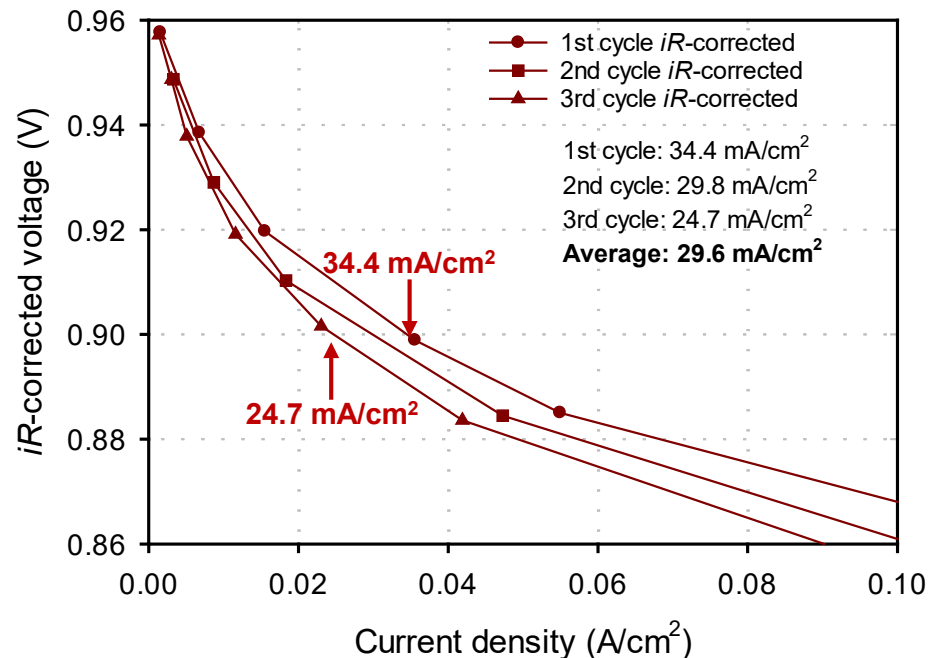
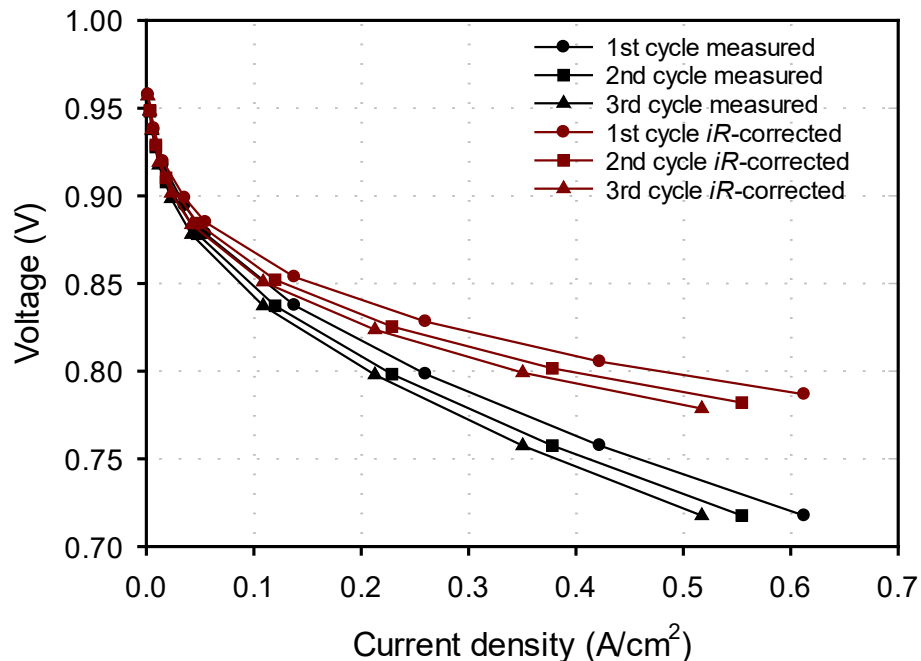
- **Support of four FY2017 FOA, five FY2019 FOA, and one FY2019 Lab Call projects (total of 10)**

- **Collaborators not directly participating in ElectroCat:**



ElectroCat FY2019 Annual Milestone

Anode: $0.2 \text{ mg}_{\text{Pt}} \text{ cm}^{-2}$ Pt/C H_2 , 500 sccm, 1.0 bar H_2 partial pressure; **Cathode:** ca. 6.8 mg cm^{-2} , CM-PANI-Fe-C(Zn), Aquivion® D83 55wt%, 1000 sccm, 1.0 bar O_2 partial pressure; **Membrane:** Nafion®211; **Cell:** differential, 5 cm^2
Test conditions: $80 \text{ }^\circ\text{C}$; 0.96 V to 0.88 V in 20 mV steps; 0.88 V to 0.72 V in 40 mV steps; 45 s/step.

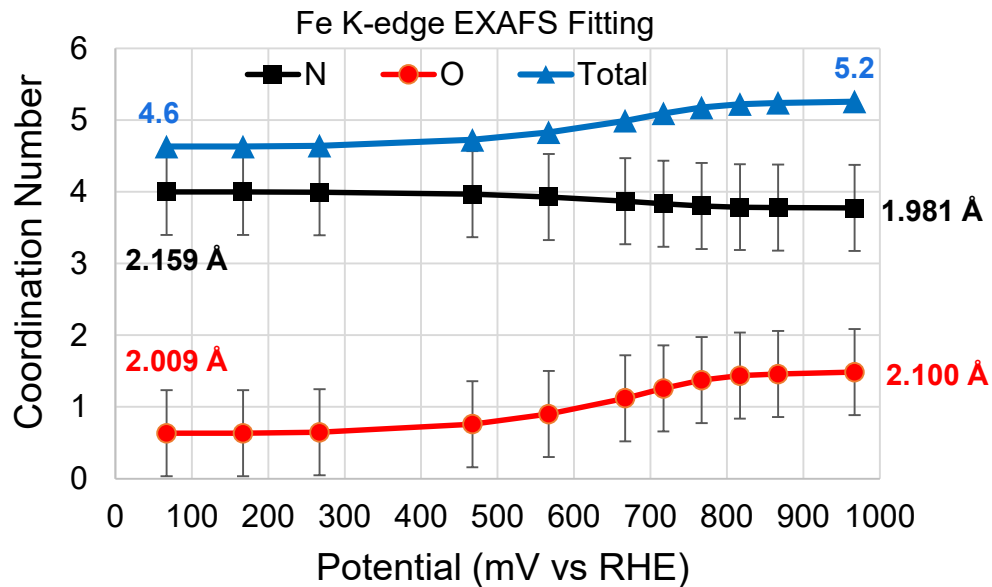
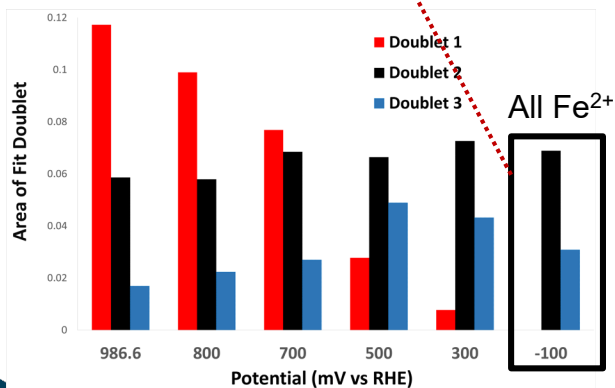
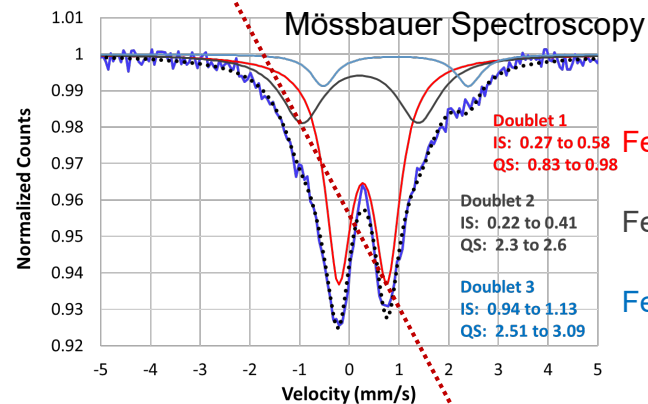
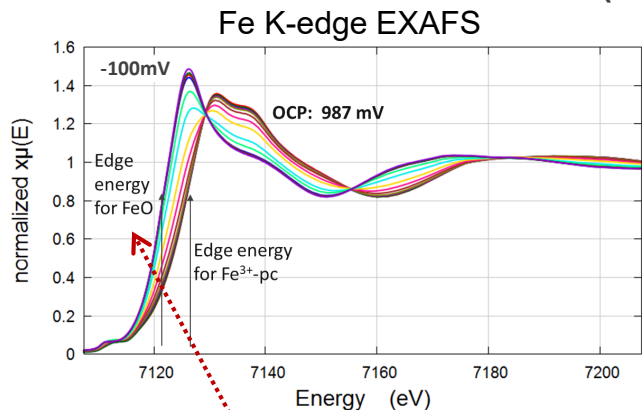


H_2/O_2 fuel cell performance of CM-PANI-Fe-C(Zn) catalyst measured at **29.6 mA cm^{-2}** (0.90 V , *iR*-free) in a differential cell by averaging the first three polarization curves, as proposed in PGM-free catalyst test protocols

ElectroCat FY2019 Annual Milestone of 29 mA cm^{-2} at 0.90 V achieved under the conditions closely matching those specified in PGM-free test protocols developed in ElectroCat and approved by DOE

Fe-N-C Site Characterization: Fe Species in (AD)Fe-N-C Catalyst

LANL (AD)⁵⁷Fe_{1.5}-N-C, deaerated 0.5 M H₂SO₄

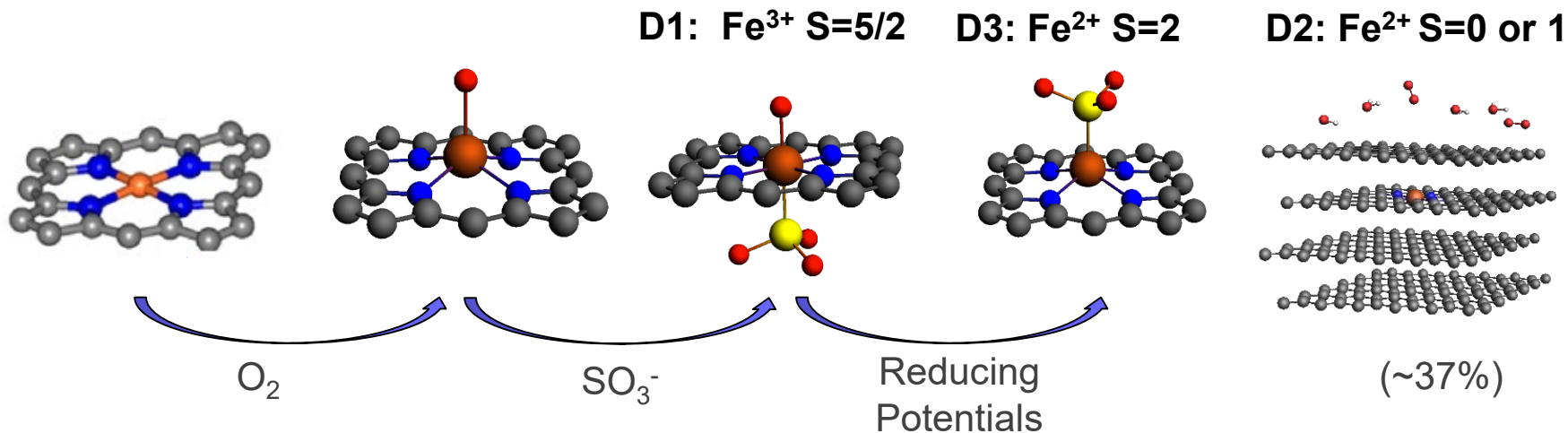


- Mössbauer: three distinct Fe species present (D1, D2, D3)
 - ✓ D1 is converted to D3 with decreasing potential. D2 content potential independent. Only D2 and D3 at -100 mV.
- EXAFS: Fe coordination number (CN) decreases from 5.2 to 4.6 and Fe average oxidation state decrease from 987 to -100 mV
- Twenty-seven possible assignments of 3 species to 3 CNs (6, 5, 4) narrowed to 2 by combining Mössbauer and EXAFS results:

	CN D1 Fe ³⁺	CN D2 Fe ²⁺	CN D3 Fe ²⁺	Fraction D1	Fraction D2	Fraction D3
Case 1	5	6	4	0.62	0.32	0.06
Case 2	6	4	5	0.62	0.37	0.01

Fe-N-C Site Characterization: Fe Coordination in (AD)Fe-N-C

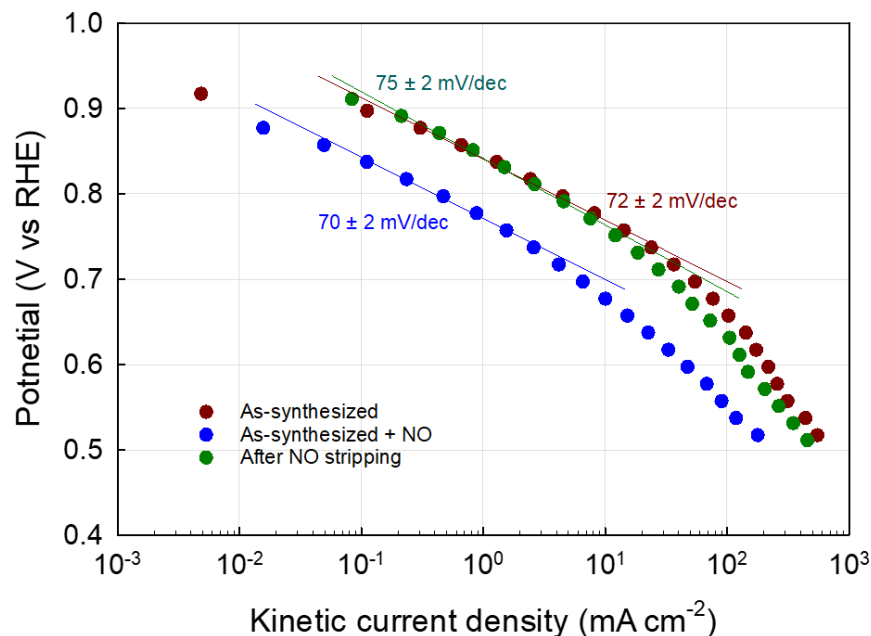
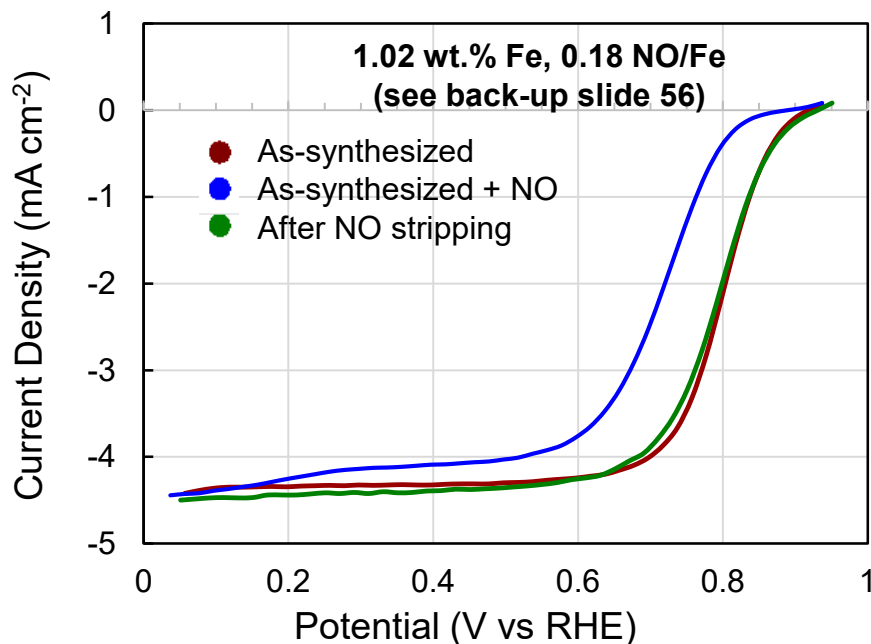
Catalyst Form	Path	Coordination Number	Bond distance (Å)
Powder	Fe-N	3.9 ± 0.5	1.939 ± 0.013
Powder after air exposure	Fe-N	3.5 ± 1.2	2.021 ± 0.033
	Fe-O	1.2 ± 0.9	1.868 ± 0.068
Electrode 990 mV (OCP)	Fe-N	3.8 ± 0.6	1.981 ± 0.015
	Fe-O	1.5 ± 0.6	2.100 ± 0.036
Electrode -100 mV	Fe-N	4.0 ± 1.3	2.159 ± 0.028
	Fe-O	0.6 ± 0.6	2.009 ± 0.028



- Increase ORR activity by eliminating formation of D2 and promoting conversion of D1 to D3 at higher potentials
- Surface Fe content can be increased by first forming N₄ sites, then adding Fe

Fe-N-C Site Characterization: ORR TOF for (AD)Fe-N-C Using NO Probe

ORR: 0.6 mg cm⁻² (AD)⁵⁷Fe_{1.5}-N-C; 0.5 M H₂SO₄; 900 rpm; 25°C; Ag/AgCl (saturated KCl) reference electrode; graphite counter electrode; steady-state potential program: 20 mV steps, 20 s/step



$$TOF(@0.8 V \text{ vs RHE}) [s^{-1}] = \frac{\Delta_{ik}@0.8 V [Ag^{-1}]}{F[A \cdot s \text{ mol}^{-1}] \times GSD [mol g^{-1}]} = \mathbf{1.1 e^{-} \text{ site}^{-1} s^{-1}}$$

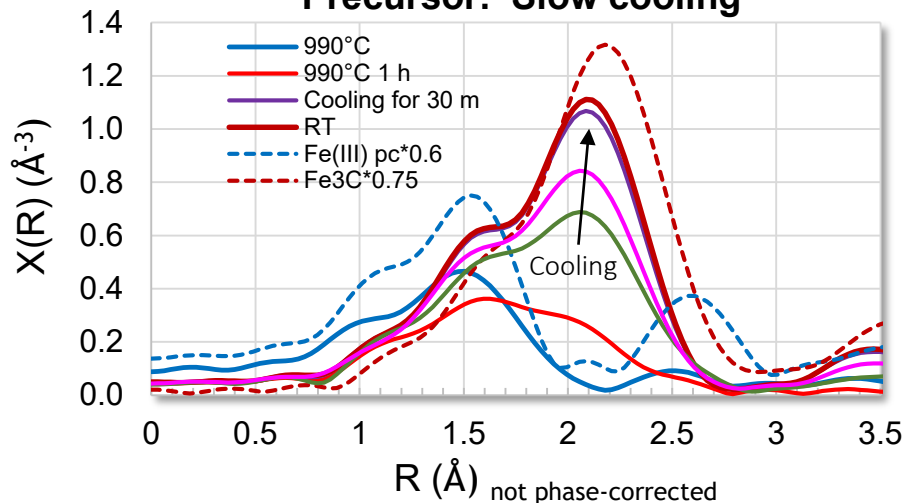
F: Faraday's constant; **G**ravimetric **S**ite **D**ensity of Fe = (wt.% Fe in catalyst/atomic weight Fe)*%Fe adsorbing NO

Active site density and ORR turnover frequency of Fe-N-C catalysts an order of magnitude lower than Pt

- ✓ **1.1 e⁻/s-site** vs. **42 e⁻/s-site** for 5 nm Pt/C at 0.8 V (vs. RHE) in RDE
- ✓ **3×10¹²** vs. **5×10¹³** sites/cm² for 40 wt.% Pt/C catalyst powder

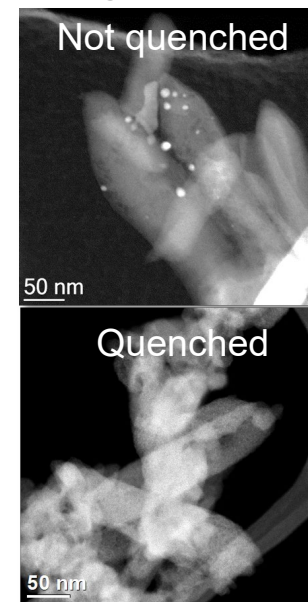
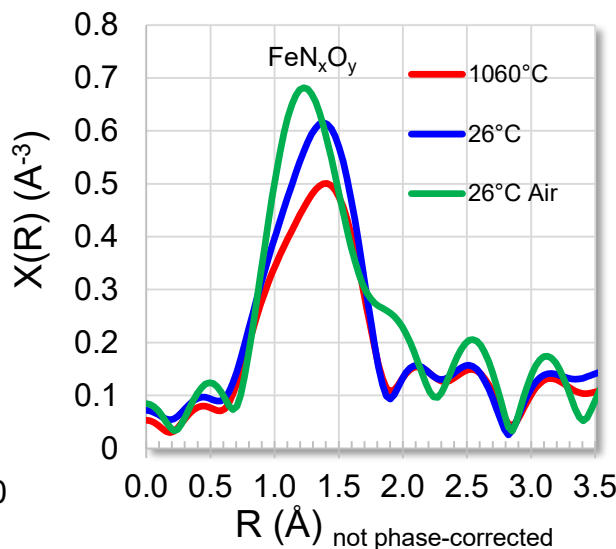
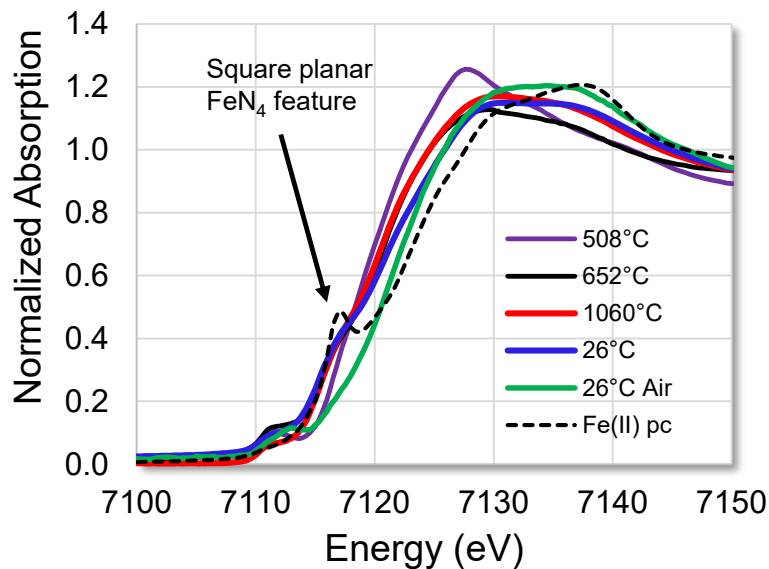
Fe-N-C Site Characterization: Increasing Activity by Eliminating Inactive Fe Species

Fe K-edge EXAFS for Fe-ZIF-L (5 at.% Fe) Precursor: Slow cooling



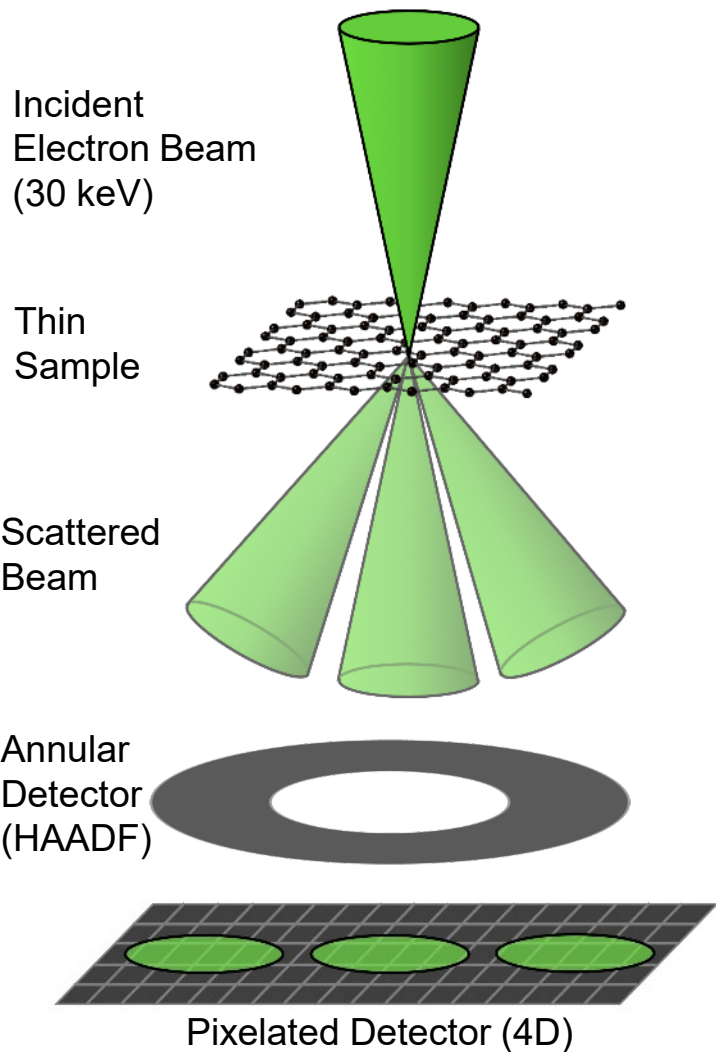
- FeN₄ in-plane structure evident at ~650°C
- **1000°C hold:** No effect on speciation with 1.5 at.% and 2.5 at.% Fe precursor; FeN_x transforms into Fe carbide during hold with 5 at.% Fe precursor
- EXAFS results suggest minimizing time at >900°C can increase FeN_x content and eliminate formation of carbide
- TEM/EELS consistent with no formation of metal or carbide clusters/particles in quenched sample

Fe K-edge EXAFS: Fe-ZIF-L (5 at.% Fe) Quenched to Room Temp. after reaching ~1000 °C

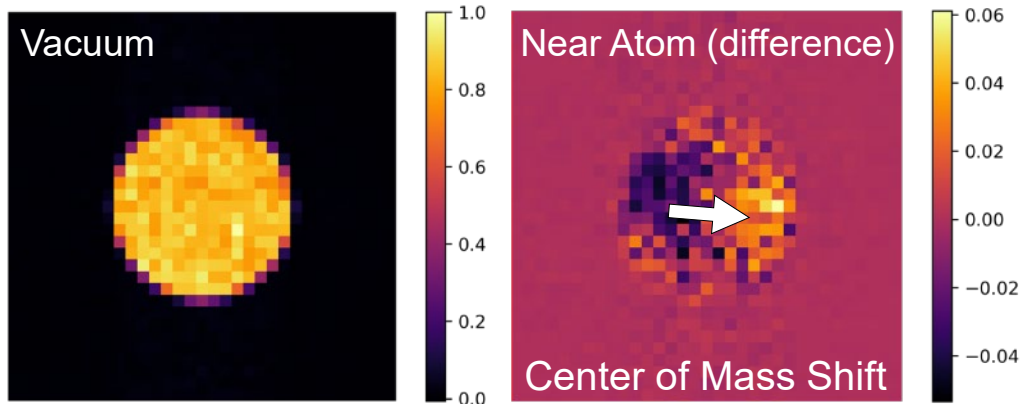


Fe-N-C Site Characterization – Capability Development: 4D STEM at 30 keV

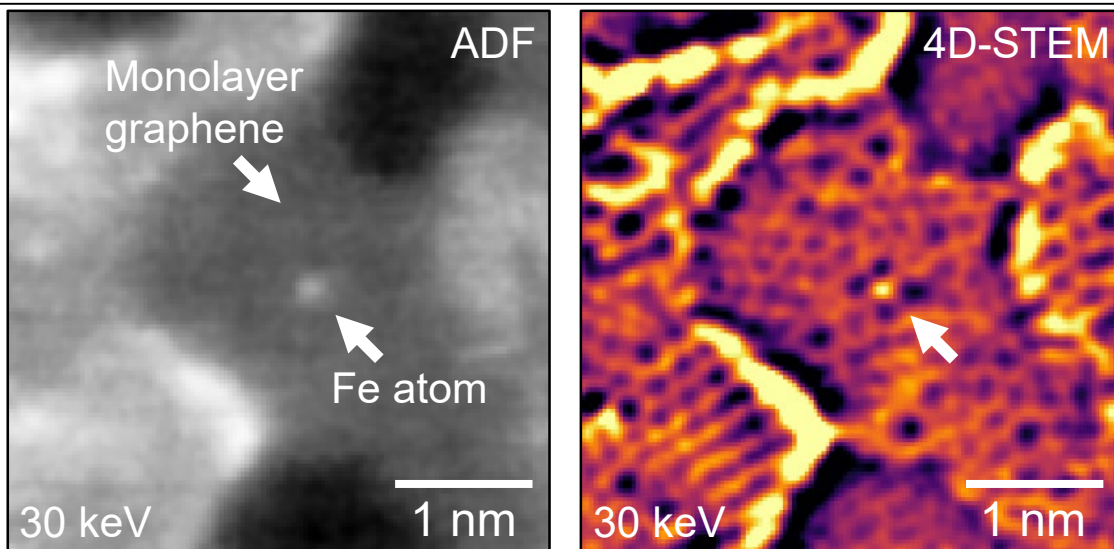
4D-STEM



Diffraction Pattern: Probe in Vacuum vs. Near Atom



HAADF vs. 4D-STEM – Restores atomic resolution at 30 keV

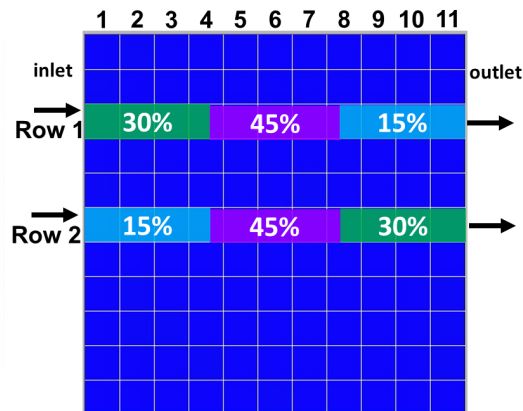
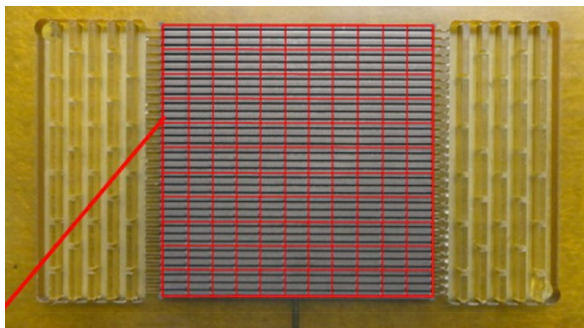


Highlight: Atomic resolution achieved at lower, less damaging electron beam voltages

* Model catalyst from D. Jung, V. Stamenkovic, ANL

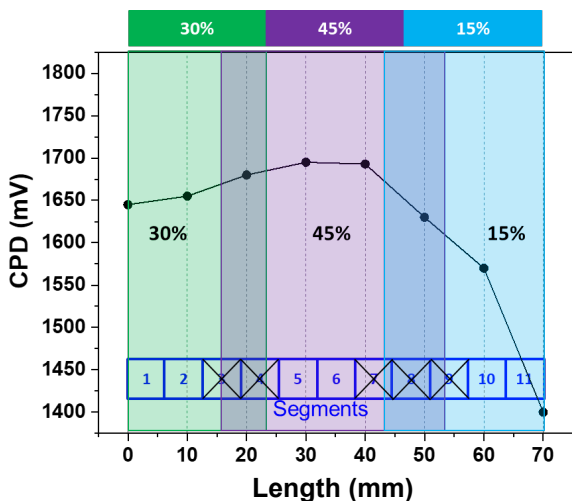
Electrode R&D – Capability: Segmented Cell for Combinatorial Screening

Parallel channel flow field of segmented cell

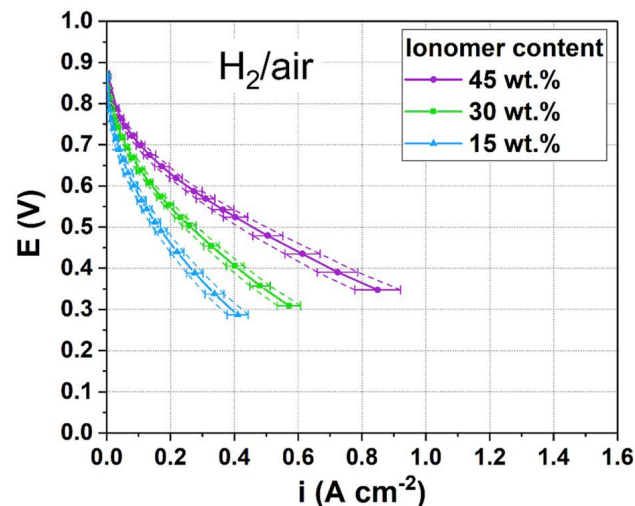
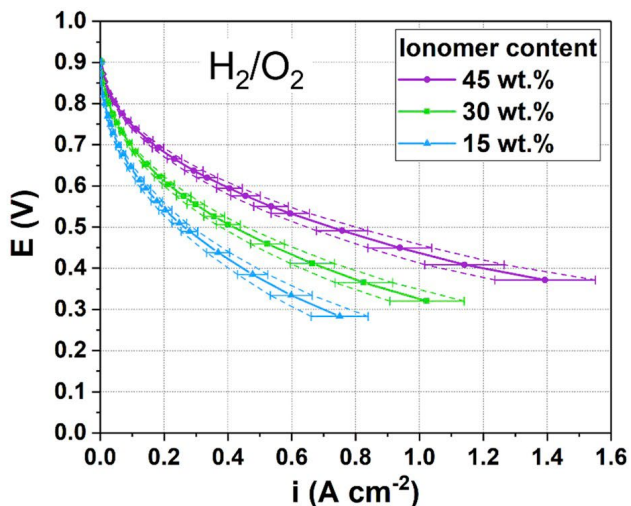


- High-throughput differential cell successfully introduced for rapid electrode composition screening
- Kelvin probe method introduced and applied to confirm ionomer content variations
- Increasing performance with ionomer content in the 15 – 45 wt.% range
- Setup applicable to studies of catalyst materials, electrode configurations, and manufacturing methods

Kelvin probe measurement of contact potential (CPD) in bar-coated GDEs



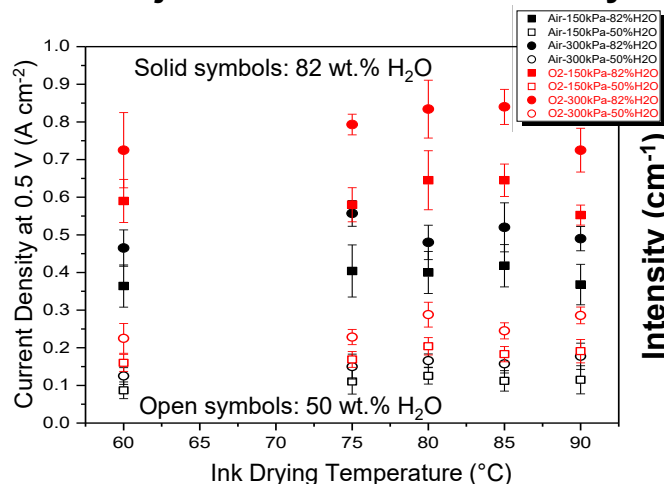
Polarization curves (Pajarito Powder electrocatalyst)



Osmieri et al., *J. Power Sources* **452**, 227829 (2020)

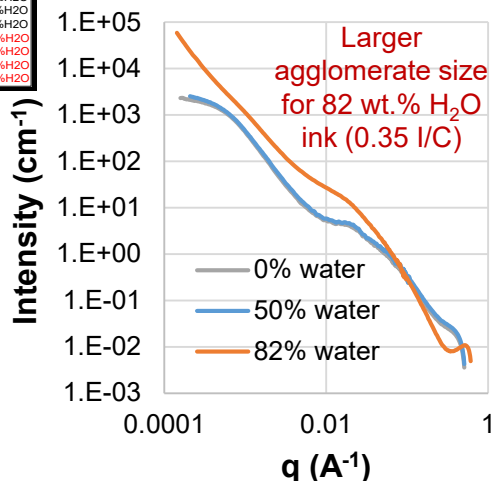
Electrode R&D: Ink Formulation vs. Ionomer Adsorption & Catalyst Agglomeration

Pajarito Powder 11904 Catalyst



Osmieri et al. *Journal of Power Sources* 452, 227829 (2020)

X-ray Scattering of Inks



Catalyst Dispersions (Catalyst only)

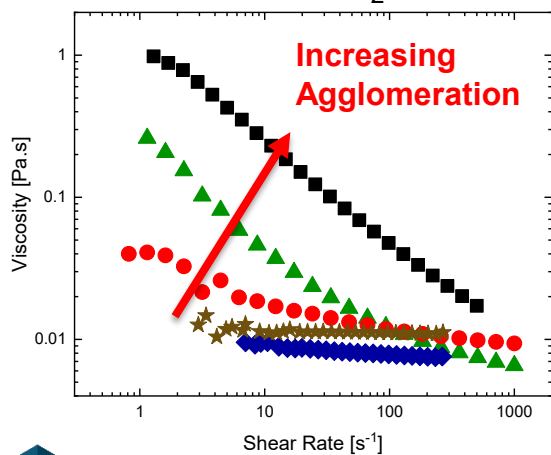
- Catalyst particles are attracted to each other and prone to agglomeration
- Level of agglomeration depends on dispersion media

Full Inks (Catalyst + Ionomer)

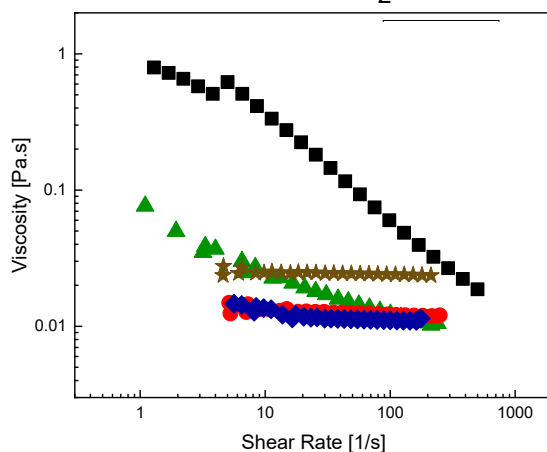
- Ionomer adsorption on catalyst depends on ink formulation
- 50 wt.% H₂O: fastest decrease in viscosity – strongest ionomer adsorption
- 82 wt.% H₂O: slow decrease in viscosity (low ionomer adsorption), then increase in viscosity (re-agglomeration)
- Largest agglomerates observed by X-ray scattering for 82 wt.% H₂O ink

Oscillatory Shear Rheology

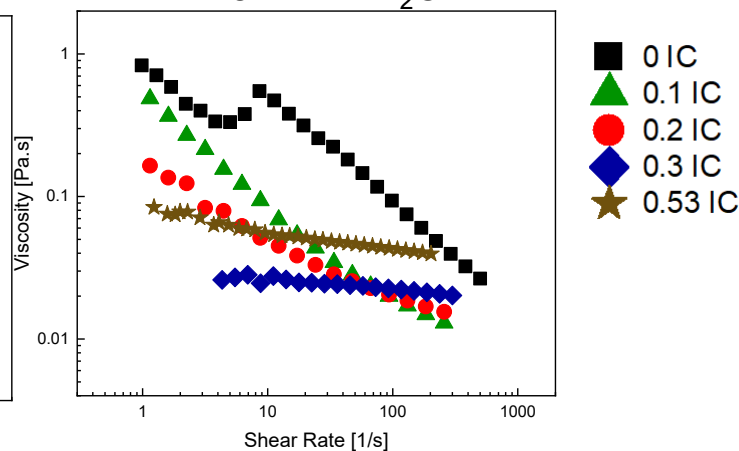
5 wt.% H₂O



50 wt.% H₂O

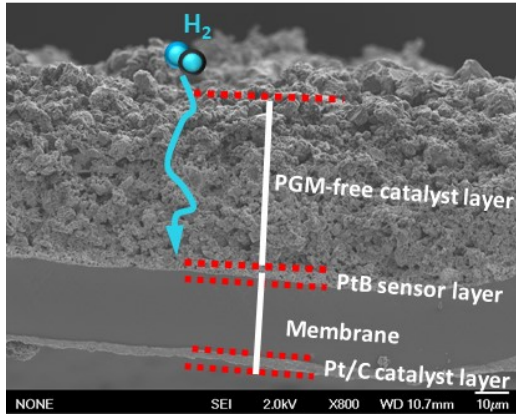


82 wt.% H₂O



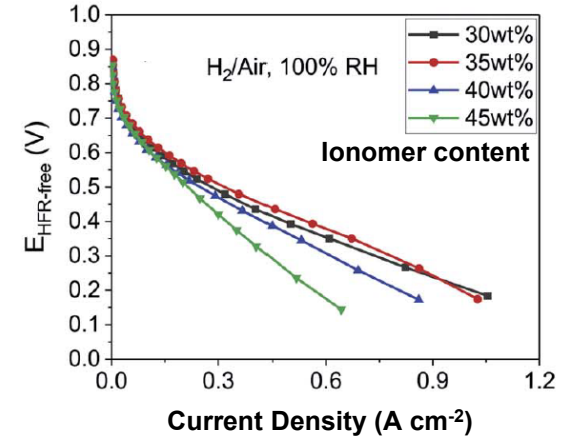
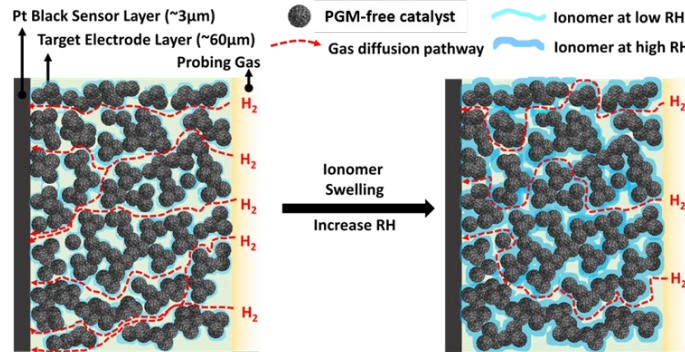
Electrode R&D – Capability Development: In-situ Electrode Diagnostics

H₂ limiting current using by Pt black sensor layer to determine bulk gas transport 5 cm² differential cell testing (Pajarito Powder Catalyst)



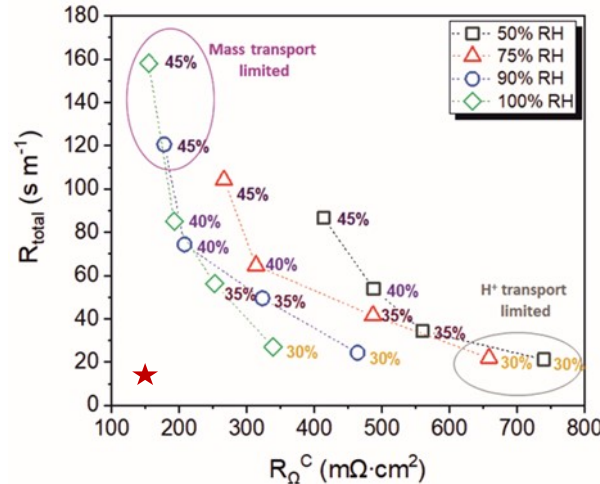
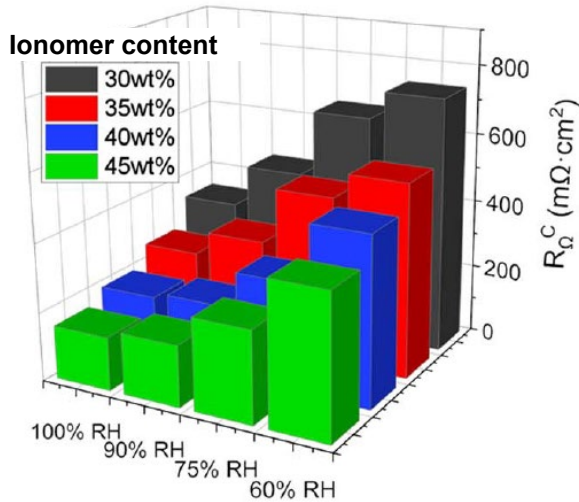
Star et al., *J. Power Sources*, 450, 227655, 2020

Effect of RH on bulk-electrode gas transport



Wang et al., *J. Electrochem. Soc.*, 167, 044519, 2020

Gas transport resistance vs. ionic resistance



- There is a trade-off between bulk-electrode gas transport (R_{total}) and electrode proton transport (R_{Ω}^c)
- Need to get off “master curve” of R_{total} vs. R_{Ω}^c by improving integration, understanding effects of ink composition and electrode fabrication processes

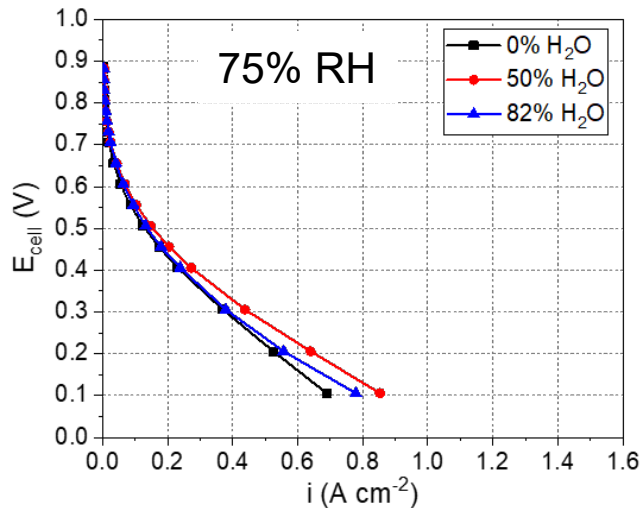
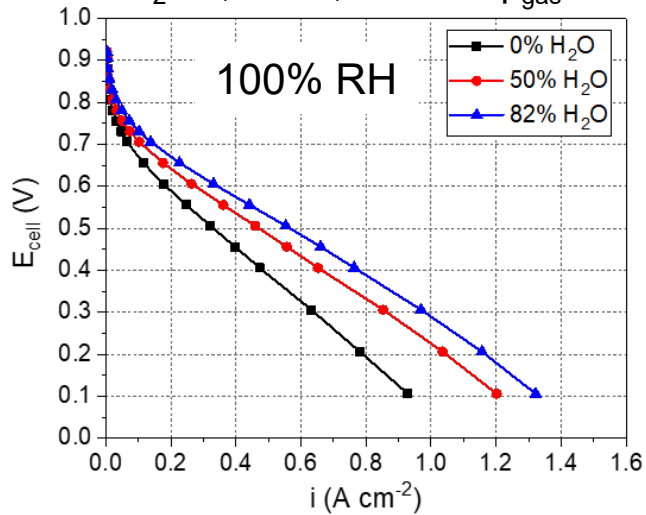
Wang et al. *JECS* 167, 044519 (2020)

★ Desired resistance region

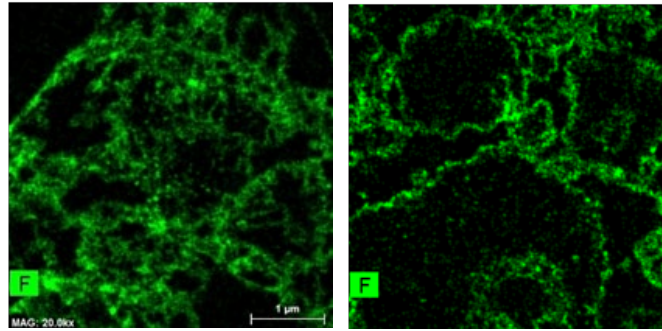
Electrode R&D: In-situ Diagnostics of Ionomer Interactions and Gas Transport

Pajarito Powder 11904 Catalyst

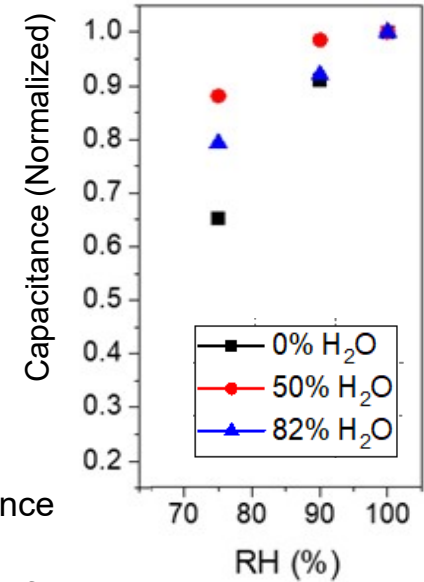
H₂/Air, 80 °C, 100 kPa p_{gas}



50 wt.% H₂O (nPA) 82 wt.% H₂O (nPA)

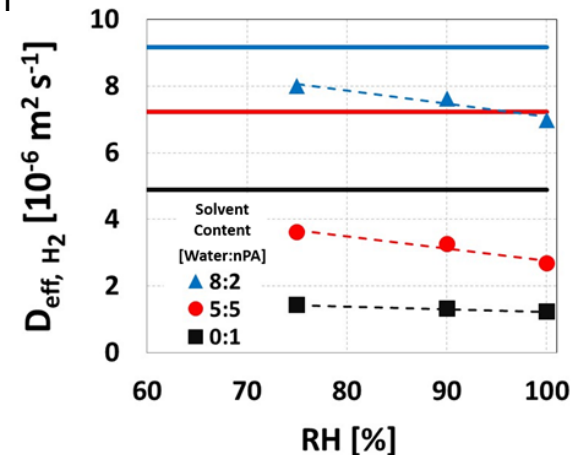
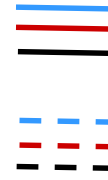


- Ionomer proximity to electrocatalyst does not necessarily indicate interaction
- Robust operation, not just maximum performance needs to be considered
- Ionomer adsorption on catalyst depends on ink formulation (see rheology data where 50 wt.% H₂O had the largest decrease in aggregation with the introduction of ionomer)
 - ✓ confirmed from normalized capacitance
- D_{eff} from transport measured in-situ yields sensitivity of ionomer within the electrode structure to RH



D_{eff,H2} calc.
Nano-CT
(~0% RH)

D_{eff,H2}
in-situ

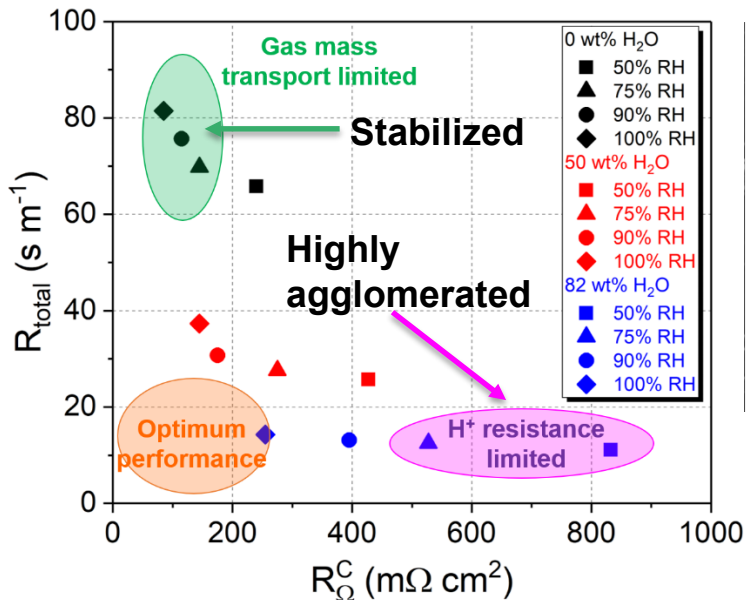


Osmieri et al. - *submitted*

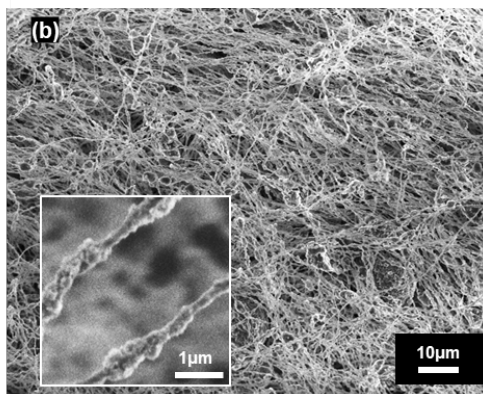
Electrode R&D – Capability Development: Electrospun Electrodes

- Current ink formulations / fabrication methods require a tradeoff between bulk-electrode and proton transport
- New formulations and/or methods are needed for optimum performance

Current Fabrication Methods

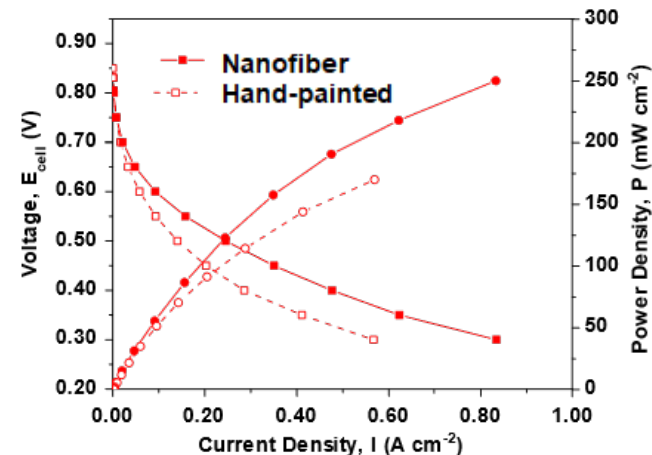


Electrospun



Kabir *et al.*, Nano Energy, accepted

(a) H₂/Air, 80°C, 150 kPa, 100% RH



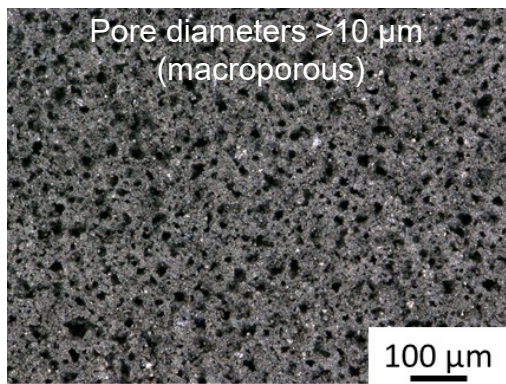
Electrospun

Ink comp	Deposition Method	Ionomer Weight [%]	D_{eff,H_2} [$\times 10^6$ m ² s ⁻¹]		
			75% RH	90% RH	100% RH
water:nPA	HP	35	3.62	3.26	2.68
water:IPA	HP	41	1.43	1.18	0.82
water:IPA	ES	41	4.19	4.08	3.97

HP: hand-painted

ES: electrospun

Current Fabrication Method with Alternative Ink Solvent

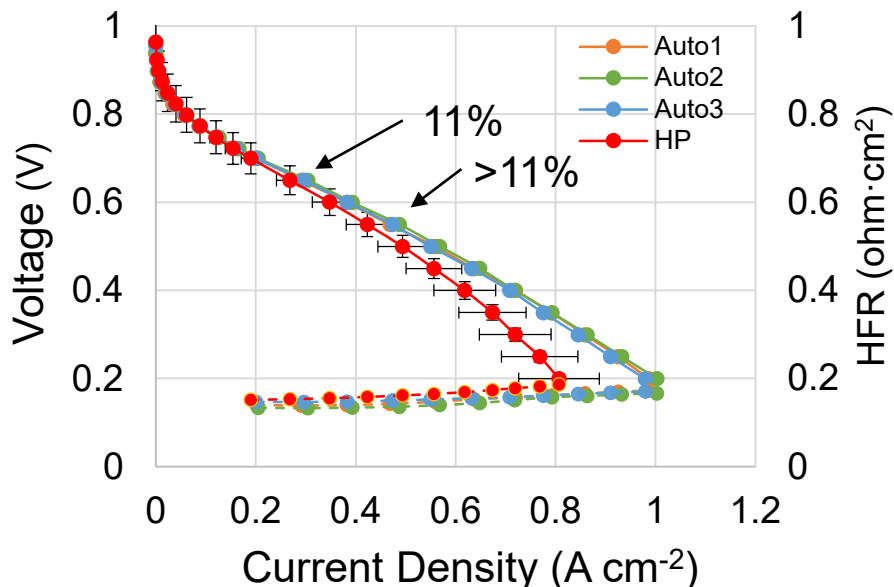


- Methods developed and utilized to generate highly porous catalyst layers
- H₂ i_{lim} results show high connectivity of pore network
- Goals are to eliminate D_{eff} dependence on RH and reduce pressure dependent bulk-electrode gas transport resistance by using alternative catalyst ink composition and electrode fabrication methods (e.g. electrospinning)
- Work ongoing to apply techniques to core national lab electrocatalysts

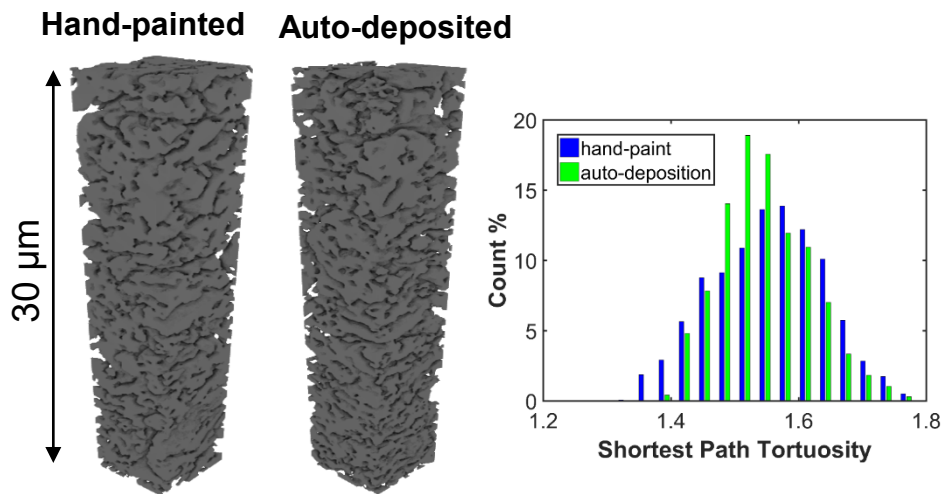
Electrode R&D: Performance Improvement using Automated Ink Deposition

Anode: 0.2 mg_{Pt} cm⁻² Pt/C, H₂, 200 sccm, 1.0 bar H₂ partial pressure, 100%RH; **Cathode:** Pajarito ammonia-treated catalyst, 4 mg cm⁻², air, 200 sccm, 1.0 bar air partial pressure, 100%RH; **Membrane:** Nafion® XL; **Cell:** 5 cm²; 80°C

Comparison of H₂-air performance of CCMs with hand-painted (HP) and auto-deposited cathodes



Nano-X-ray computed tomography



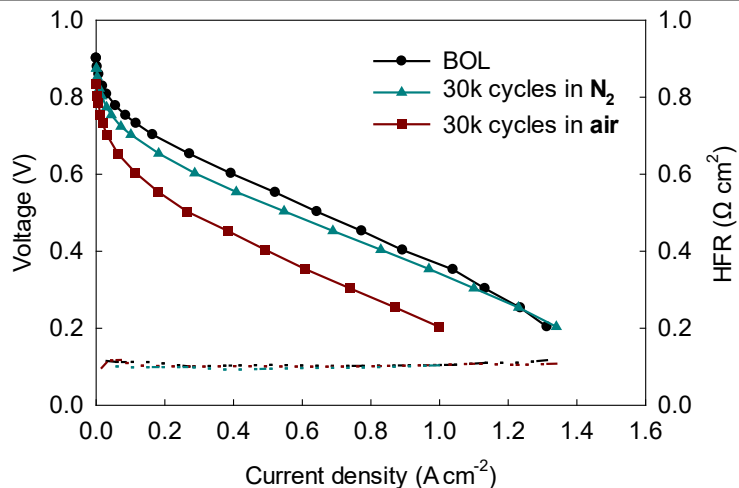
Auto-deposited electrode has higher porosity (0.46 vs. 0.40) and a less tortuous pore network

- **GPRA Milestone:** Automated deposition of PGM-free catalyst-ionomer inks shows 10% current density improvement versus the standard fabrication technique at <0.7V. Automated deposition of PGM-free catalyst-ionomer inks shows reproducibility of hydrogen-air fuel cell current density at <0.7 V within 5%.
- **Milestone met:** The average polarization curve for three auto-deposited electrodes shows >10% higher current density than that for the hand-painted electrode at <0.7 V. Three polarization curves for auto-deposited electrodes fall within 5% standard deviation in current density.

AST Protocols & Round-Robin Testing: Introduction

Polarization Curves Before and After Cycling Between 0.60 V and OCV

Anode: 0.2 mg_{Pt} cm⁻² Pt/C H₂, 1.0 bar partial pressure, 500 sccm, 100% RH
Cathode: ~ 4 mg/cm² Fe_{1.5}-N-C catalyst, 1.0 bar partial pressure, 2000 sccm, 100% RH
Membrane: Nafion® 211 **Cell:** differential, 5 cm² electrode area, **Cell temperature:** 80 °C

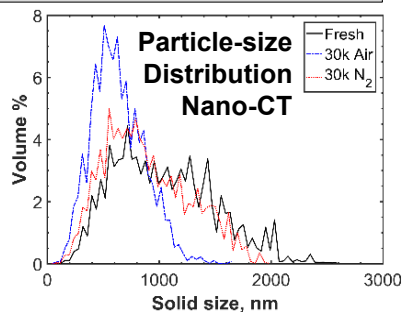


AST Protocol in H₂-Air Fuel Cell (Excerpts)

- Square-wave cycle; steps between 0.60 V (3 s) and OCV (but no higher than 0.925 V to minimize carbon corrosion) (3 s); rise time of 0.5 s or less
- Cell temperature 80 °C; 100 kPa N₂ + O₂ pressure
- Single differential cell ≥ 5 cm² (below)
- Anode/cathode gas flows of 0.7/ 1.7 SLPM
- Anode/cathode relative humidity (RH) 100%/100%
- H₂-air polarization curves recorded after 0, 100, 1k, 5k, 10k, 30k cycles in voltage range OCV-0.20 V
- Non-stabilized membrane
- **Catalysts tested:** Pajarito Powder 011904
LANL's Fe_{1.5}-N-C

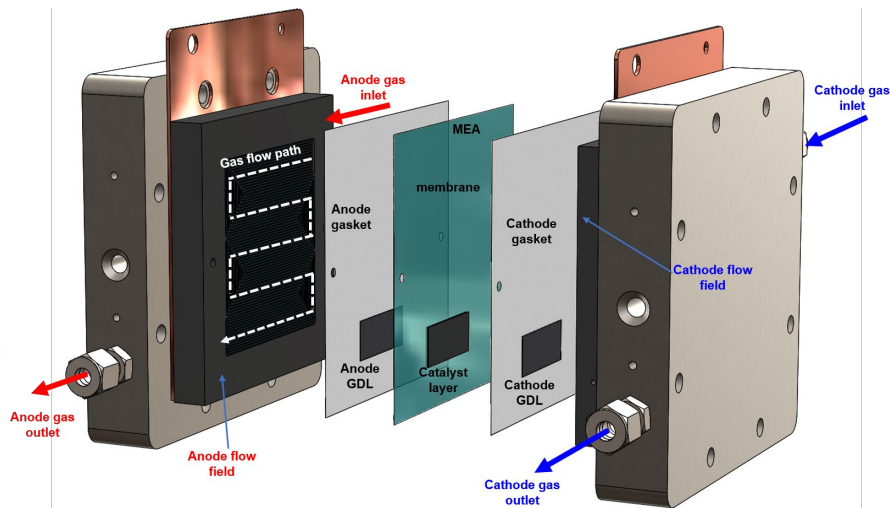
Characterization Before and After Cycling Between 0.60 and 0.95 V (2019 AMR)

MEA Tested	at.% (EDS)	
	N	Fe
Fresh MEA	1.71	0.09
MEA after AST in N ₂	1.50	0.04
MEA after AST in air	1.25	0.01

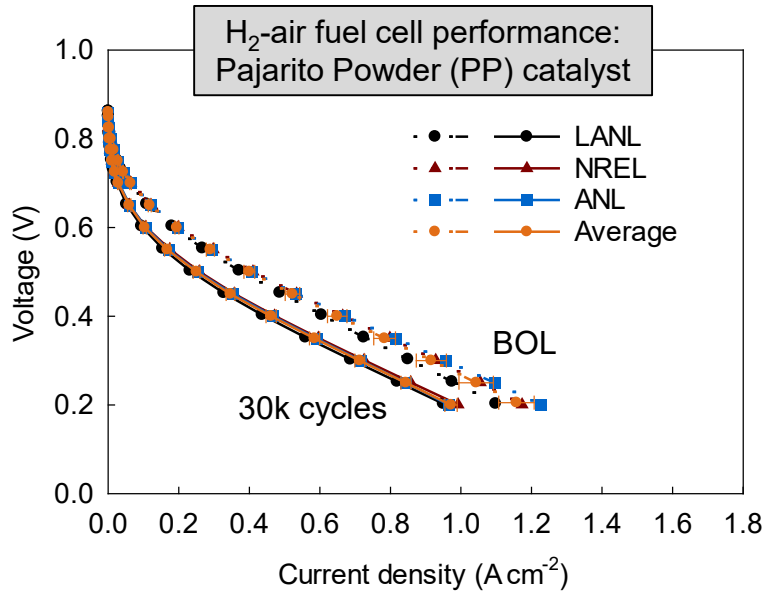


Unlike for PGM catalysts, effective durability testing of PGM-free catalysts requires cycling in air rather than N₂

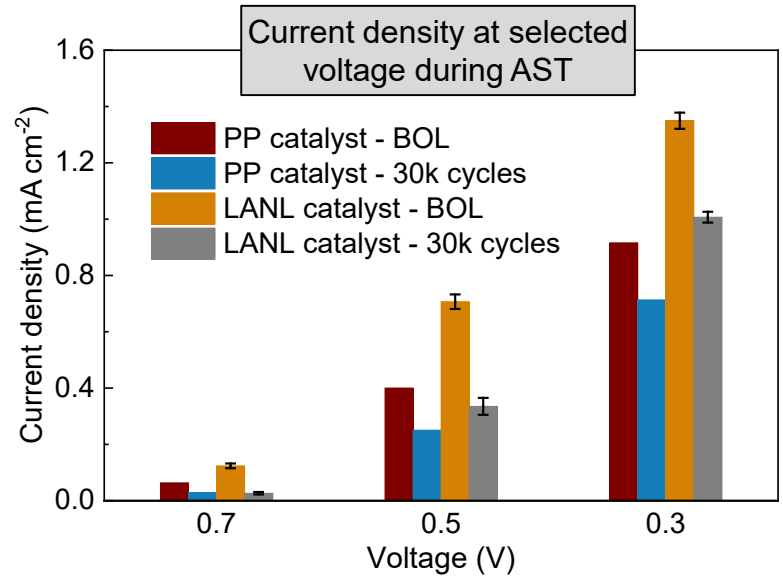
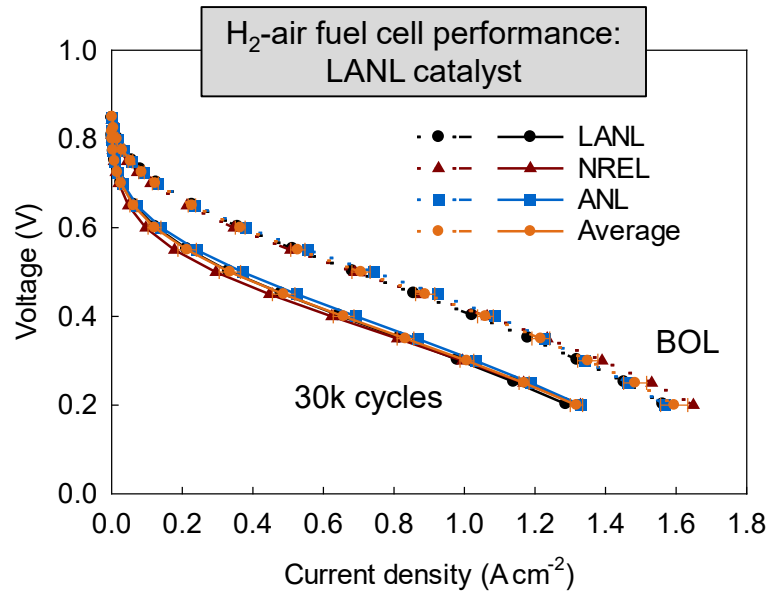
Schematic Diagram of Differential Cell



AST Protocols & Round-Robin Testing: Testing in H₂-Air Fuel Cells



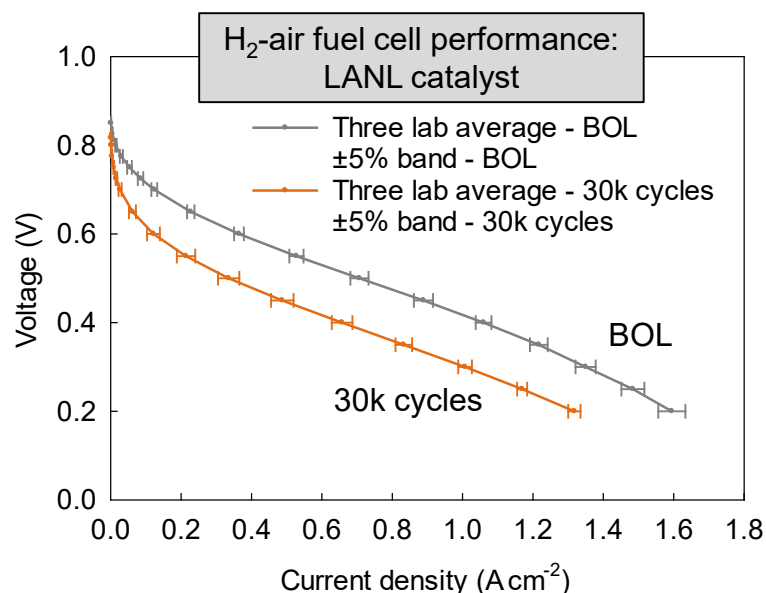
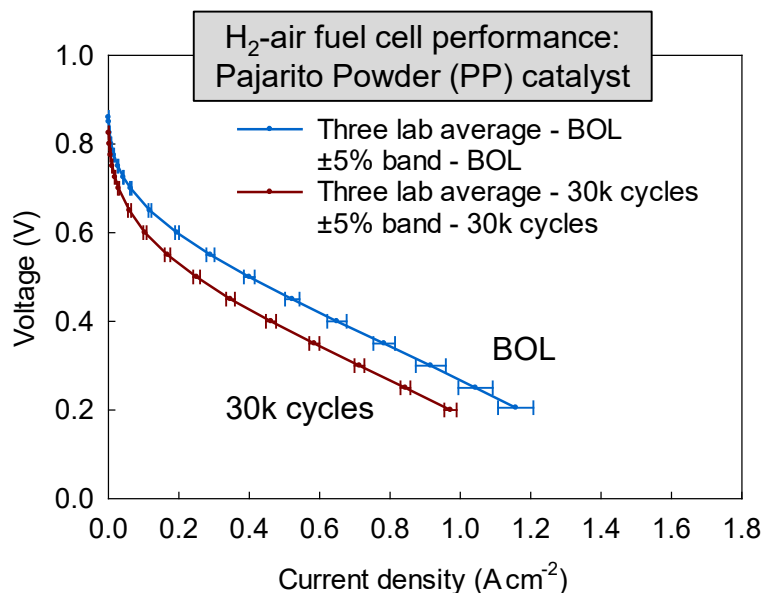
Anode: Pt/C, 0.1 mg_{Pt}/cm²; H₂: 1.0 bar partial pressure, 700 sccm; 100% RH. **Cathode:** Pajarito Powder 011904 and LANL Fe_{1.5}-N-C catalysts, 4 mg/cm²; Air: 1.0 bar partial pressure, 1700 sccm; 100% RH. **Membrane:** Nafion®211. **Cell:** Differential cell, 5 cm² electrode area. **Cell temperature:** 80 °C.



Excellent agreement in test results using Pajarito Powder 011904 and LANL Fe_{1.5}-N-C catalysts at three ElectroCat labs (LANL, ANL, and NREL)

AST Protocols & Round-Robin Testing: Testing in H₂-Air Fuel Cells

Anode: Pt/C, 0.1 mg_{pt}/cm²; H₂: 1.0 bar partial pressure, 700 sccm; 100% RH. **Cathode:** Pajarito Powder 011904 & LANL Fe_{1.5}-N-C catalysts, 4 mg/cm²; 1.0 bar air partial pressure, 1700 sccm; 100% RH. **Membrane:** Nafion®-211. **Cell:** Differential cell, 5 cm² active area. **Cell temperature:** 80 °C.



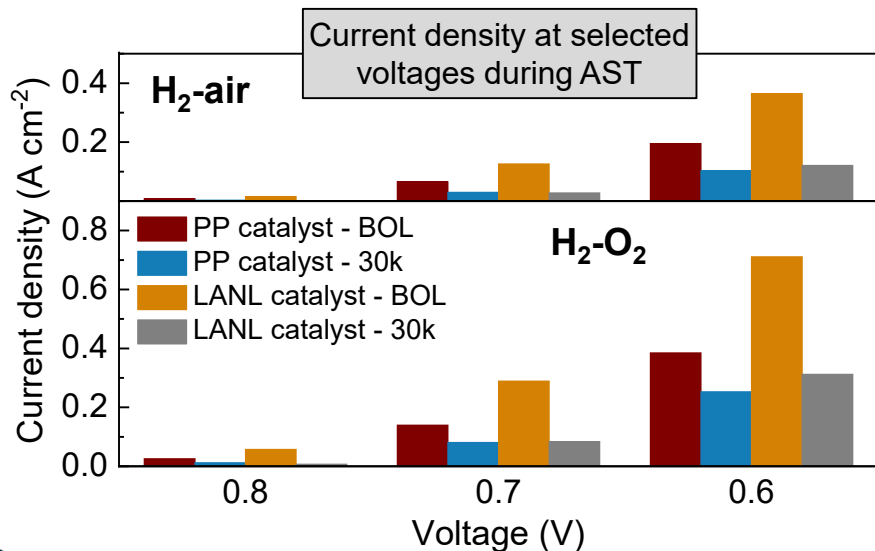
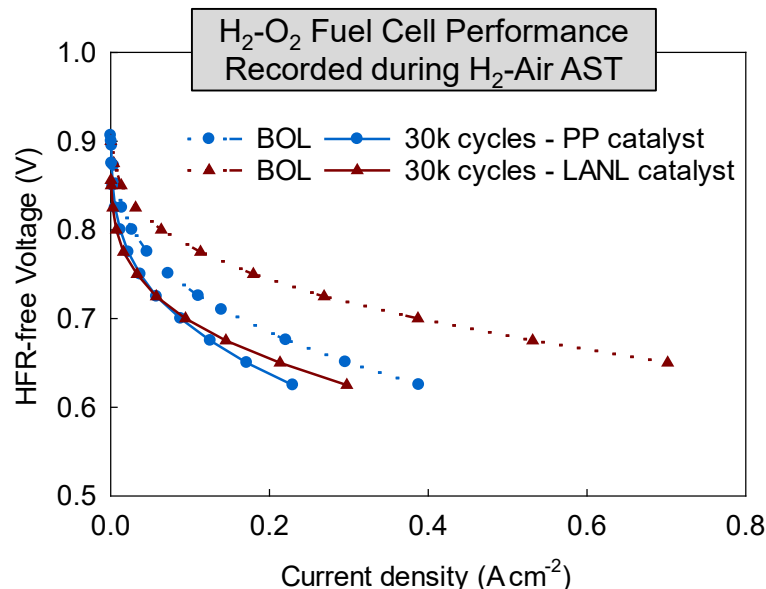
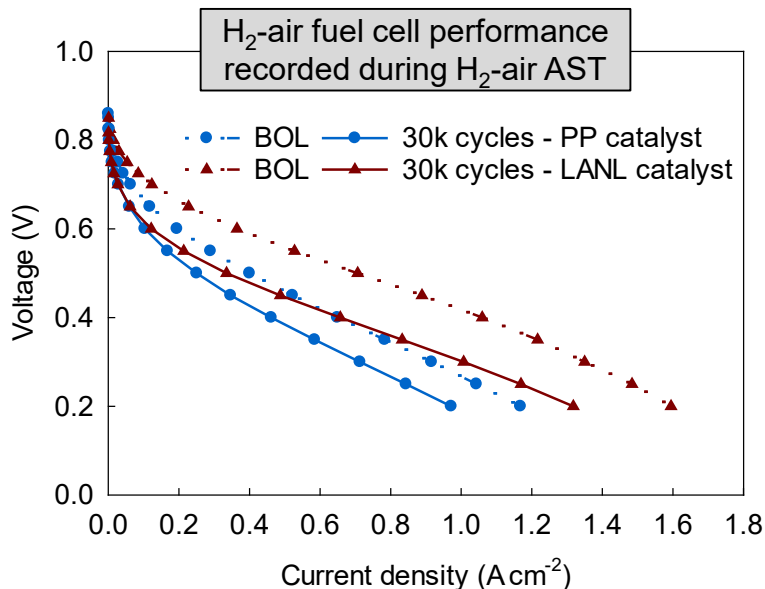
Standard Deviation Values in MEA Round Robin Tests

Voltage (V)	PP Catalyst		LANL Catalyst	
	BOL	30k	BOL	30k
0.7	3.7%	4.8%	6.7%	16.8%
0.5	3.8%	3.9%	3.6%	9.0%
0.3	4.7%	2.0%	2.1%	1.9%

- **Highlight:** GPRA Milestone achieved with less than 5% standard deviation using Pajarito Powder 011904 catalyst in round-robin testing
- Very good agreement also accomplished in LANL catalyst testing
- **Highlight:** Utility of PGM-free catalyst AST durability protocol validated

AST Protocols & Round-Robin Testing: Air vs. Oxygen Performance

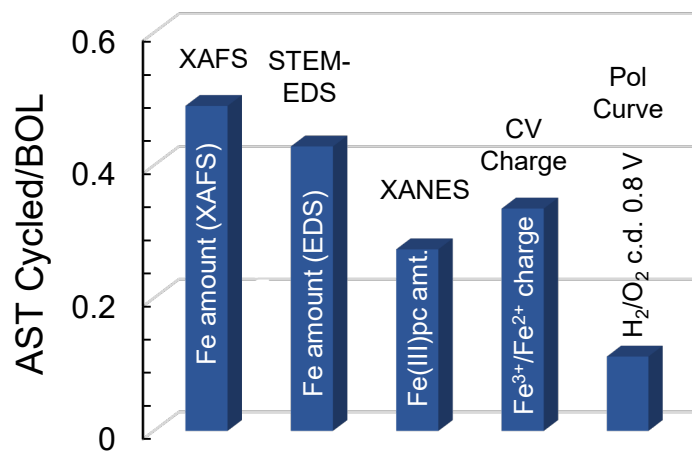
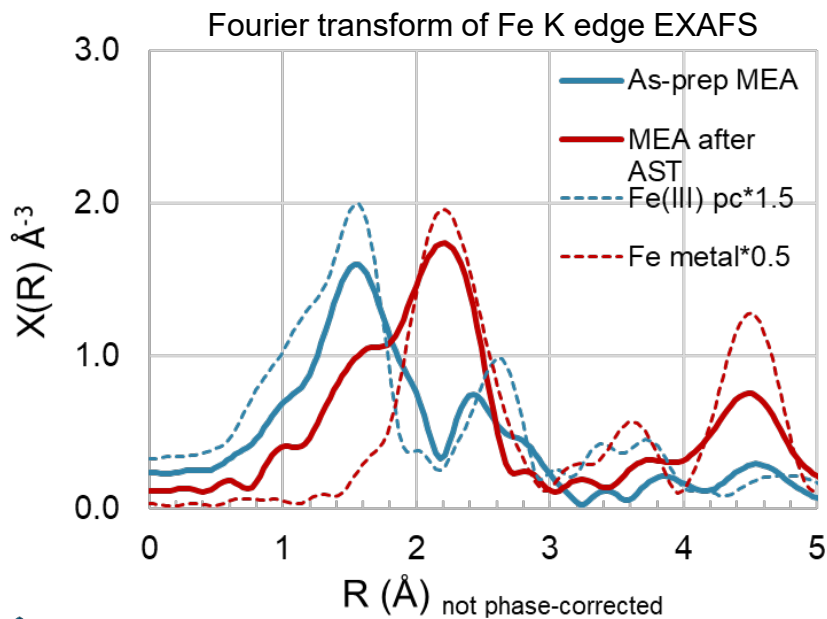
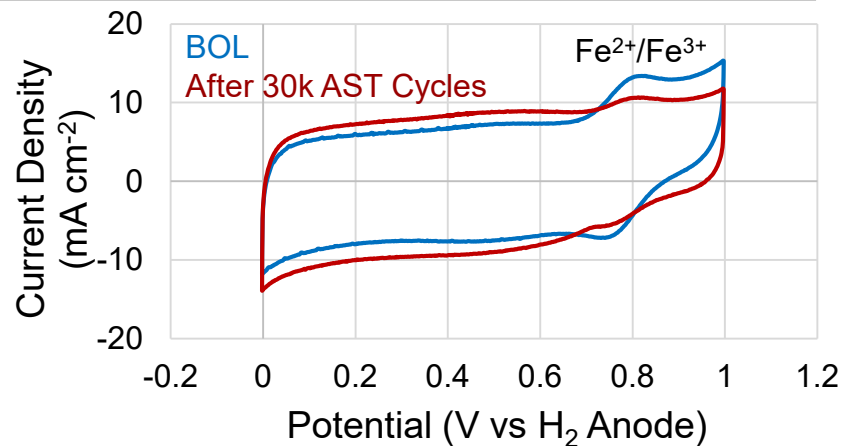
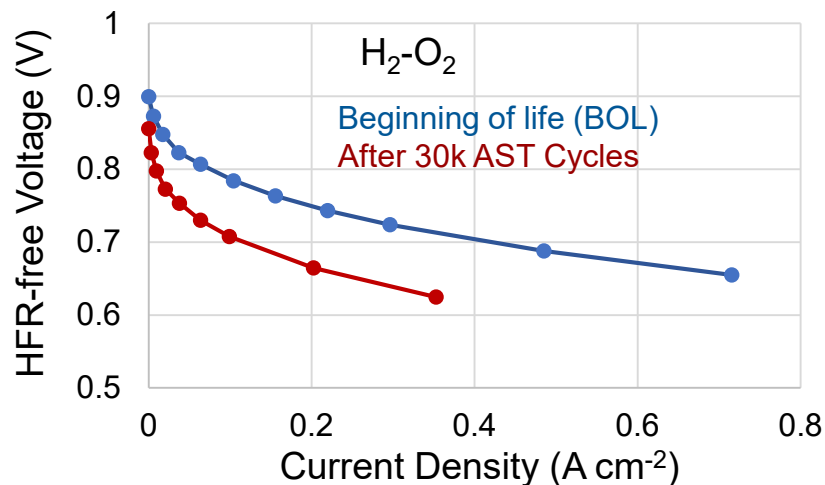
Anode: Pt/C, 0.1 mg_{Pt}/cm²; 1.0 bar H₂ partial pressure, 700 sccm; 100% RH. **Cathode:** Pajarito Powder 011904 or LANL Fe_{1.5}-N-C catalyst, 4 mg/cm²; 1.0 bar gas partial pressure, 1700 sccm; 100% RH. **Membrane:** Nafion™ 211. **Cell:** differential, 5 cm² electrode area. **Cell temperature:** 80 °C.



- ElectroCat-developed PGM-free durability protocol successfully applied in accelerated stress testing in three core consortium labs
- Activity-durability trade-off observed with two catalysts, with less active Pajarito catalyst incurring less voltage loss than more active LANL catalysts

AST Protocols & Round-Robin Testing: Impact of AST Protocol on Cathode

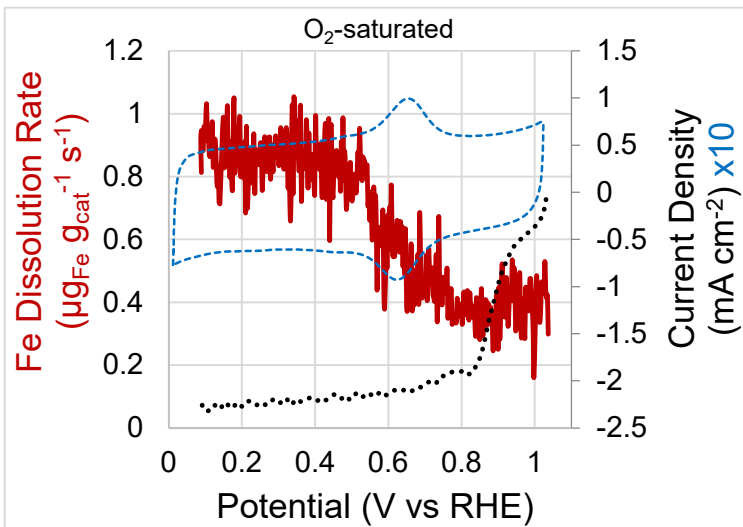
Anode: Pt/C, 0.1 mg_{Pt}/cm²; H₂: 1.0 bar partial pressure, 700 sccm; 100% RH. **Cathode:** LANL Fe_{1.5}-N-C catalyst, 4 mg/cm²; O₂ (left) N₂ (right), 1.0 bar partial pressure, 1700 sccm; 100% RH. Membrane: Nafion[®]211. **Cell:** Differential cell, 5 cm² electrode area. **Cell temperature:** 80 °C.



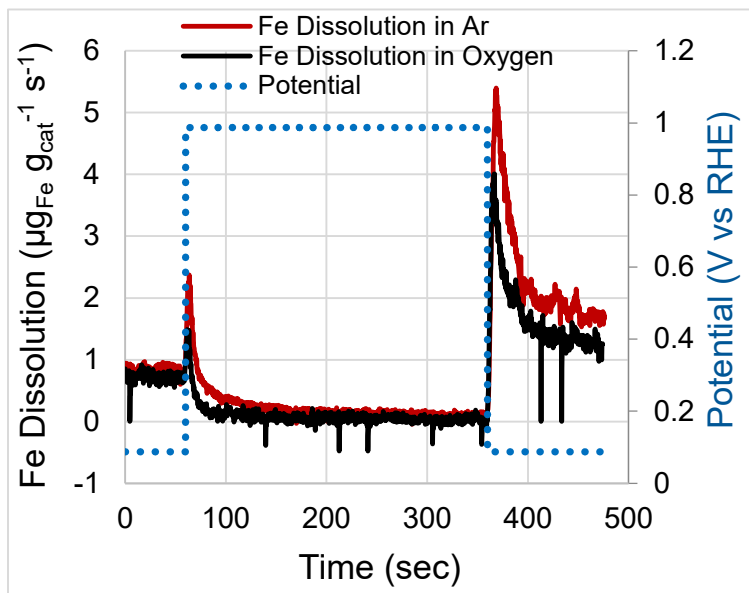
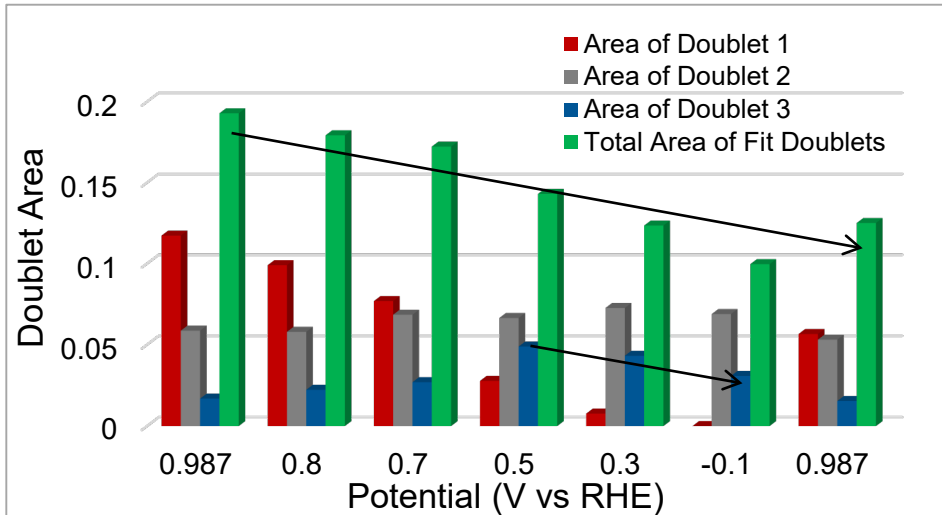
- ASTs in air cause a >50% loss in Fe content, a 73% loss of FeN₄ content, and an 88% loss of current density at 0.8 V (H₂-O₂)
- Fe is lost from cathode catalyst layer and FeN₄ is converted to Fe metal

Durability: Fe Dissolution from (AD)Fe-N-C Catalyst

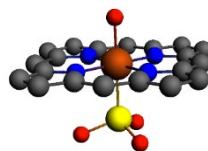
Dissolution measurements: ICP-MS Probe on RDE
0.5 M H₂SO₄ electrolyte



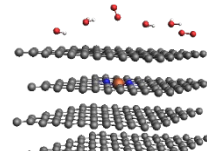
Mössbauer Spectroscopy
0.5 M H₂SO₄ deaerated electrolyte, 24 h/potential



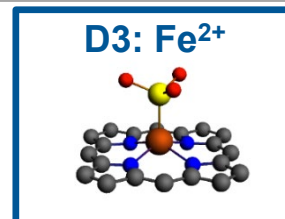
D1: Fe³⁺



D2: Fe²⁺



D3: Fe²⁺

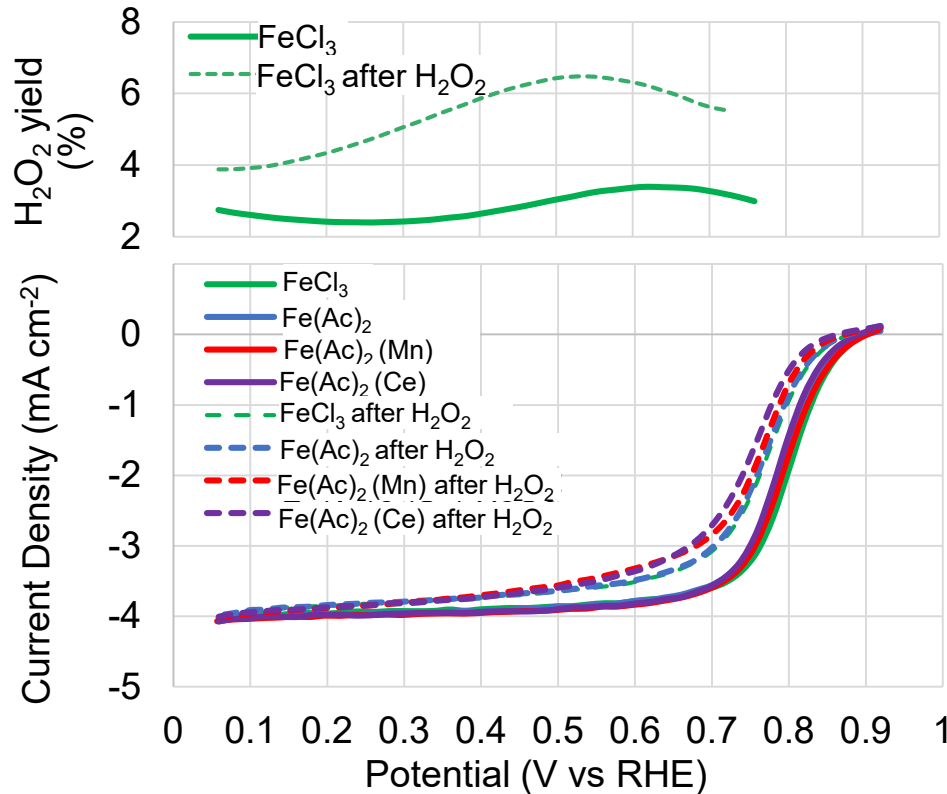


Soluble Species

- D1 converted to D3 with decreasing potential to 500 mV
- At <700 mV D3 is lost to the electrolyte (or converted to species that is not Mössbauer active)
- D1 content decreases after potential cycle
- Dissolution data shows Fe dissolution is highest during transition from high to low potentials, corresponds with potential range for loss of D3
- Dissolution is not increased by presence of O₂ in aqueous electrolyte

Durability: Effect of Peroxide on ORR Activity in Aqueous Electrolyte

ORR: 0.6 mg cm⁻² catalysts from high-throughput system #3; 0.5 M H₂SO₄; 900 rpm; 25°C; Ag/AgCl (saturated KCl) reference electrode; graphite counter electrode; steady-state potential program: 20 mV steps, 20 s/step

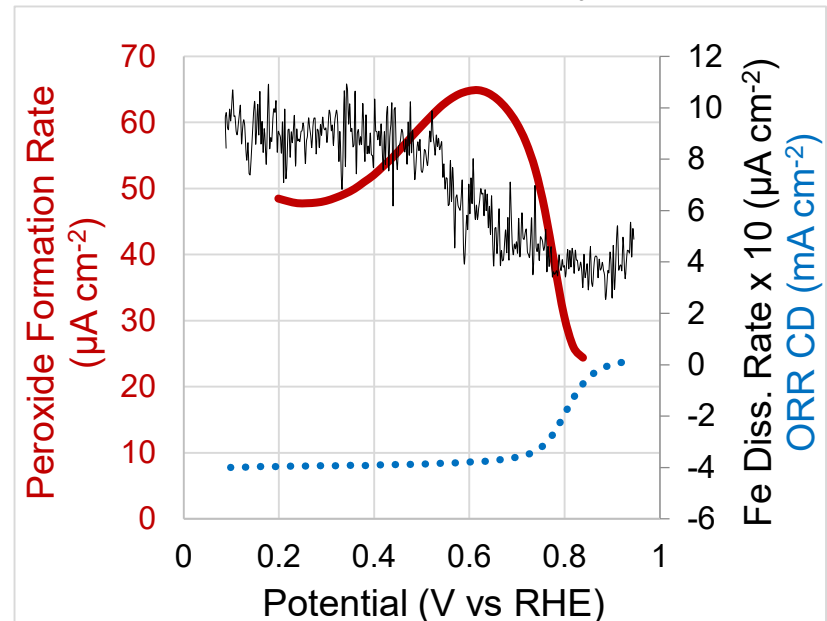


- Peroxide causes substantial loss in ORR activity of Fe-N-C catalysts, regardless of presence of dopant metal
- Peroxide formation rate is highest at 0.5 to 0.7 V, coincident with Fe dissolution

Ex situ peroxide treatment procedure:

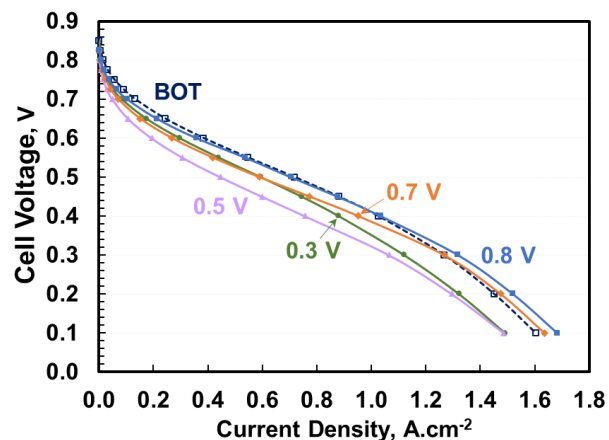
- Voltammetry of 0.6 mg cm⁻² RDE in O₂-saturated 0.5 M H₂SO₄, 900 rpm
- Soak RDE tip/catalyst layer in room temperature 5 wt.% hydrogen peroxide in deaerated 0.5 M H₂SO₄ solution for 2 h at open circuit with electrode rotated at 2000 rpm
- Repeat ORR voltammetry

Peroxide Formation Rate during ORR, RRDE, 0.6 mg cm⁻² FeCl₃(N-C)



Durability: (AD)Fe-N-C Catalyst in MEA

- Utilized four differential cells with (AD)Fe-N-C cathode catalyst
- Monitored current decay at constant cell voltages for 24 h, and measured changes in voltammetry and H₂-O₂ and H₂-air polarization performance



Kinetic Region

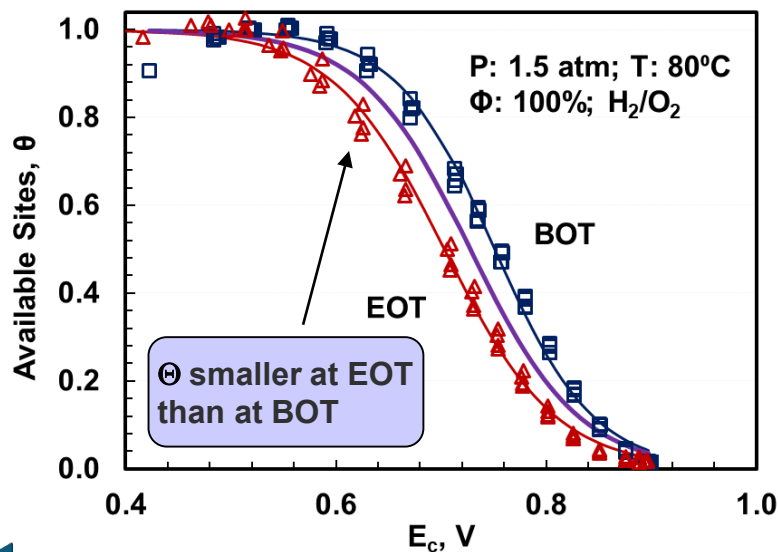
▪ ΔE at 0.8 V < 0.7 V ~ 0.3 V < 0.5 V

High Current Density Region

▪ ΔE at 0.8 V < 0.7 V < 0.3 V ~ 0.5 V

Available Site Degradation ($\Delta\theta$) from H₂-O₂ Polarization Data at BOT and EOT

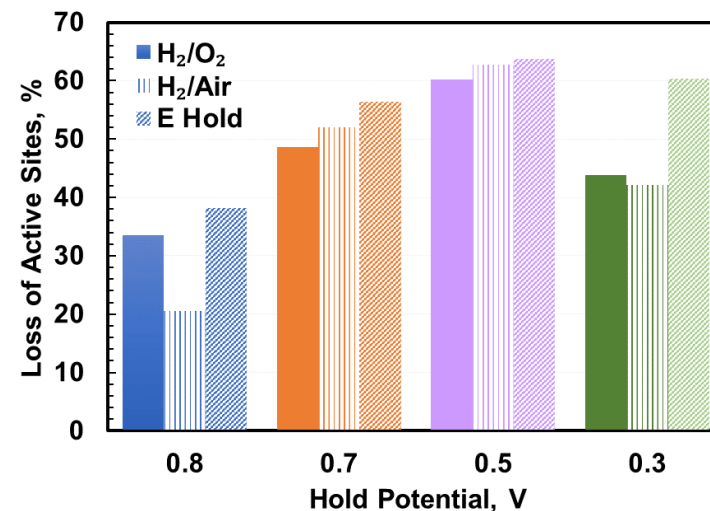
- Observable degradation in θ after 24 h, independent of hold potential



Active Site Degradation from H₂-Air Polarization Data at BOT and EOT

- Highest degradation after 24 h at 0.5 V

Active site loss smallest at 0.8 V, highest at 0.5 V



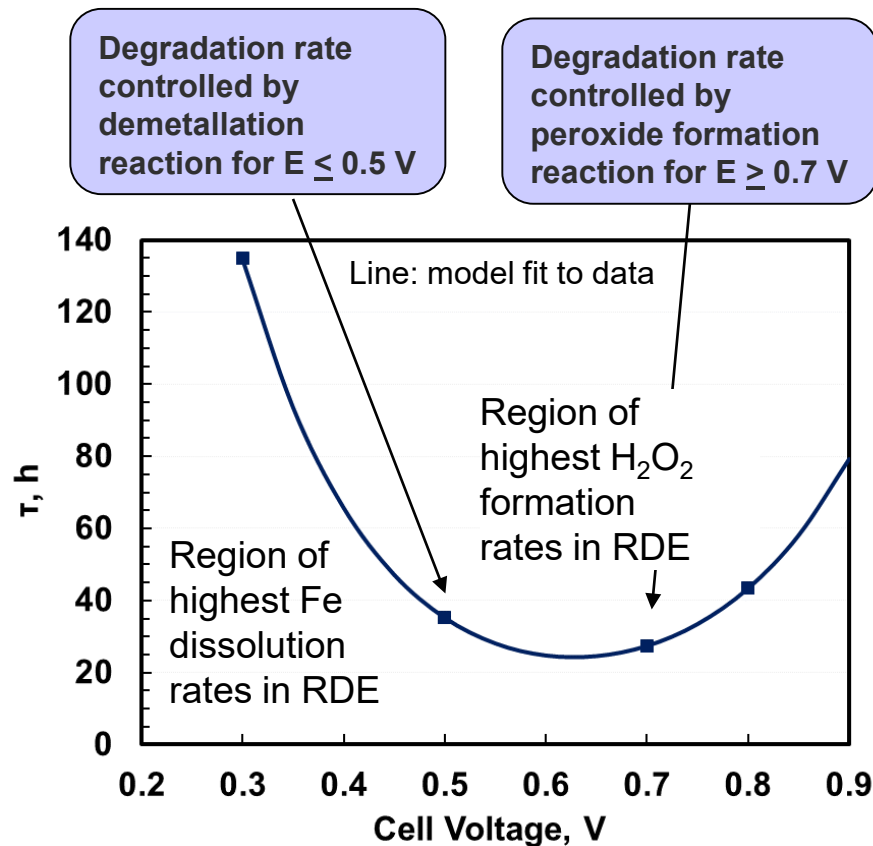
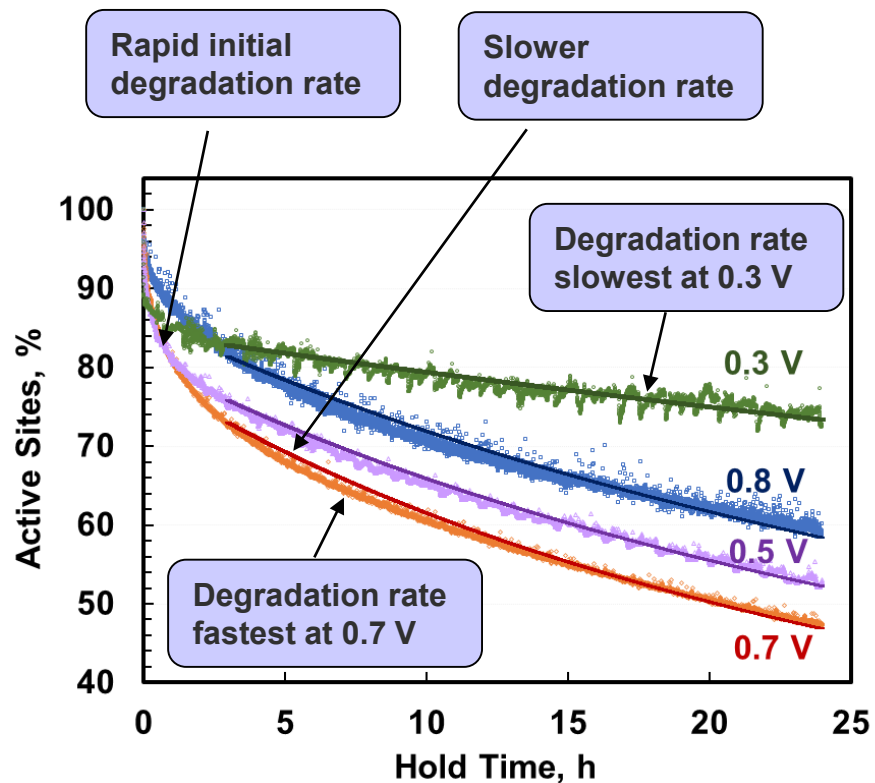
Durability: Degradation Kinetics of (AD)Fe-N-C in MEA at Constant Voltage

Modified Logistic Decay Model

- $X + O_2 + 2H^+ + 2e^- = X + H_2O_2$
 $X + H_2O_2 + 2H^+ + 2e^- = X_D + 2H_2O$
- $\frac{d\Psi}{dt} = -\left(\frac{1}{\tau}\right)\psi^2$
- Degradation rate:
 $0.3\text{ V} < 0.8\text{ V} < 0.5\text{ V} < 0.7\text{ V}$

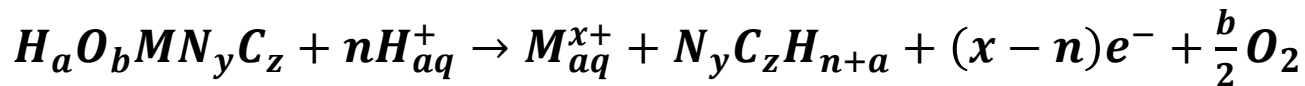
Degradation Time Constant

- $\tau = \tau_1 + \tau_2$
- τ_1 : peroxide formation time constant
- τ_2 : demetallation time constant

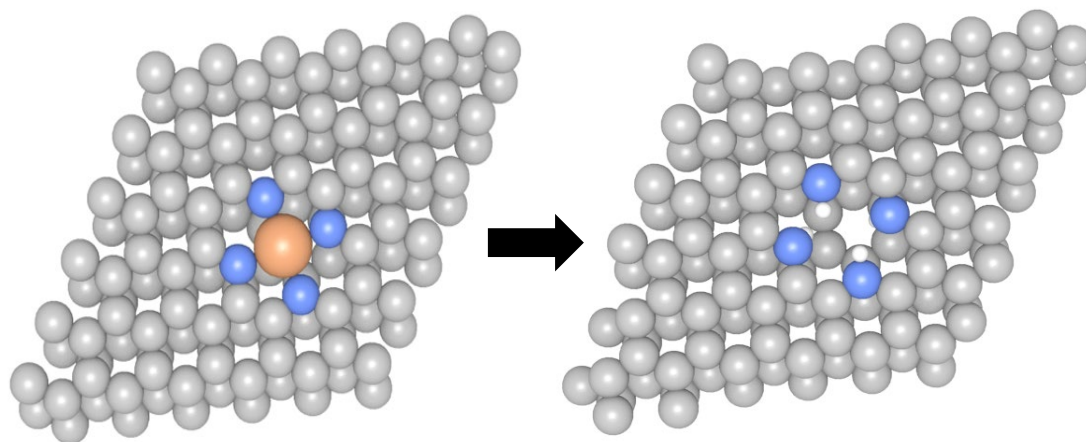
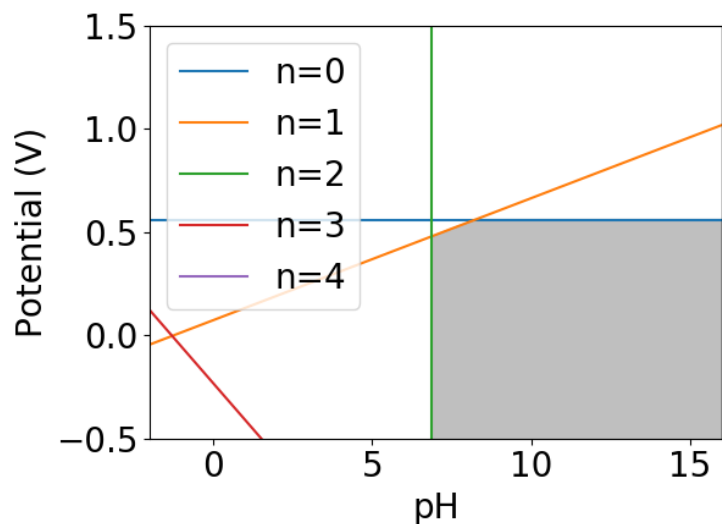


Durability: DFT-Derived Dissolution Descriptor

Dissolution reaction:



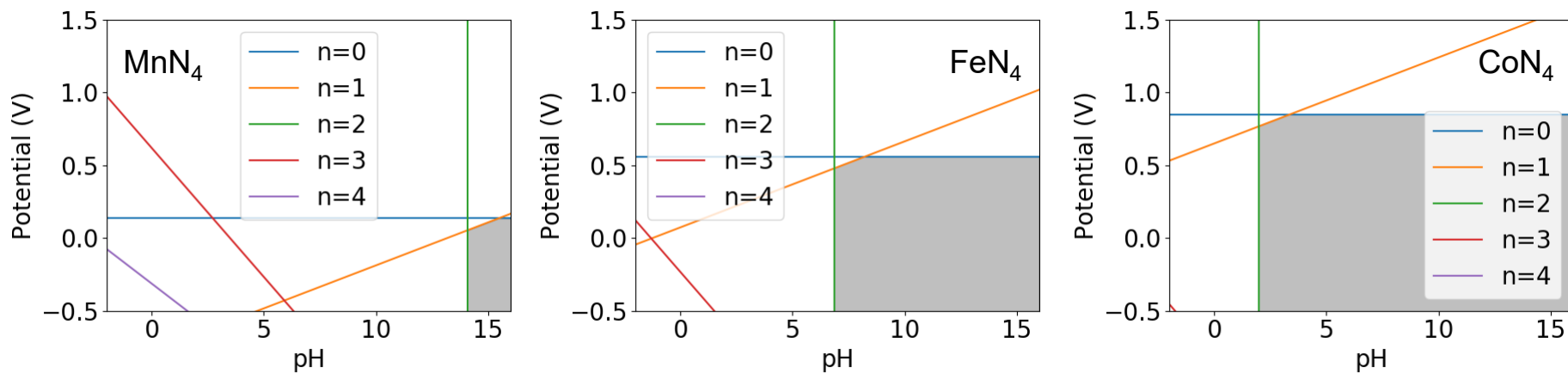
- DFT energetics of reactant (active site) and product (metal ion, metal-free site, *etc.*) states serve as model input
- Methodology accounts for potential, pH, ionic concentration, and temperature
- Provides Pourbaix-like diagram for metastable active site structures



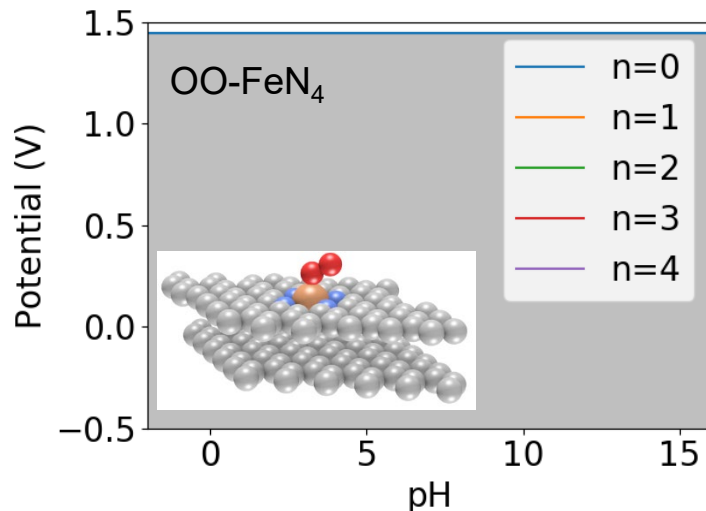
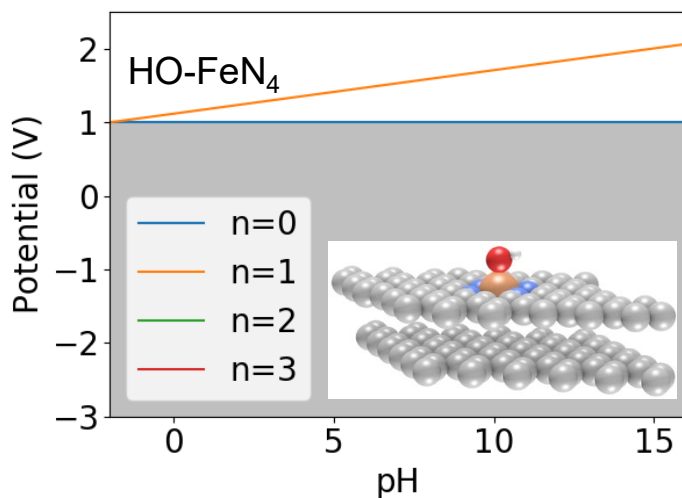
Holby, Wang, and Zelenay, in preparation

Highlight: Derived, scripted, and applied thermodynamically consistent method for determining stability requirements as a function of active site structure/ligation based on DFT input

Durability: DFT-Derived Dissolution Descriptor; Role of Metal Speciation & Ligation



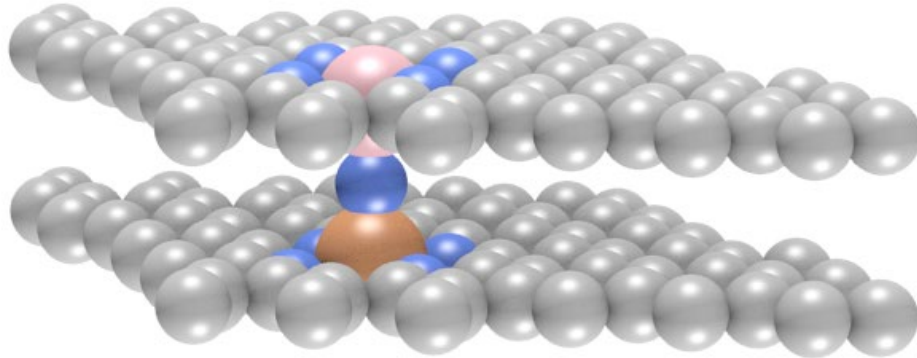
Stable vs. dissolution



- **Highlight:** Metal speciation and ligation state play important roles in dissolution of metals from active sites
- Free radical attack of stabilizing ligands leading to dissolution captures many experimental trends in activity loss

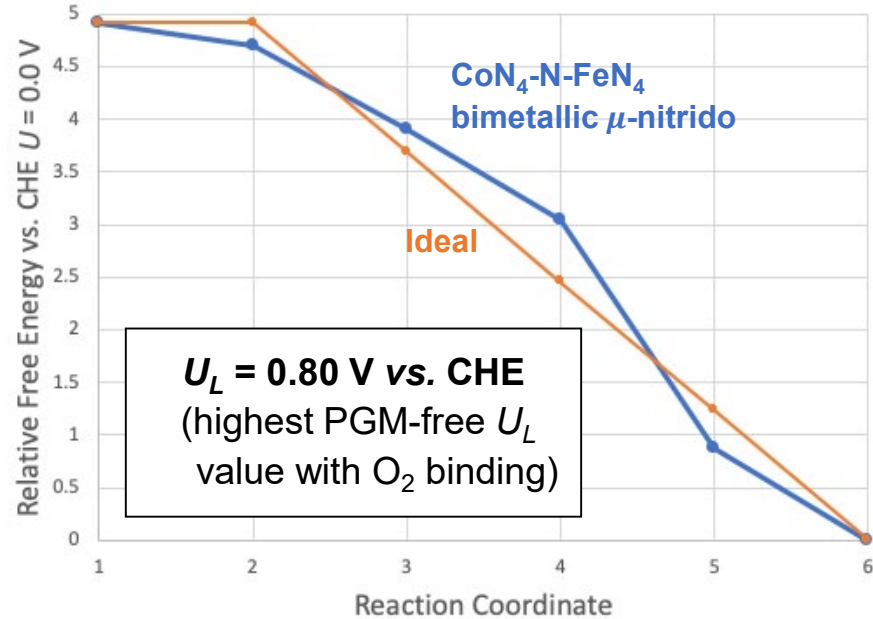
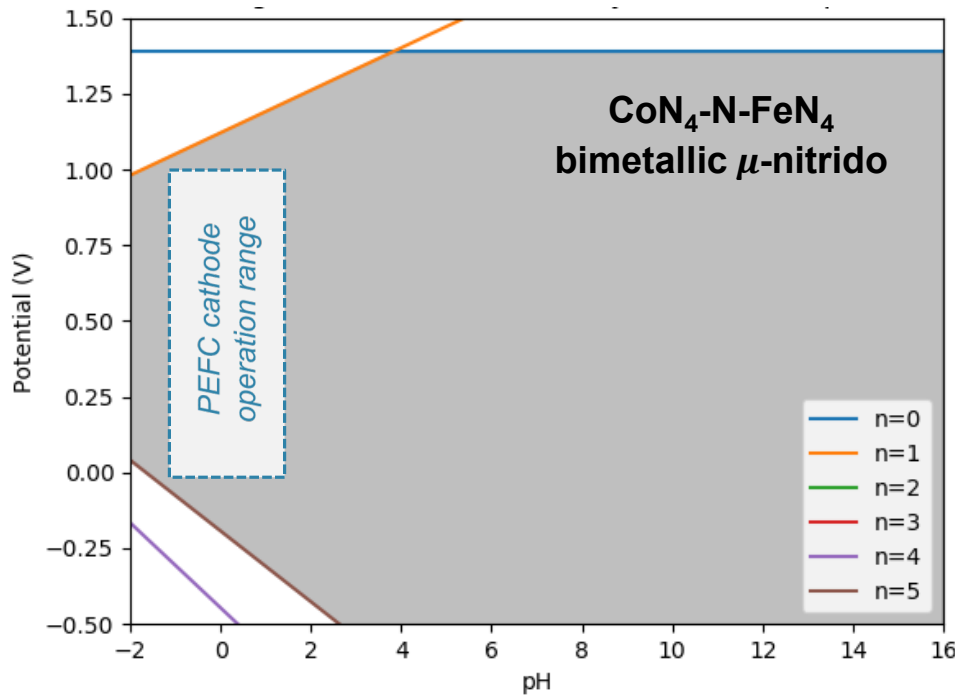
Holby, Wang, and Zelenay, in preparation

Enhancing Activity & Durability: Learning from DFT-Derived Descriptors



Proposed target active site structure:

CoN₄-N-FeN₄ bimetallic μ-nitrido based on input from both activity and dissolution studies – *simultaneous optimization possible!*



Highlight: Structure prescribed with simultaneously high activity and dissolution tolerance

Holby, in preparation.

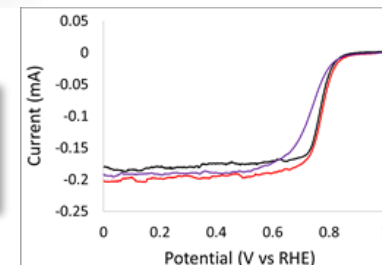
Enhancing Activity & Durability: High-throughput Synthesis of Three Systems

Catalyst system 1: Solution phase synthesis of (Fe)Zn – ZIF; **40** unique samples

Catalyst system 2: Physical mixtures (ball milling) of Fe salt, carbon-nitrogen precursor, carbon support (e.g., Zitolo *et al.*, *Nat. Mater.*, 14, 937, 2015); **160** unique samples

Catalyst system 3: Two step synthesis; formation of nitrogen-doped carbon followed by incorporation of Fe (based on J. Li, D, Myers, Q. Jia *et al.*, *J. Am Chem. Soc.*, 142, 1417, 2020)

- Physical mixtures (ball milling) of carbon-nitrogen precursors pyrolyzed and heat-treated in NH_3 to form nitrogen-doped carbon (N-C)
- Physical mixtures (ball milling) of N-C and Fe salt pyrolyzed and heat treated in NH_3
- **Parameters varied to obtain 50 unique samples:**
 - ✓ Fe precursor
 - ✓ Fe loading
 - ✓ Fe vs Mn
 - ✓ Fe addition in first step only or first and second step
 - ✓ Ball milling vs no ball milling in second step
 - ✓ Ammonia treatment
 - ✓ Temperature of second heat treatment step
 - ✓ Addition of transition metal dopants and radical scavengers to N-C



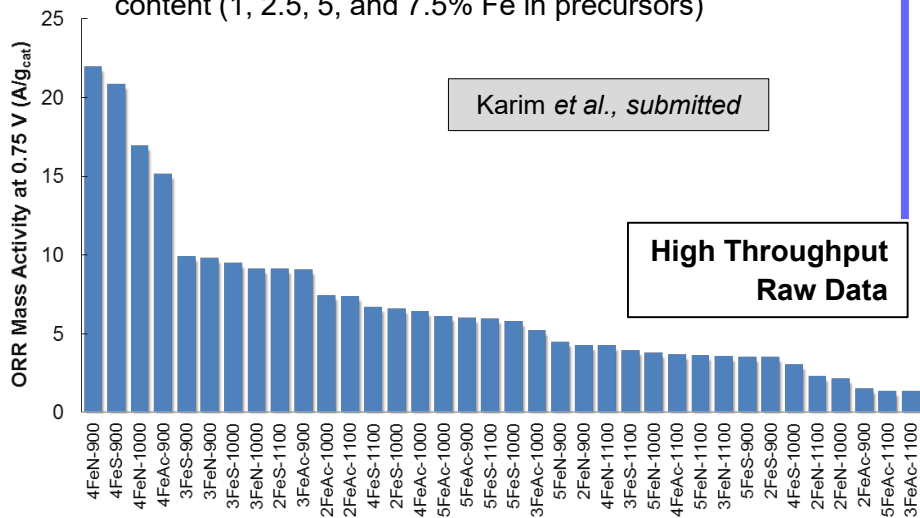
Enhancing Activity & Durability: Machine Learning for Improved ORR Activity

Motivation to use machine learning approaches: (1) How is synthesis best optimized for high ORR activity? **(2)** What should the next set of experiments be to efficiently explore defined search space to enhance ORR activity and improve an activity surrogate model?

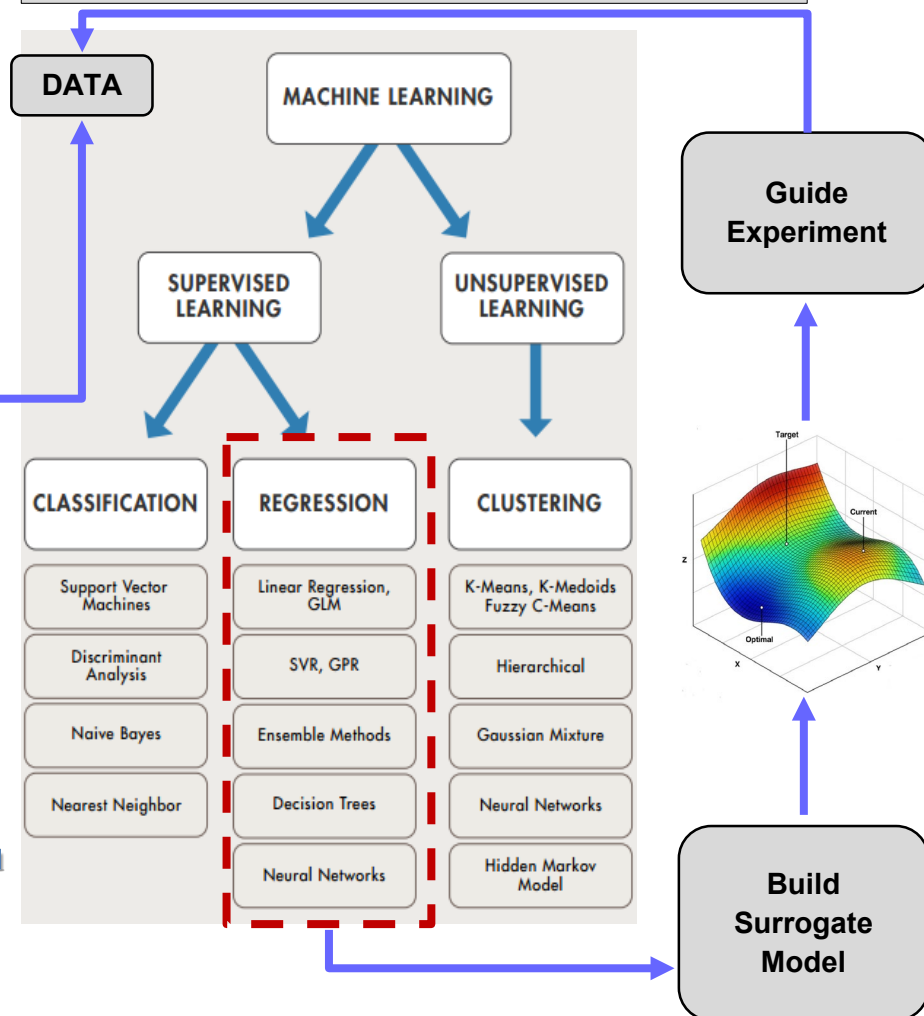
Precursor Synthesis: CM Protégé Robot



- 36 unique batches synthesized and m-CFDE cell tested for ORR mass activity (LANL's $(\text{Zn}_x\text{Fe}_{1-x})\text{ZIF}$ catalyst)
- Temperature of heat treatment: 900, 1000, 1100 °C
- Fe precursor: nitrate, sulfate, acetate
- Fe to Zn ratio in precursor varied to control initial Fe content (1, 2.5, 5, and 7.5% Fe in precursors)

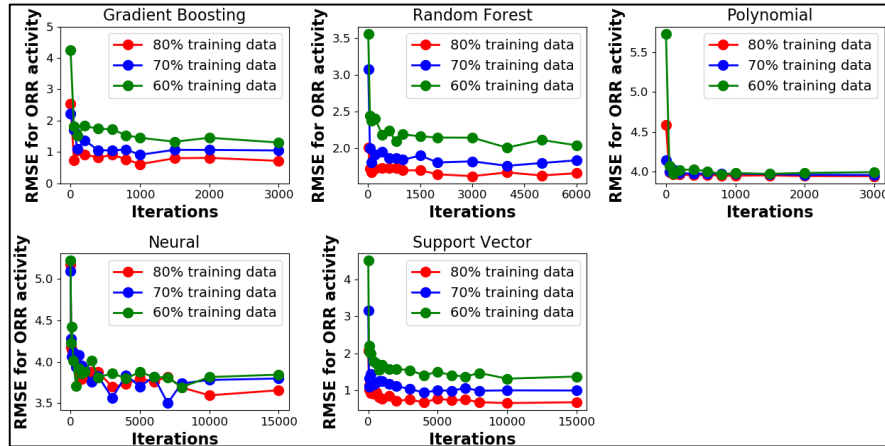


Data Used to Build Surrogate Model

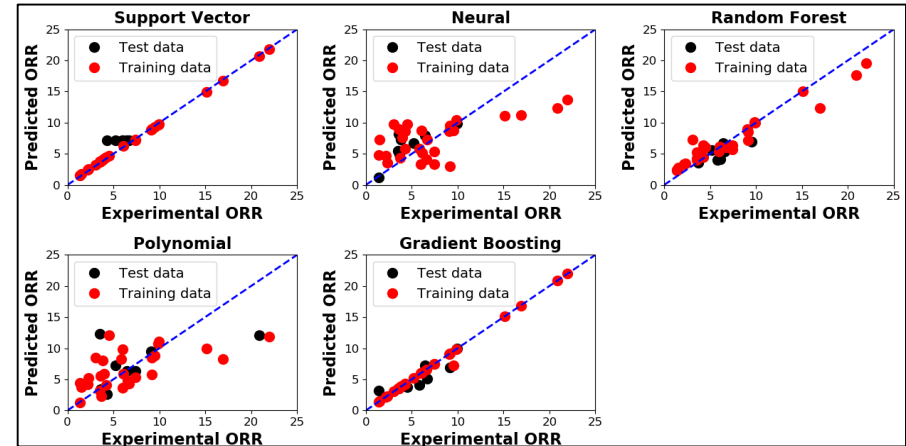


Enhancing Activity & Durability: Prediction Accuracy & Error Analysis

Root-mean square error (RMSE) for different regression training methods



Accuracy Test: Prediction vs. experimental data for different regression methods



METHODOLOGY

- Step 1:** Randomly select 60-80% data as “training set” and build surrogate model
- Step 2:** Use this surrogate model to predict ORR on 40-20% “test set” and estimate RMS error comparing predicted and experimental ORR values
- Step 3:** Repeat Step 1 and Step 2 until the RMS error converges to a minimum value

Highlight: Machine learning-based surrogate model method accurately predicting the RR ORR activity for high-throughput data set with low mean average percent error, MAPE, using gradient boosting regression and support vector regression

ML Algorithm	MAPE (%)
Gradient Boosting	4.47
Support Vector	6.87
Neural	45.04
Random Forest	34.97
Polynomial	58.68

$$MAPE = \frac{100}{n} \sum_{i=1}^n \frac{|Y_i - Y'_i|}{Y_i}$$

MAPE = Mean Absolute Percent Error

Y_i = Experimental ORR

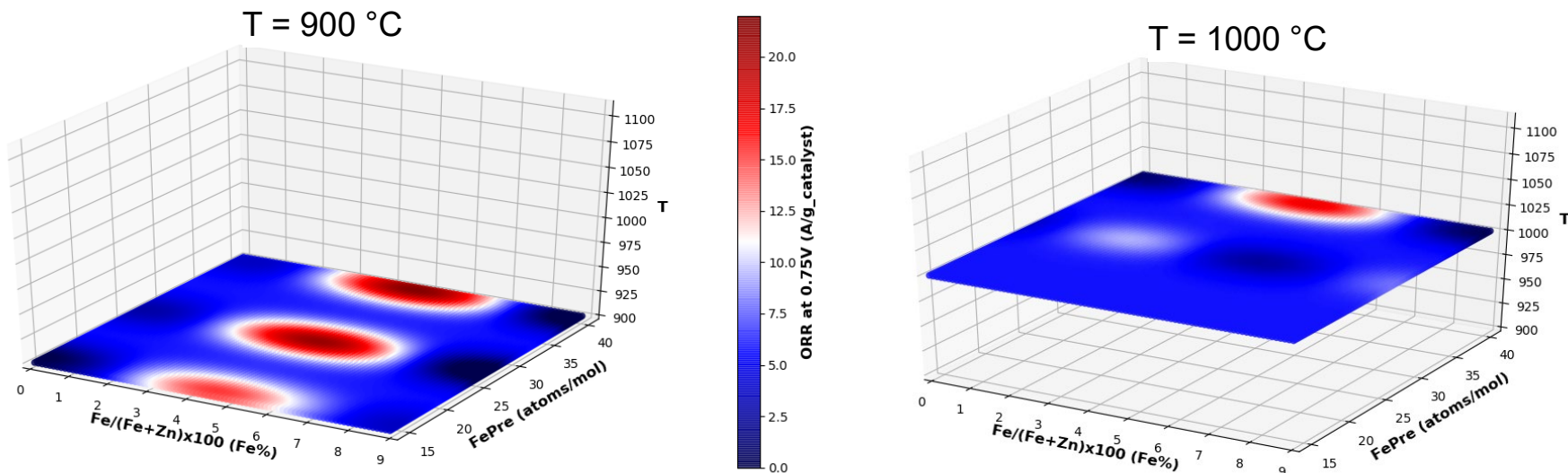
Y'_i = Predicted ORR

n = number of samples

Karim *et al.*, submitted

Enhancing Activity & Durability: Surrogate Model Application

Example heat maps from optimized support vector regression approach at two temperatures



Validation: Catalyst from Follow-up Synthesis

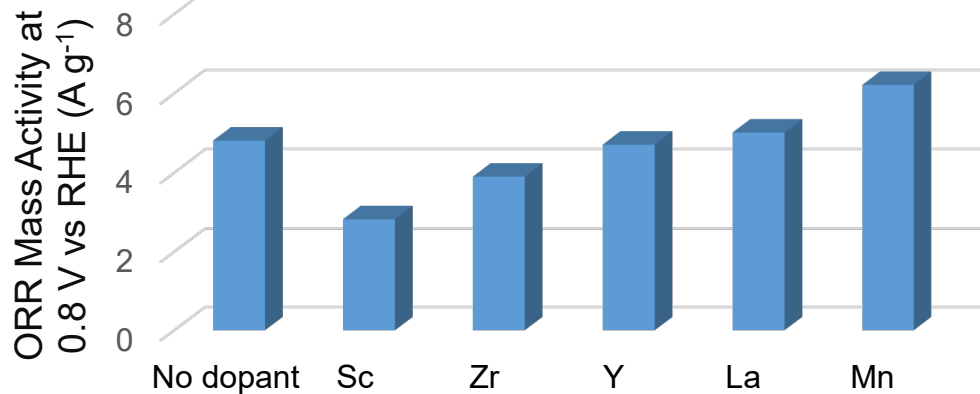
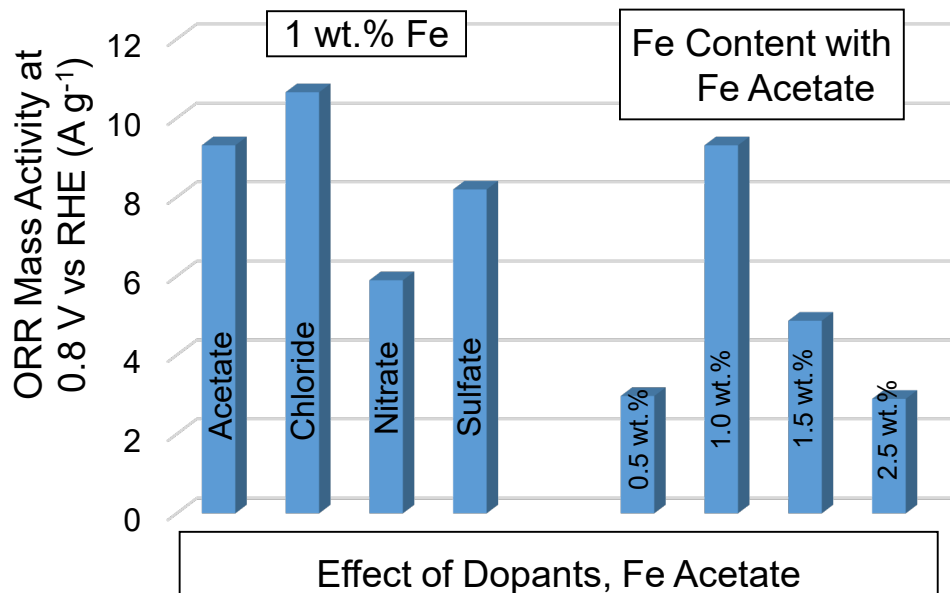
Fe/(Fe+Zn)×100%	Fe Precursor (atoms/molecule)	Heat-Treatment Temperature	ORR Activity at 0.75 V
4.8(%)	FeN (40)	900 °C	30.3 A/g

Highlight: Synthesis under conditions derived from machine learning resulted in **~36% activity improvement** over previous best catalyst

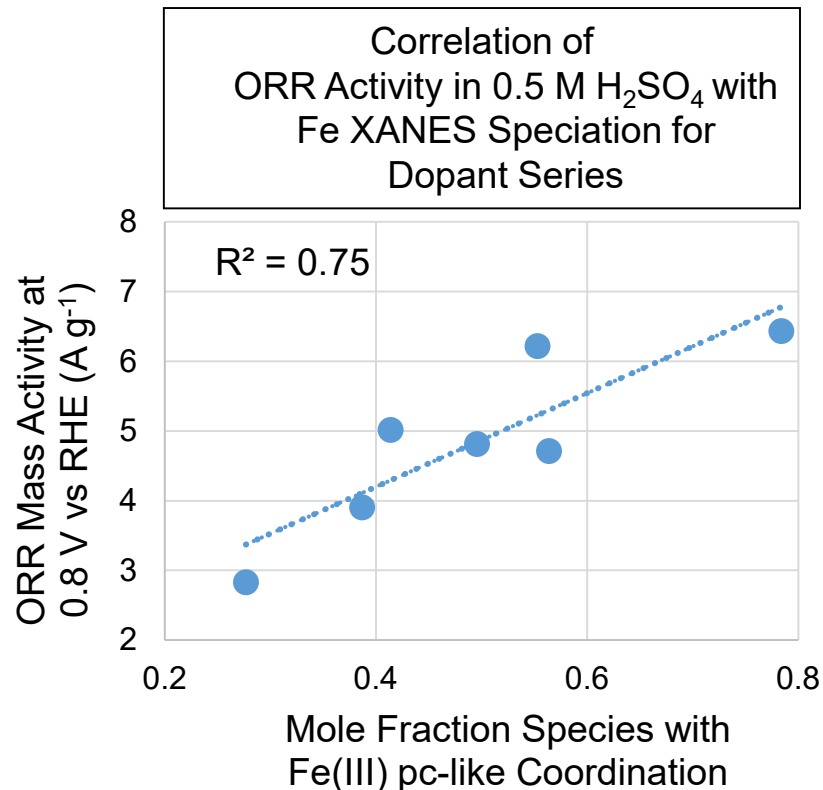
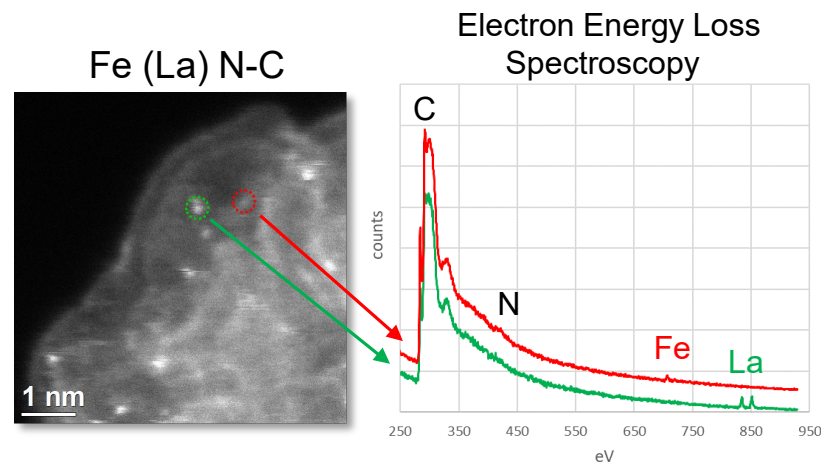
- **Fe/(Fe+Zn)×100%** – at.% of Fe versus the sum of Fe and Zn
- **Fe Precursor** – FeS, FeN or FeAc (atoms/molecule)
- **T** – heat-treatment temperature (in °C)
- Color bar-mapped with target function of ORR activity per gram of catalyst at 0.75 V (A/g)

Karim *et al.*, submitted.

Enhancing Activity & Durability: High-Throughput Synthesis (Catalyst System 3)

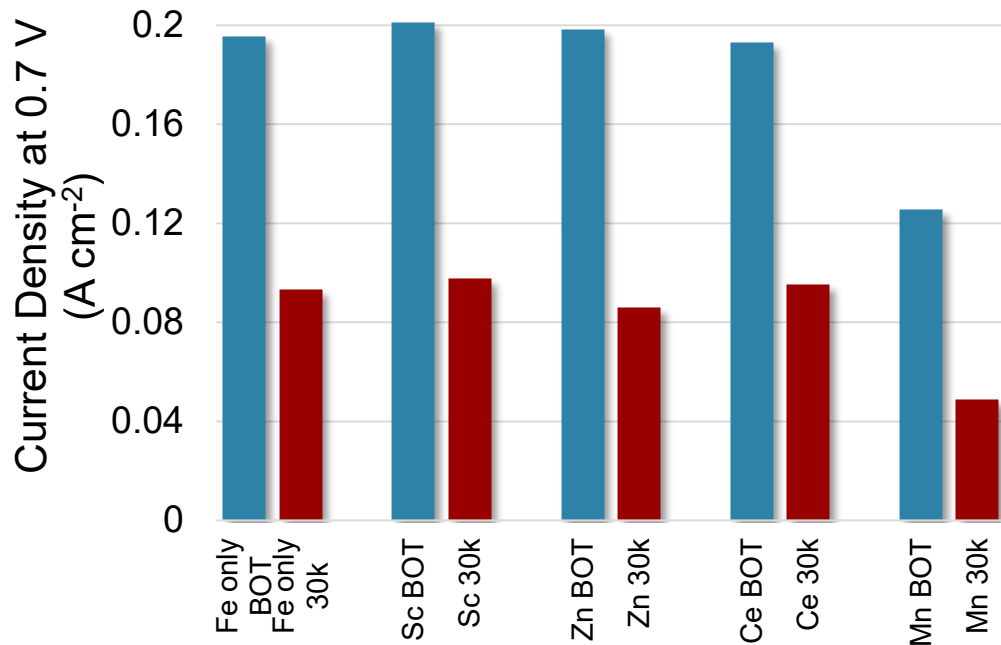


- 1 wt.% Fe content in precursor and Fe acetate and Fe chloride salts in precursor show highest ORR activity
- Dopants affect ORR activity in aqueous electrolyte, correlating with extent of formation of FeN₄-like coordination



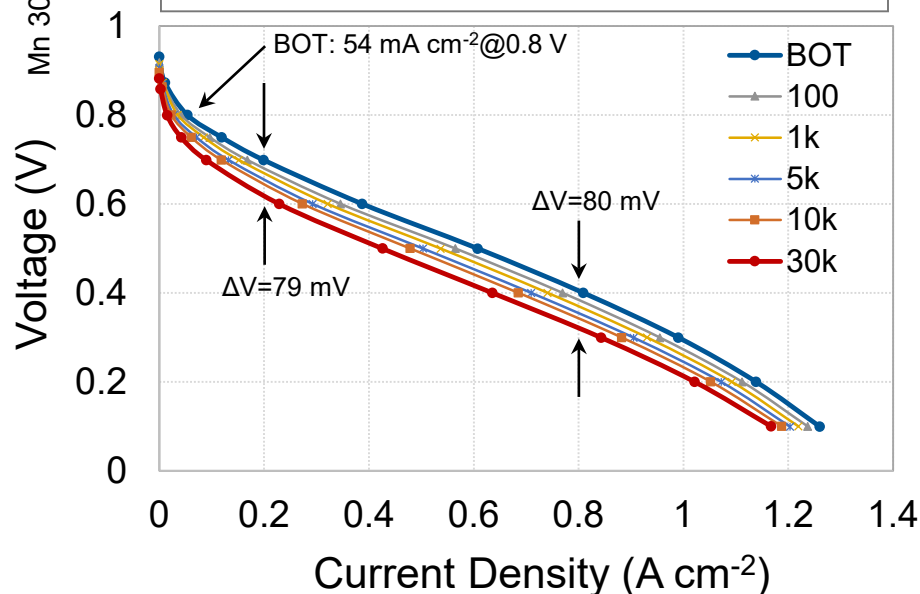
Enhancing Activity & Durability: MEA Performance & Durability (Catalyst System 3)

Anode: 0.2 mg_{Pt} cm⁻² Pt/C H₂, 200 sccm, 1.0 bar H₂ partial pressure; **Cathode:** ~4 mg cm⁻² air, 200 sccm, 1.0 bar air partial pressure; **Membrane:** Nafion®XL; **Cell:** 5 cm²; 80°C



- >50% loss of H₂-air current density observed after 30k AST cycles (0.6 to OCV in air) irrespective of presence of dopant and dopant identity
- Mn-doped catalyst showed significantly worse beginning-of-test (BOT) performance, but highest ORR activity in RDE

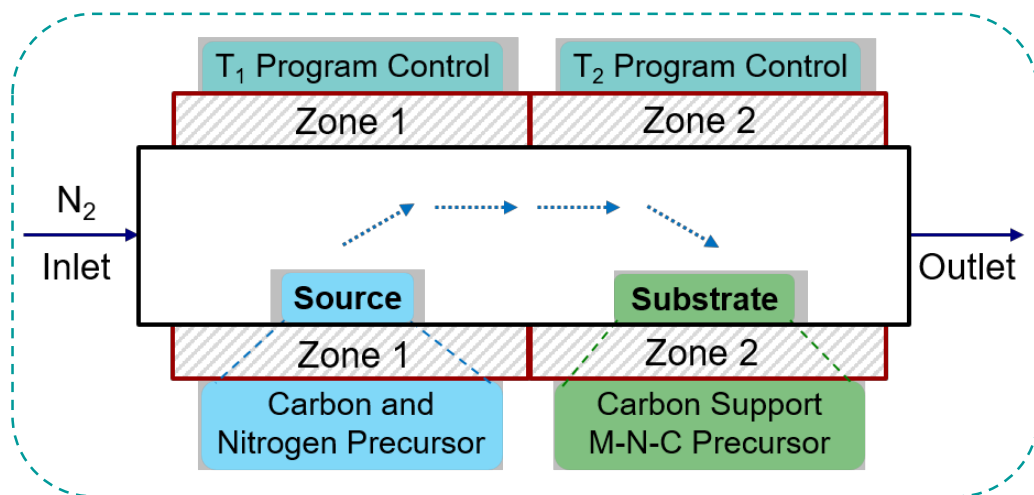
Anode: 0.2 mg_{Pt} cm⁻² Pt/C H₂, 200 sccm, 1.0 bar H₂ partial pressure; **Cathode:** ~4 mg cm⁻² 1 wt.% Fe(N-C), air, 200 sccm, 1.0 bar air partial pressure; **Membrane:** Nafion®211; **Cell:** standard single serpentine 5 cm² flow field; 80 °C. AST: 0.6 V to OCV square wave 3 s hold, in air



- CCM with Fe(N-C) catalyst shows 55% loss in current density at 0.7 V after 30k AST cycles in air
- **Highlight:** ΔV of 79 mV at 200 mA cm⁻² after 30k AST cycles in air **exceeds** FY20 Q2 GPRA QPM
 - ✓ GPRA QPM: 15 mV improvement in ΔV at 200 mA cm⁻² after 30k AST cycles vs baseline ΔV of 100 mV (from round robin task)

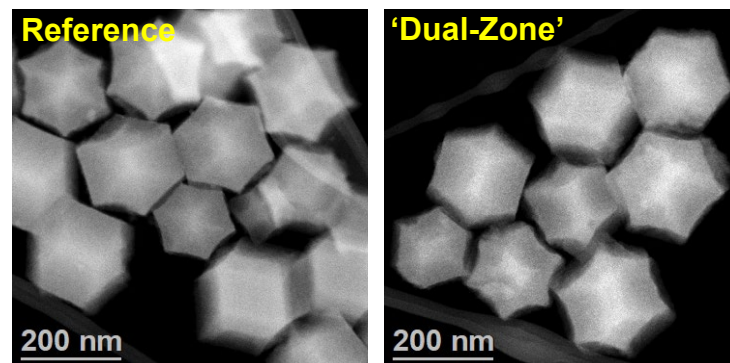
Major Progress in Durability: 'Dual-Zone' Catalyst Synthesis & Characterization

'Dual-Zone' Chemical Vapor Deposition Setup



- Precise temperature control of both furnace zones during evaporation of source precursors and deposition onto substrate
- Carbon-phase in the substrate in Zone 2 modified via deposition of carbon species and nitrogen precursors, e.g., cyanamide, from Zone 1
- Approach resulting in seemingly more robust carbon structure in of PGM-free catalyst in Zone 2 and much improved durability of thus-obtained 'dual-zone' catalyst

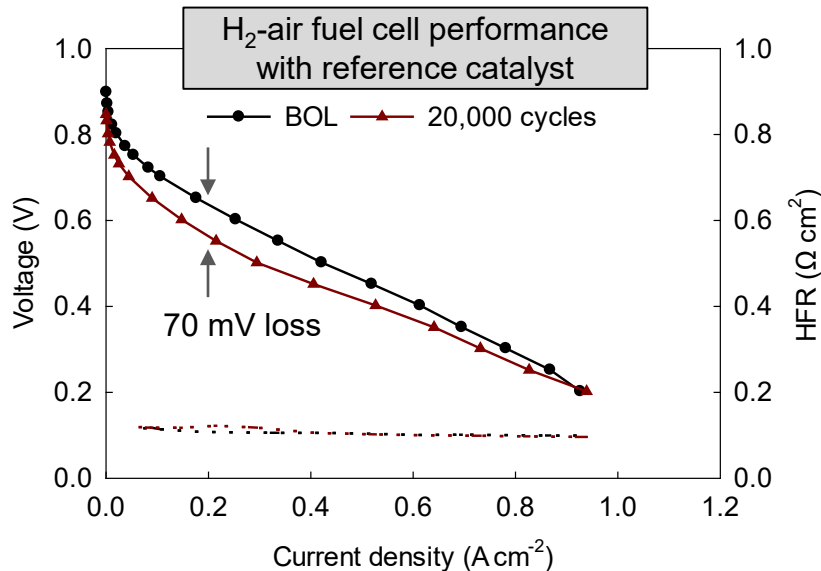
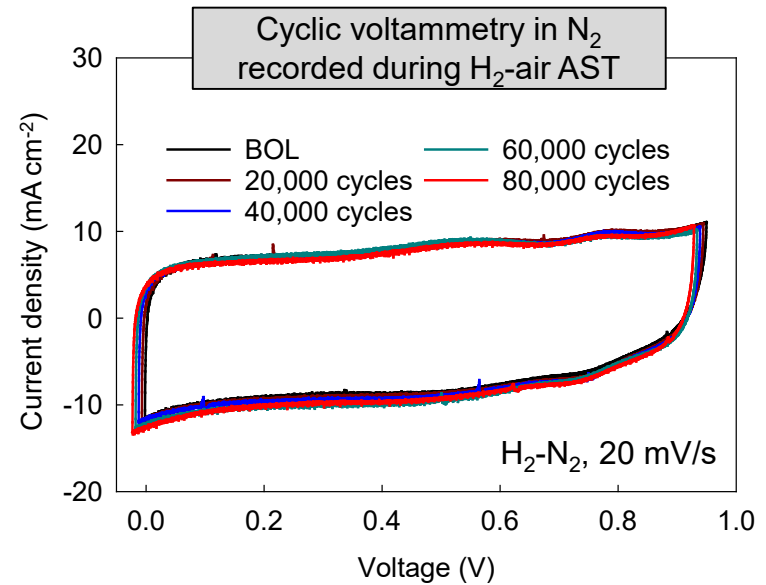
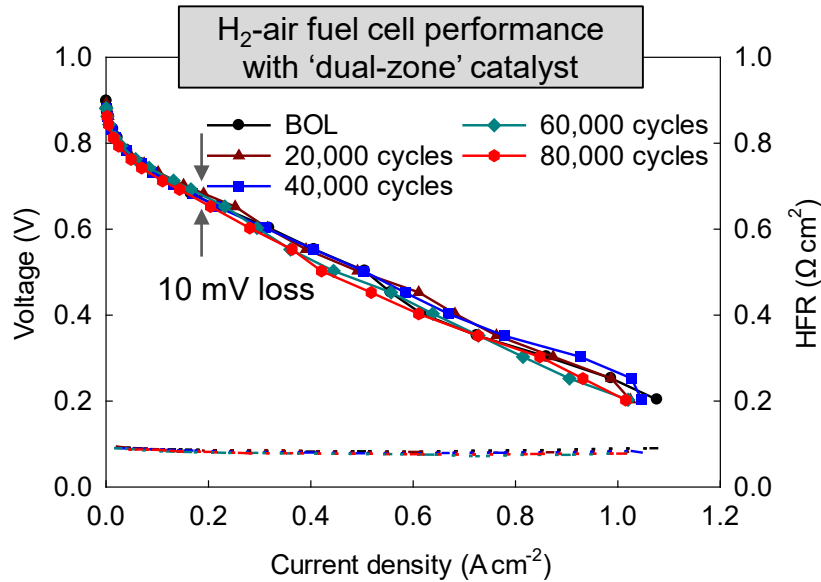
Reference vs. 'Dual-Zone' Catalyst



Name	Reference B.E.	at. %	'Dual-Zone' B.E.	at. %
C (sp ²)	284.6	77.7	284.5	81.1
C (sp ³ /C-N)	285.8	10.1	285.8	8.4
C (C=O)	287.5	3.0	287.4	2.9
C (O=C-O)	289.0	1.6	288.8	1.5
O (O=C)	532.2	4.4	532.1	3.5
N (pyrid)	398.6	1.1	398.5	0.9
N (pyrrol)	400.9	1.2	400.9	1.2
N (O-N)	402.6	0.4	402.8	0.3
Fe	710.7	0.2	710.3	0.2
Zn	1021.6	0.2	1021.3	0.1
Na	1072.1	0.1	1071.1	0.0

Major Progress in Catalyst Durability: AST of 'Dual-Zone' Catalyst

Anode: 0.3 mg_{Pt} cm⁻² Pt/C; H₂: 1.0 bar partial pressure and 700 sccm; 100% RH. **Cathode:** ~ 4 mg/cm² 'dual-zone' catalysts catalyst; air: 1.0 bar O₂+N₂ and 1700 sccm; 100% RH. **Membrane:** Nafion®211. **Cell:** differential cell with 5 cm² electrode area. **Cell temperature:** 80 °C.



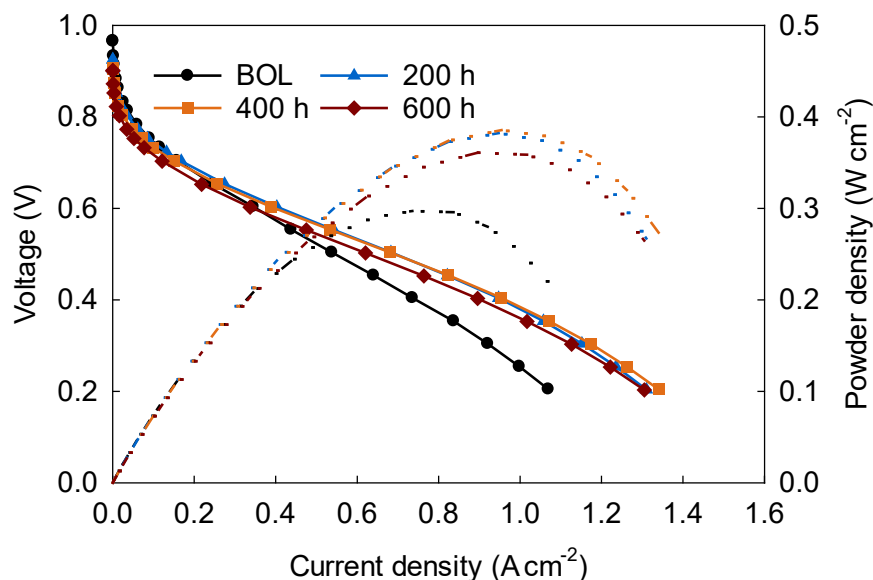
Catalyst	Voltage loss at 200 mA/cm ²	Number of cycles
'Dual-Zone' catalyst	10 mV	80,000
LANL "round-robin" catalyst	100 mV	30,000
LANL reference catalyst	70 mV	20,000

- Highlight:** Excellent durability achieved with 'dual-zone' catalyst for up to 80,000 AST cycles in H₂-air fuel cell (~0.12 μV/cycle loss at 0.2 A/cm²)
- No change seen in double-layer charging current
- Significant degradation of the reference catalyst after only 20,000 AST cycles (test ongoing)

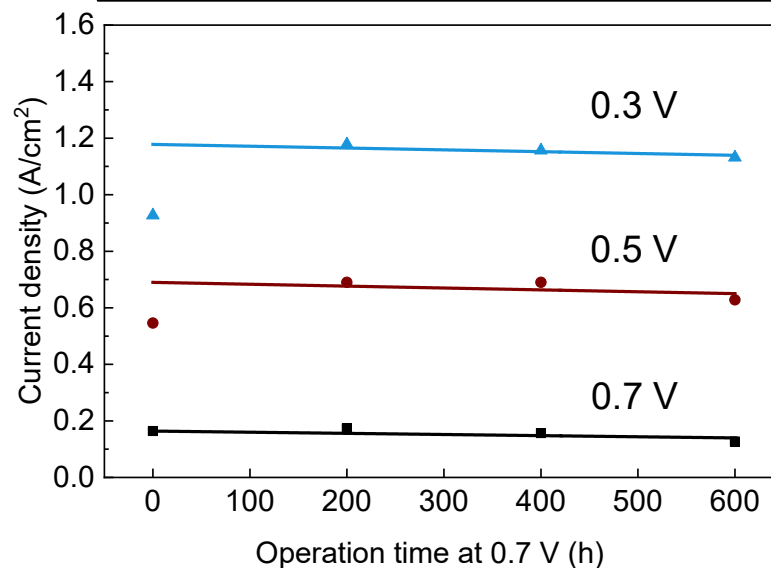
Enhancing Activity & Durability: 'Dual-Zone' Catalyst – Life Test at 0.7 V (H₂-Air)

Anode: 0.3 mg_{Pt} cm⁻² Pt/C; H₂: 1.0 bar partial pressure and 700 sccm; 100% RH. **Cathode:** ~ 4 mg/cm² 'dual-zone' catalyst; air: 1.0 bar O₂+N₂ and 1700 sccm; 100% RH. **Membrane:** Nafion®.211. **Cell:** differential cell with 5 cm² electrode area. **Cell temperature:** 80 °C.

H₂-air fuel cell performance recorded at different times of life test at 0.7 V



Current density recorded at selected cell voltages during life test at 0.7 V



- **Highlight:** Much improved fuel cell durability accomplished during constant-voltage test with 'dual-zone' catalyst than with conventional PGM-free catalysts
- 70% of the original performance at 0.7 V retained after a 600-hour life test
- Only slight degradation in H₂-air fuel cell polarization curves after 600 hours

Remaining Challenges and Barriers

- Much improved, but still inadequate durability of PGM-free cathodes under steady-state and load-cycling conditions, as well as under AST cycling in air
- Improved, but still inadequate understanding of the catalyst and electrode degradation mechanism(s) making development of mitigation strategies more challenging
- Low density of active sites and oxygen reduction reaction turnover frequency (TOF) leading to H₂-Air performance below DOE targets
- Limited materials and synthesis approaches for increasing active site density without forming spectator species (e.g., metal and metal carbide clusters)
- Electrode design targeting thick electrodes, which may still be required in spite of expected further activity improvements in ORR activity of PGM-free catalysts

Proposed Future Work

- **ElectroCat Development**

- ✓ Populate ElectroCat DataHub with published data and publicly publish the datasets to the Materials Data Facility (<https://materialsdatafacility.org/>)

- **Improvement in Performance and Durability of Catalysts and Electrodes**

- ✓ Expand probe molecule studies to degraded catalysts; implement selective desorption of probe molecule; couple with ORR activity and FTIR characterization to determine adsorption sites of probe molecule
- ✓ Further identify primary factors governing the durability of PGM-free catalysts and electrodes and continue to develop means to prevent performance degradation
- ✓ Advance performance of catalysts by maximizing volumetric density and accessibility of active sites, through alternative synthetic methods
 - Complete construction of dual-zone vertical furnace with rapid cooling capability and utilize furnace to synthesize catalysts from precursors with higher Fe content
- ✓ Optimize the fuel cell performance of the Fe (N-C) catalyst (from high-throughput system 3) by subjecting it to high-throughput ink optimization, cell testing, and associated ink characterization and cell diagnostics
- ✓ Scale-up synthesis of Fe (N-C) catalyst (from system 3) and subject it to AST cycles in air in differential cell hardware with pre- and post-test characterization to understand degradation mechanism and source of improved durability
- ✓ Subject “dual-zone” catalyst to round-robin testing and pre- and post-test characterization to understand mechanism of improved durability

Any proposed future work is subject to change based on funding levels

Accomplishments and Progress: Summary

• ElectroCat Development and Communication

- ✓ Consortium is supporting ten FOA/Lab Call projects with ten capabilities
- ✓ Consortium-wide meetings were held on August 13-14, 2019 and January 13-14, 2020 to kick off new FOA projects. Protocol and consortium information distributed to consortium members; select information available through public website and data management hub (electrocat.org; <https://datahub.electrocat.org>)
- ✓ Disseminated accelerated stress test protocols to U.S. and international research communities in more than 10 presentations
- ✓ 16 papers published, 39 presentations given (24 invited), 1 patent issued, 1 patent application and 4 invention disclosures submitted

• Progress in Performance and Performance Durability

- ✓ ElectroCat FY19 Annual Milestone of PGM-free cathode MEA performance of 29 mA cm^{-2} at 0.90 V (H_2/O_2 , iR -free, average of three consecutive pol curves) exceeded: 30 mA cm^{-2}
- ✓ Six-fold improvement of the H_2 -air fuel cell performance at 0.80 V of an atomically-dispersed catalyst, from 9 mA cm^{-2} to 54 mA cm^{-2} since 2017 AMR
- ✓ Exceeded FY20 Q3 hydrogen-air fuel cell performance durability quarterly progress measure (15 mV improvement in loss): Voltage degradation at 200 mA cm^{-2} of 79 mV after 30k AST cycles for Fe(N-C) catalyst and 10 mV after 80k AST cycles for “dual-zone” catalyst versus 100 mV for baseline “round robin” catalyst
- ✓ Synthesized over 50 unique catalysts using high-throughput approach, with > 20% enhancement in ORR activity ($\text{H}_2\text{-O}_2$ at 0.8 V) and > 30% performance improvement (H_2 -air at 0.7 V) versus ElectroCat baseline ZIF catalyst

- **Characterization and Capability Development**

- ✓ Determined ORR turnover frequency of $1.1 \text{ e}^- \text{ site}^{-1} \text{ s}^{-1}$ on (AD)Fe-N-C using gas-phase NO probe
- ✓ Combined *in situ* EXAFS and Mössbauer spectroscopy results to determine speciation of Fe as a function of potential and dissolving species
- ✓ Determined dominant degradation mechanisms of (AD)Fe-N-C catalyst in MEA under H₂-air constant voltage holds
- ✓ Developed 4D-STEM technique for achieving atomic resolution at lower, less damaging electron beam energy (30 keV)
- ✓ Further developed segmented cell capability for simultaneous differential condition testing of 6 to 12 catalysts/electrodes combinations
- ✓ Developed hydrogen limiting current electrode construction and method for determining gas phase transport resistance of electrodes
- ✓ Established and disseminated an accelerated stress test and polarization curve protocol and verified protocol in “round robin” testing at three national laboratories

- **ORR active-site modeling**

- ✓ Determined that metal speciation and ligation state play important roles in dissolution of metals from active sites
- ✓ Identified new structure with simultaneously high ORR activity and dissolution tolerance

Reviewers' Comments from 2019 Annual Merit Review

- *“Much more focus needs to be placed on durability in the immediate term.” “At this stage of the project, additional expertise is required [...] on degradation.” “Additional work on durability, and articulating whether this class of catalysts may ever have sufficient durability, is encouraged.” “The focus should be only two areas: determining the degradation mechanism and whether it can be prevented. Any other area is a waste of funding.” “To date, the progress made toward addressing durability appears to be modest.” “More work should be done on understanding the degradation mechanism and whether it can be prevented.” “If this catalyst cannot be stabilized, alternative processes need to be identified.” “The project should focus on degradation.” “The fundamental mechanism responsibility for the losses in the kinetic region need to be identified.”*

Much of the previous year's effort was focused on activity loss including:

- ✓ New experimental and theoretical insights regarding possible degradation pathways and understanding of how multiple mechanisms may be linked (explaining much of the confusion regarding potential dependence for activity loss)
- ✓ Identification of how synthesis can be modified to achieve higher stability
- ✓ Developing alternative synthesis routes and materials with better durability
- *“Machine learning and high-throughput catalyst development has additional relevance but may not be as goal oriented as the key performance indicators.”*

As demonstrated by the initial generation of catalysts (slides 31-33), we believe that collaborative and novel approach combining high-throughput catalyst synthesis with machine learning is capable of furthering ORR activity and, possibly, catalyst durability.

- *“There is a nice combination of theory, analysis, and experimental and synthetic work. The project aims to develop advanced PGM-free catalysts and electrodes.”*

We have actively worked to maintain this integrated approach within the consortium, across labs and FOA partners.

- *“More modeling work would be useful to guide the work on electrode structure.” “It appears that the team is depending mostly on electrospun electrodes to provide improved mass transport and high-current-density performance. However, no indication was provided on feasibility or the rationale behind those expectations.”*

We are modeling the transport properties of electrodes based on structures and component distributions determined using TEM and nano-CT. We are also studying the effect of ink solvent, mixing method, and ionomer to catalyst ratio on the break-up of catalyst agglomerates and on the resulting structure of the electrodes. The fundamental understanding of the impact of ink composition on structure provide us with the tools to modify the electrode structure to improve transport properties. The use of ink composition, electrospinning, and alternative ink deposition methods are only some of the methods we are using to improve the high current density performance.



PGM-free catalyst development, electrochemical and fuel cell testing, atomic-scale modeling

Piotr Zelenay (PI), Hoon Chung, Hanguang Zhang, Ted Holby, Towfiq Ahmed, Mohammad Rezaul Karim, Xi Yin, Siddharth Komini Babu, Bianca Ceballos, Burak Koyotürk, Vijay Bhooshan Kumar, Ulises Martinez, Gerie Purdy, John Weiss



High-throughput techniques, mesoscale models, X-ray studies, aqueous stability studies

Debbie Myers (PI), Jaehyung Park, Magali Ferrandon, Nancy Kariuki, Ahmed Farghaly, Ted Krause, Evan Wegener, Jeremy Kropf, Josh Wright, Rajesh Ahluwalia, Xiaohua Wang, Firat Cetinbas, Voja Stamenkovic, Haifeng Lv, Pietro Papa Lopes, Ben Blaiszik, Marcus Schwarting



Advanced fuel cell characterization, rheology and ink characterization, segmented cell studies

K.C. Neyerlin (PI), Luigi Osmieri, Guanxiong Wang, Hao Wang, Sadia Kabir, Scott Mauger, Guido Bender, Michael Ulsh, Sunil Khandavalli, Kristin Munch, Courtney Pailing



Advanced electron microscopy, atomic-level characterization, XPS studies

David Cullen (PI), Michael Zachman, Shawn Reeves, Harry Meyer, Haoran Yu, Karren More

Publications (since 2019 AMR presentation submission)

1. "Preparation of Non-precious Metal Electrocatalysts for the Reduction of Oxygen Using a Low-Temperature Sacrificial Metal;" T. Al-Zoubi, Y. Zhou, X. Yin, B. Janicek, C.-J. Sun, C. Schulz, X. Zhang, A. Gewirth, P. Huang, P. Zelenay, H. Yang, *J. Am. Chem. Soc.*, **142** (12), 5477-5481 (2020).
2. "Evolution Pathway from Iron Compounds to Fe₁(II)-N₄ Sites through Gas-Phase Iron during Pyrolysis;" J. Li, L. Jiao, E. Wegener, L. L. Richard, El Liu, A. Zitolo, M. T. Sougrati, S. Mukerjee, Z. Zhao, Y. Huang, F. Yang, S. Zhong, H. Xu. A. J. Kropf, F. Jaouen, D. J. Myers, Q. Jia, *J. Am. Chem. Soc.*, **142**, 1417-1423 (2020).
3. "Mass transport characterization of platinum group metal-free polymer electrolyte fuel cell electrodes using a differential cell with an integrated electrochemical sensor;" A. G. Star, G. Wang, S. Medina, S. Pylypenko, K.C. Neyerlin, *J. Power Sources*, **450** (29), 227655 (2020).
4. "Elucidating the role of ionomer in the performance of platinum group metal-free catalyst layer via in situ electrochemical diagnostics;" G. Wang, L. Osmieri, A. G. Star, J. Pfeilsticker, K.C. Neyerlin, *J. Electrochem. Soc.*, **167**, 044519 (2020).
5. "Use of a segmented cell for the combinatorial development of platinum group metal-free electrodes for polymer electrolyte fuel cells;" L. Osmieri, S. Mauger, M. Ulsh, K.C. Neyerlin, G. Bender, *J. Power Sources*, **452** 227829 (2020).
6. "Thermally Driven Structure and Performance Evolution of Atomically Dispersed FeN₄ Sites for Oxygen Reduction;" J. Li, H. Zhang, W. Samarakoon, W. Shan, D. A. Cullen, S. K., M. Chen, D. Gu, K. L. More, G. Wang, Z. Feng, Z. Wang, G. Wu, *Angew. Chem. Int. Ed.*, **59**, 18971-18980 (2019).
7. "Heat-Treated Iron Porphyrin Aerogels for Oxygen Reduction Reaction;" N. Zion, D. A. Cullen, P. Zelenay, L. Elbaz, *Angew. Chem. Int. Ed.*, **58**, 2-9 (2019).
8. "2,2'-Dipyridylamine as Heterogeneous Organic Molecular Electrocatalyst for Two-Electron Oxygen Reduction Reaction in Acid Media;" X. Yin, L. Lin, U. Martinez, P. Zelenay*, *ACS Appl. Energy Mater.*, **2**, 7272-7278 (2019).

Publications II

9. “Resolving Active Sites in Atomically Dispersed Electrocatalysts for Energy Conversion Applications;” D. A. Cullen, K. L. More, K. C. Neyerlin, H. T. Chung, P. Zelenay, D. Myers, *Microsc. Microanal.*, **25** S2 2066-2067 (2019).
10. “Elucidation of Fe-N-C electrocatalyst active site functionality via in-situ X-ray absorption and operando determination of oxygen reduction reaction kinetics in a PEFC;” L. Osmieri, R. K. Ahluwalia, X. Wang, H. T. Chung, X. Yin, A. J. Kropf, J. Park, D. A. Cullen, K. L. More, P. Zelenay, D. J. Myers, K. C. Neyerlin, *Appl. Catal., B*, article 117929, **257** 2019.
11. “Atomically Dispersed Iron Catalysts for Polymer Electrolyte Fuel Cells;” H. Zhang, H. T. Chung, D. A. Cullen, S. Wagner, U. I. Kramm, K. L. More, P. Zelenay, G. Wu, *Energy Environ. Sci.*, **12**, 2548-2558 (2019).
12. “Highly active atomically dispersed CoN₄ fuel cell cathode catalysts derived from surfactant-assisted MOFs: carbon-shell confinement strategy;” Y. He, S. Hwang, D. A. Cullen, M. A. Uddin, L. Langhorst, B. Li, S. Karakalos, A. J. Kropf, E. C. Wegener, J. Sokolowski, M. Chen, D. Myers, D. Su, K. L. More, G. Wang, S. Litster, G. Wu, *Energy Environ. Sci.*, **12**, 250-260 (2019).
13. “PGM-free ORR catalysts designed by templating PANI-type polymers containing functional groups with high affinity to iron;” X. Yin, H. T. Chung, U. Martinez, L. Lin, K. Artyushkova, P. Zelenay, *J. Electrochem. Soc.*, **166** (7), F3240-F3245, 2019.
14. “Experimental and Theoretical Trends of PGM-free Electrocatalysts for the Oxygen Reduction Reaction with Different Transition Metals;” U. Martinez, E. F. Holby, S. Komini Babu, K. Artyushkova, L. Lin, S. Choudhury, P. Zelenay, *J. Electrochem. Soc.*, **166** (7), F3136-F3142 2019.
15. “Performance of Polymer Electrolyte Fuel Cell Electrodes with Atomically Dispersed (AD) Fe-C-N ORR Catalyst;” R. K. Ahluwalia, X. Wang, L. Osmieri, J-K Peng, H. T. Chung, and K. C. Neyerlin, *J. Electrochem. Soc.*, **166** F1096-F1104 (2019).
16. “Nitrogen-Doped Graphene Oxide Electrocatalysts for the Oxygen Reduction Reaction;” J. H. Dumont, U. Martinez, K. Artyushkova, G. M. Purdy, A. M. Dattelbaum, P. Zelenay, A. Mohite, P. Atanassov, G. Gupta, *ACS Appl. Nano Mater.*, **2**, 1675-1682, 2019.

Presentations (since 2019 AMR presentation submission)

1. University of Cincinnati Department of Chemistry Colloquium, Cincinnati, Ohio, February 21, 2020. Title: "New opportunities and challenges for hydrogen fuel cells;" D. A. Cullen (**invited lecture**).
2. Telluride Science Research Center (TRSC) Workshop, Platinum Group Metal-free Electrocatalysts: Small Molecules Activation and Conversion, January 21-24, 2020. Title: "PGM-free Electrocatalysis at Crossroads: How to Assure Much Needed Progress?" P. Zelenay (**invited lecture**).
3. Giner Inc. Newton, Massachusetts, December 22, 2019. Title: "Atomic-level insights into fuel cell catalysts;" D. A. Cullen (**invited lecture**).
4. CNMS Seminar Series, Oak Ridge, Tennessee, December 11, 2019. Title: "Atomic-level insights into the next generation of fuel cell catalysts;" D. A. Cullen (**invited lecture**).
5. Royal Institute of Technology (KTH), School of Engineering Sciences in Chemistry, Biotechnology and Health, Stockholm, Sweden, November 4, 2019. Title: "Oxygen Reduction Reaction on Fe-derived Platinum Group Metal-Free Electrocatalysts;" P. Zelenay (**invited lecture**).
6. 4th Israeli Fuel Cell Consortium Workshop, Tel Aviv-Haifa, Israel, October 28-31, 2019. Title: "Durability of Platinum Group Metal-Free Catalysts for Oxygen Reduction: A Formidable Challenge;" P. Zelenay (**invited lecture**).
7. AVS 66th International Symposium & Exhibition. Columbus, Columbus, Ohio, October 20-25, 2019. Title: "Enabling hydrogen as an energy carrier through analytical electron microscopy;" D. A. Cullen (**invited lecture**).
8. 236th Meeting of the Electrochemical Society, Atlanta, Georgia, October 13-17, 2019. Title: "Electrochemical Characterization Methods of Fe-Based Oxygen Reduction Reaction Electrocatalysts for Polymer Electrolyte Fuel Cells;" J. Park, M. Ferrandon, D. J. Myers, H. T. Chung, S. Komini Babu, P. Zelenay.
9. 236th Meeting of the Electrochemical Society, Atlanta, Georgia, October 13-17, 2019. Title: "Nuclear Resonance Vibration Spectroscopy Study of 57-Fe-Enriched Atomically Dispersed (AD)Fe-N-C Oxygen Reduction Reaction Catalyst for Polymer Electrolyte Fuel Cells;" H. Chung*, J. Park, N. Kariuki, J. Zhao, D. Cullen, K. More, D. Myers, E. Alp, P. Zelenay.

Presentations II

10. 236th Meeting of the Electrochemical Society, Atlanta, Georgia, October 13-17, 2019. Title: “Activity and Composition of Fe-Based Oxygen Reduction Reaction Electrocatalysts Synthesized and Characterized Using High-Throughput Approaches” D. J. Myers, M. Ferrandon, J. Park, H. Lv, V. R. Stamenkovic, A. J. Kropf, E. C. Wegener.
11. 236th Meeting of the Electrochemical Society, Atlanta, Georgia, October 13-17, 2019. Title: “Layered PGM-Free Electrode for Improved Mass Transport;” S. Komini Babu*, X. Yin, U. Martinez, D. Cullen, G. Purdy, P. Zelenay.
12. 236th Meeting of the Electrochemical Society, Atlanta, Georgia, October 13-17, 2019. Title: “ElectroCat: Expediting PGM-Free Fuel Cell Catalyst and Electrode Development;” D. Papageorgopoulos, S. Thompson, D. Myers, K. More, K. C. Neyerlin, P. Zelenay (**invited lecture**).
13. UTSI MABE Departmental Series Seminar, Tullahoma, Tennessee, October 9, 2019. Title: “Accelerated Catalyst Development for the Emerging Hydrogen Economy;” D.A. Cullen (**invited lecture**).
14. Advanced Photon Source Upgrade (APS-U) Workshop, Catalysis Research at APS-U, Lemont, IL, October 4, 2019. Title: “X-ray Absorption, Scattering, Tomography, and Nuclear Resonance Vibrational Spectroscopy Studies of Platinum Group Metal-free Oxygen Reduction Reaction Catalysts and Electrodes.” D. Myers (presenter), A.J. Kropf, J. Wright, C. F. Cetinbas, R. Ahluwalia, J. Park, N. Kariuki, A. Farghaly, E. Alp, J. Yang, H. Chung, P. Zelenay (**invited lecture**).
15. Advanced Manufacturing and Characterization of Fuel Cells and Electrolyzers Workshop, University of Connecticut, Storrs, Connecticut, September 23-24, 2019. Title: “Advanced Microscopy Methods to Interrogate Materials and Interfaces in Fuel Cell Catalyst Layers;” K. L. More (**invited lecture**).
16. Electrolysis and Fuel Cells Discussions (EFCD 2019), La Grande Motte, France, September 15-18, 2019. Title: “Platinum Group Metal-Free Catalysts for Oxygen Reduction: State of the Art, Mechanistic Insights, and Challenges;” P. Zelenay, H. T. Chung, E. F. Holby, U. Martinez, S. Komini Babu, V. Bhooshan Ramani, X. Yin (**invited keynote lecture**).
17. 257th ACS National Meeting & Exposition, San Diego, California, August 25-29, 2019. Title: “Understanding Electrode Design and Degradation in Fuel Cells;” D. A. Cullen, K. L. More (**invited lecture**).

Presentations III

18. University of Padua, Department of Industrial Engineering, Padua, Italy, August 2, 2019. Title: “Electrocatalysis at Noble Metal-free Materials. Part II: (a) Test protocols for platinum group metal-free ORR catalysts; (b) Molecular catalysts for hydrogen evolution and two-electron oxygen reduction;” P. Zelenay (**invited lecture**).
19. University of Padua, Department of Industrial Engineering, Padua, Italy, July 31, 2019. Title: “Electrocatalysis at Noble Metal-free Materials Part I: “Progress in Performance and Understanding of the Mechanism of Oxygen Reduction Reaction (ORR);” P. Zelenay (**invited lecture**).
20. European Fuel Cells Forum, Lucerne, Switzerland, July 2-5, 2019. Title: “Platinum Group Metal-free Electrocatalysts for Fuel Cell Applications;” X. Yin, H. T. Chung, S. Komini Babu, U. Martinez, G. M. Purdy, E. F. Holby, P. Zelenay (**invited lecture**).
21. First Telluride Science Research Center (TSRC) Workshop on PGM-free Electrocatalysis, Telluride, Colorado, June 24-29, 2019. Title: “PGM-free Catalyst Durability (or lack of thereof);” P. Zelenay (**invited lecture**).
22. First Telluride Science Research Center (TSRC) Workshop on PGM-free Electrocatalysis, Telluride, Colorado, June 24-29, 2019. Title: “*In Situ* and Operando Characterization of PGM-free Electrodes via Electrochemical Diagnostics;” K. C. Neyerlin (**invited lecture**).
23. First Telluride Science Research Center (TSRC) Workshop on PGM-free Electrocatalysis, Telluride, Colorado, June 24-29, 2019. Title: “Atomic-level insights into platinum group metal-free electrocatalysts derived from metal organic frameworks;” D. A. Cullen (**invited lecture**).
24. 235th Meeting of the Electrochemical Society, Dallas, Texas, May 26-30, 2019. Title: “Structure-Activity Data Mining for Hydrogen Evolution Reaction at Organic Molecular Electrocatalysts;” X. Yin, E. F. Holby, P. Zelenay.
25. 235th Meeting of the Electrochemical Society, Dallas, Texas, May 26-30, 2019. Title: “High-Throughput Synthesis and Characterization of PGM-Free PEFC Cathode Catalysts”, J. Park, M. Ferrandon, E. Coleman, N. N. Kariuki, V. R. Stamenkovic, D. J. Myers.
26. 235th Meeting of the Electrochemical Society, Dallas, Texas, May 26-30, 2019. Title: “Precious Metal-Free Electrocatalysis: Accomplishments and Challenges;” P. Zelenay (**invited lecture**).

Presentations IV

27. 235th Meeting of the Electrochemical Society, Dallas, Texas, May 26-30, 2019. Title: “Microstructure Characterization of PGM-Free Catalyst Ink Using in-Situ Ultra Small Angle X-Ray Scattering”, J. Park, N. N. Kariuki, D. J. Myers, H. Zhang, G. Wu.
28. 235th Meeting of the Electrochemical Society, Dallas, Texas, May 26-30, 2019. Title: “*In Situ* Mössbauer and X-Ray Absorption Spectroscopy Studies of Atomically-Dispersed Fe-N-C Oxygen Reduction Reaction Catalysts;” D. J. Myers*, E. E. Alp, H. T. Chung, P. Zelenay, D. E. Brown, W. Bi, H. Mistry, A. J. Kropf, J. Park, N. N. Kariuki, K. L. More, D. A. Cullen.
29. 235th Meeting of the Electrochemical Society, Dallas, Texas, May 26-30, 2019. Title: “Electrode Layer Development and in Situ Diagnostic Characterization in Low Temperature Fuel Cells;” K. C. Neyerlin, T. Van Cleve, G. Wang, A. G. Star, S. Kabir, L. Osmieri, S. Khandavalli, M. Wang, M. Ulsh, S. A. Mauger, S. Medina, S. Pylypenko.
30. 235th Meeting of the Electrochemical Society, Dallas, Texas, May 26-30, 2019. Title: “PGM-Free Electrode Development and Optimization Using H₂ Limiting Current;” G. Wang, A. G. Star, L. Osmieri, K. C. Neyerlin.
31. 235th Meeting of the Electrochemical Society, Dallas, Texas, May 26-30, 2019. Title: “Use of a Segmented Cell for the Development of PGM-Free Cathode Catalyst Layers for Polymer Electrolyte Fuel Cells;” L. Osmieri, S. A. Mauger, E. Klein, M. Ulsh, K. C. Neyerlin, G. Bender.
32. 235th Meeting of the Electrochemical Society, Dallas, Texas, May 26-30, 2019. Title: “On-Line Inductively-Coupled Plasma Mass Spectrometry Characterization of Transition Metal Dissolution in Electrochemical Environments;” D. J. Myers, N. N. Kariuki (**invited lecture**).
33. 235th Meeting of the Electrochemical Society, Dallas, Texas, May 26-30, 2019. Title: “Nuclear Resonance Vibrational Spectroscopy and Mössbauer Spectroscopy Studies of Atomically Dispersed (AD)⁵⁷Fe-N-C Oxygen Reduction Reaction Catalysts for Polymer Electrolyte Fuel Cells; H. T. Chung, E. F. Holby, S. Komini Babu, J. Park, N. N. Kariuki, A. A. Farghaly, J. Zhao, W. Bi, D. A. Cullen, H. M. Meyer, III, E. E. Alp, K. L. More, D. J. Myers, P. Zelenay.

Presentations V

34. 235th Meeting of the Electrochemical Society, Dallas, Texas, May 26-30, 2019. Title: “Electron microscopy study of degradation mechanisms in platinum group metal-free catalysts;” D.A. Cullen, K. L. More, L. Osmieri, K.C. Neyerlin.
35. 235th Meeting of the Electrochemical Society, Dallas, Texas, May 26-30, 2019. Title: “Structure-Function Relationships of PGM-Free ORR Electrocatalysts from Density Functional Theory;” E. F. Holby, U. Martinez, S. Komini Babu, X. Yin, H. T. Chung, P. Zelenay.
36. Cornell Center for Materials Research (CCMR) Symposium on Electrochemical Energy Storage and Conversion, Ithaca, New York, May 22, 2019. Title: “Beyond Platinum Alloy Cathode Catalysts for Polymer Electrolyte Fuel Cells.” D. Myers. (**invited lecture**)
37. 2019 MRS Spring Meeting & Exhibit, Phoenix, Arizona, April 22-26, 2019. Title: “Searching for the Active Site in Carbon-Based Noble Metal-Free Oxygen Reduction Electrocatalysts;” P. Zelenay, S. Komini Babu, H. T. Chung, U. Martinez, X. Yin, G. M. Purdy, E. F. Holby (**invited lecture**).
38. 2019 MRS Spring Meeting & Exhibit, Phoenix, Arizona, April 22-26, 2019. Title: “High-Throughput Synthesis and Characterization of PGM-Free Oxygen Reduction Electrocatalysts for Polymer Electrolyte Fuel Cells”, D. Myers, M. Ferrandon, J. Park, H. Lv, N. Kariuki, C. Yang, A. J. Kropf, and E. Wegener. (**invited lecture**).
39. 2019 MRS Spring Meeting & Exhibit, Phoenix, Arizona, April 22-26, 2019. Title: “Atomic-Level Insights into Platinum Group Metal-Free Electrocatalysts Derived from Metal Organic Frameworks;” D. Cullen, K. More, G. Wu, D. Myers, K.C. Neyerlin, H. T. Chung, P. Zelenay.

Issued Patent

1. B.-Z. Zhan, Z. He, H. T. Chung, P. Zelenay; “Metal nanoparticle-deposited, nitrogen-doped carbon adsorbent produced by e.g. contacting nitrogen precursor and metal-containing salt in first strong acid solution and heating used to remove sulfur compounds from hydrocarbon feed stream;” U.S. Patent US2019262798-A1 issued on August 29, 2019.

Patent Application

1. X. Yin, P. Zelenay, “2,2'-dipyridylamine as a Catalyst for An Electrochemical Cell;” U.S. Patent Application No. 62/860,964 filed on June 13, 2019 (Triad Ref. No. S133691.000).

Invention Disclosures

1. H. Zhang, H. T. Chung, P. Zelenay. “Highly durable and active platinum group metal-free catalysts developed via chemical vapor deposition approach for proton exchange membrane fuel cells;” LANL invention disclosure S133864, February 2020.
2. M. Ferrandon, J. Park, D. J. Myers, ANL Case #: IN-19-124 "Metal Dopants in iron-based Electrocatalysts for Platinum Metal Group (PGM)-free PEMFCs".
3. T. Chung, P. Zelenay; “ZIF-L derived atomically dispersed (AD)Fe-N-C catalysts for polymer electrolyte fuel cells;” LANL invention disclosure 2729, April 17, 2019.

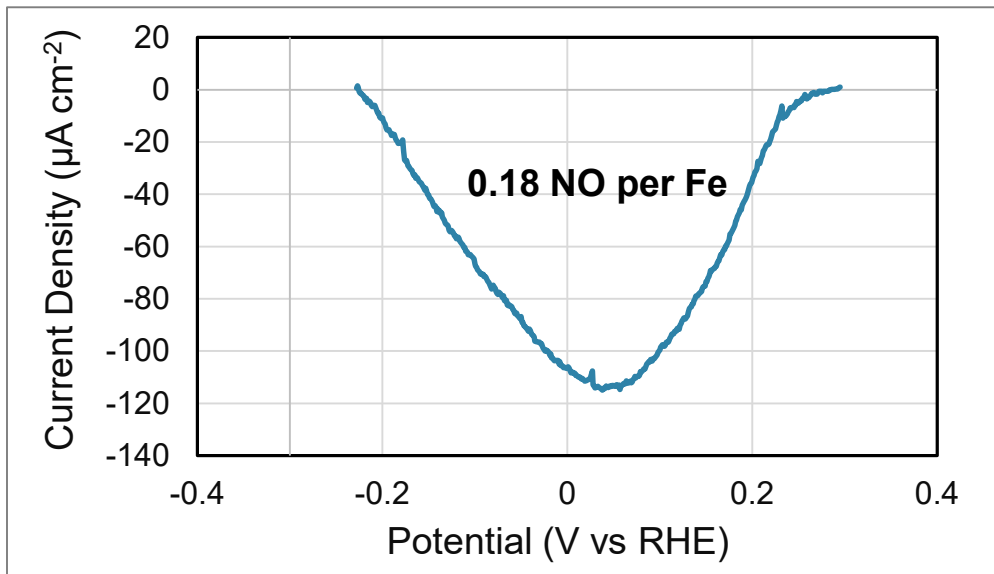
Technical Back-Up Slides

Fe-N-C Site Characterization: Gas Phase Probe (NO) Study of (AD)Fe-N-C

As-prepared (AD)⁵⁷Fe-N-C: 1.02 wt.%, 0.22 at.% Fe

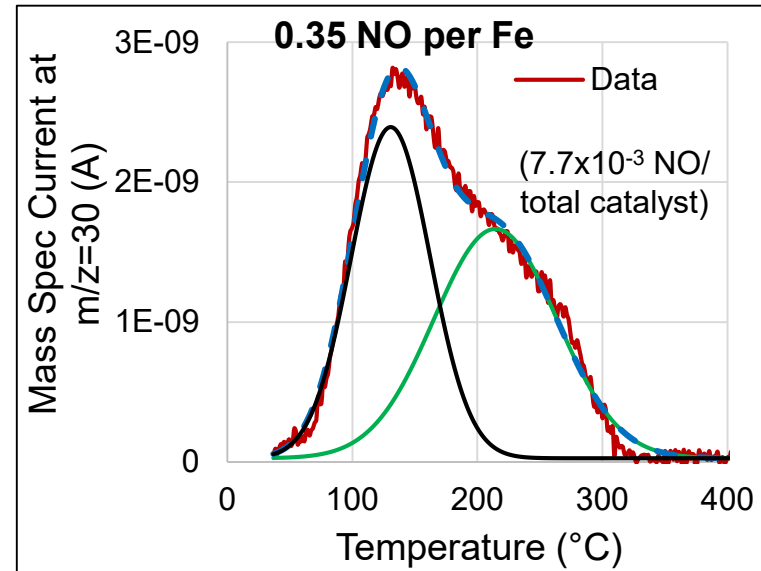
Electrochemical stripping of adsorbed NO

0.6 mg cm⁻², deaerated 0.5 M H₂SO₄, 20 mV sec⁻¹



Temperature-programmed desorption of adsorbed NO

25 mg catalyst, 5 °C min⁻¹



- NO adsorbs to surface Fe sites in as-synthesized (AD)Fe-N-C catalyst (2019 AMR, NRVS and Mössbauer results)
- NO can be electrochemically stripped in 0.3 to -0.3 V potential region and thermally desorbed at 50-300 °C
- NO is desorbed in two temperature regimes, i.e., on sites with two distinctly different adsorption energies (also shown in 2019 AMR for NO₂⁻)
- Fe coverage of NO is 0.18 to 0.35 NO/Fe

- Computational results show that NO binding to FeN₄C_x is more favorable than oxygenated ligands

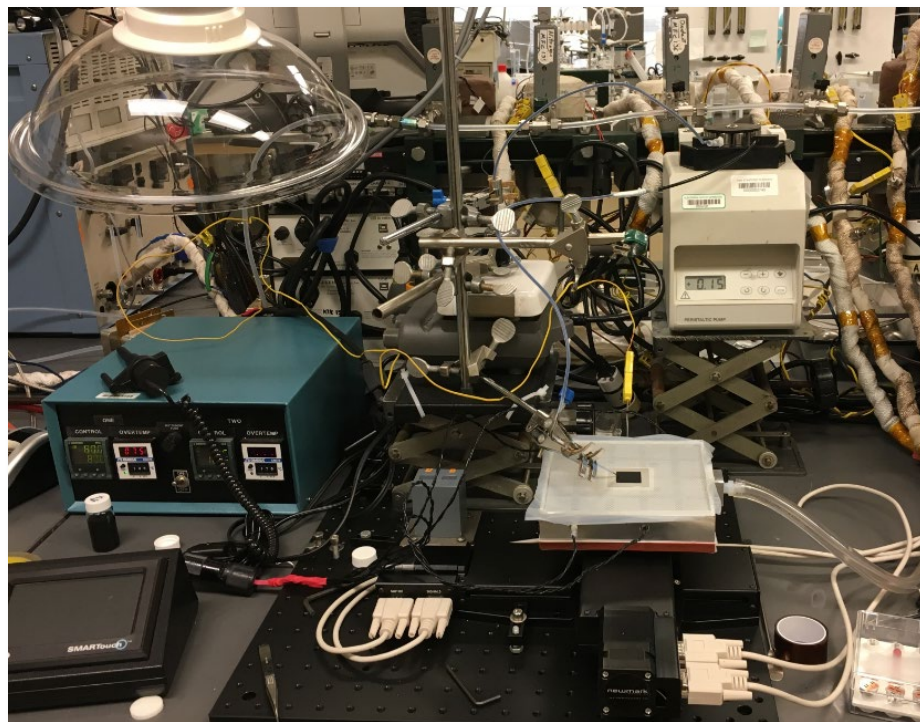
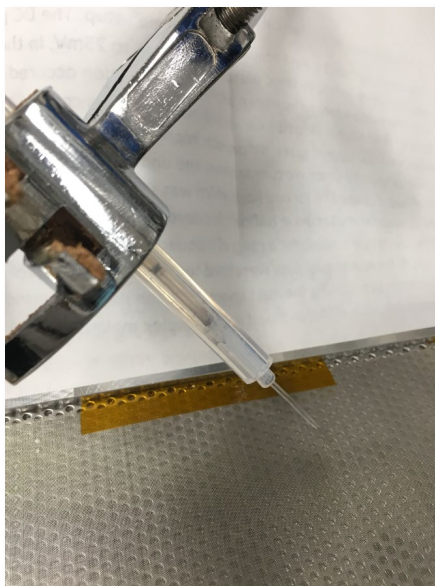
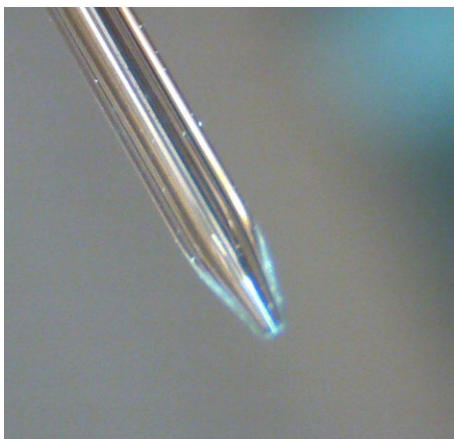
Functional	Adsorbing molecule		
	E _{ads} (eV)		
	OH	NO	O ₂
PBE	0.39	-1.88	-0.53
HSE	1.1	-0.52	0.34
RPA@PBE	1.19	-0.49	0.9

PBE: Standard DFT, RPA: High-Fidelity;
HSE: Intermediate between PBE and RPA

Enhancing Activity & Durability: Automated Ink Deposition System

System:

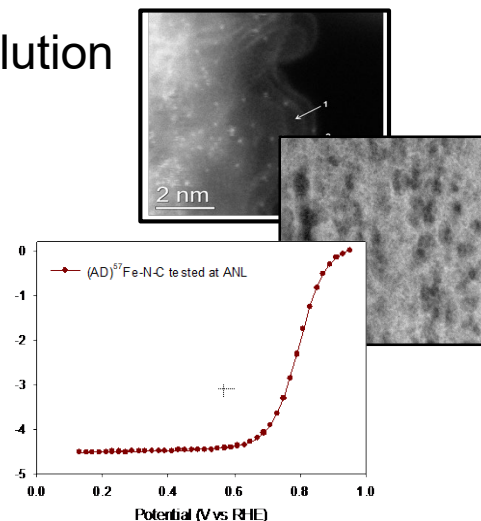
Catalyst ink delivered to heated membrane using peristaltic pump and nanopipette. Membrane mounted on heated vacuum table translated using computer-controlled x-y stage.



Catalyst system 1 (Year 1): LANL's Fe salt-ZIF-F system: solution phase synthesis of (Fe)Zn - ZIF

Parameters varied to obtain 40 unique samples:

- ✓ Fe-to-Zn ratio: 0, 1, 2.5, 5, and 7.5 at.% Fe in precursors
- ✓ Fe salts: sulfate, nitrate, acetate
- ✓ Heat-treatment temperatures: 900, 1000, 1100 °C



Catalyst system 2 (Year 2): Physical mixtures (ball milling) of Fe salt, carbon-nitrogen precursor, carbon support (e.g., Zitolo *et al.*, *Nature Materials*, 14 (2015) 937.)

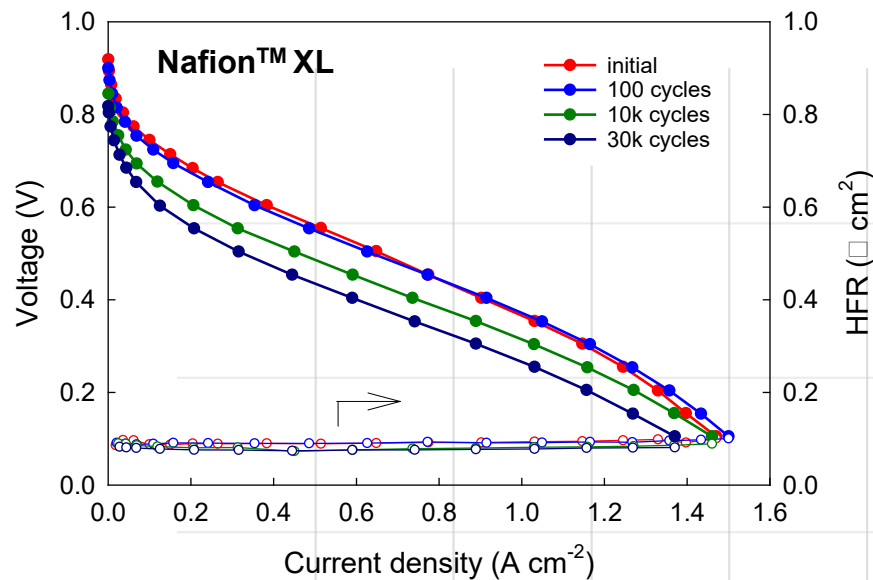
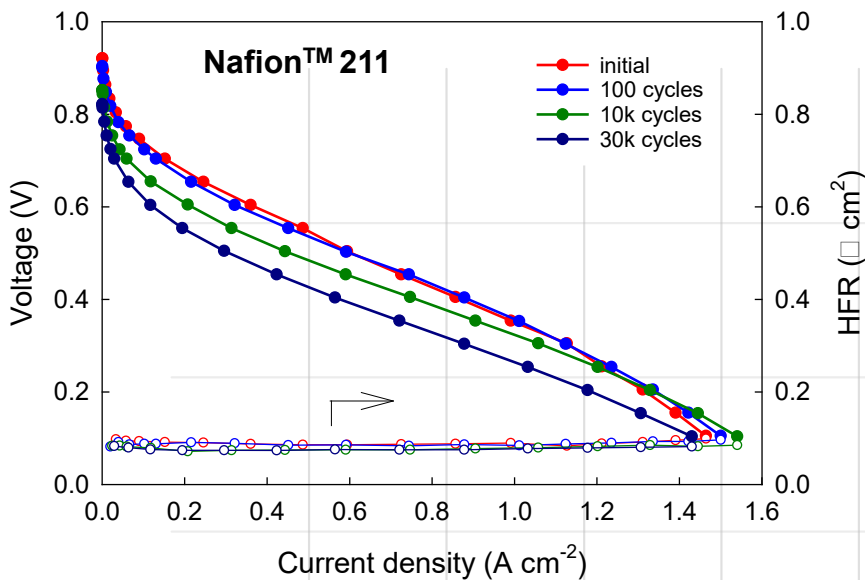
Parameters varied to obtain 160 unique samples:

- ✓ Carbon-nitrogen macrocycle to carbon support ratio
- ✓ Carbon-nitrogen macrocycle to ZIF ratio
- ✓ Identity of carbon-nitrogen macrocycle
- ✓ Fe loading
- ✓ Fe precursor
- ✓ Identity of transition metal dopant
- ✓ Weight loading of transition metal dopant

Enhancing Activity & Durability: Peroxide Unmitigated vs. Mitigated Membrane

Anode: 0.2 mg_{Pt} cm⁻² Pt/C H₂, 1.0 bar partial pressure, 500 sccm, 100% RH **Cathode:** ~ 4 mg/cm² (AD)Fe_{1.5}-N-C catalyst, 1.0 bar partial pressure, 2000 sccm, 100% RH **Membrane:** Nafion[®] 211 and XL membrane **Cell:** differential cell with 5 cm² electrode area, **Cell temperature:** 80 °C

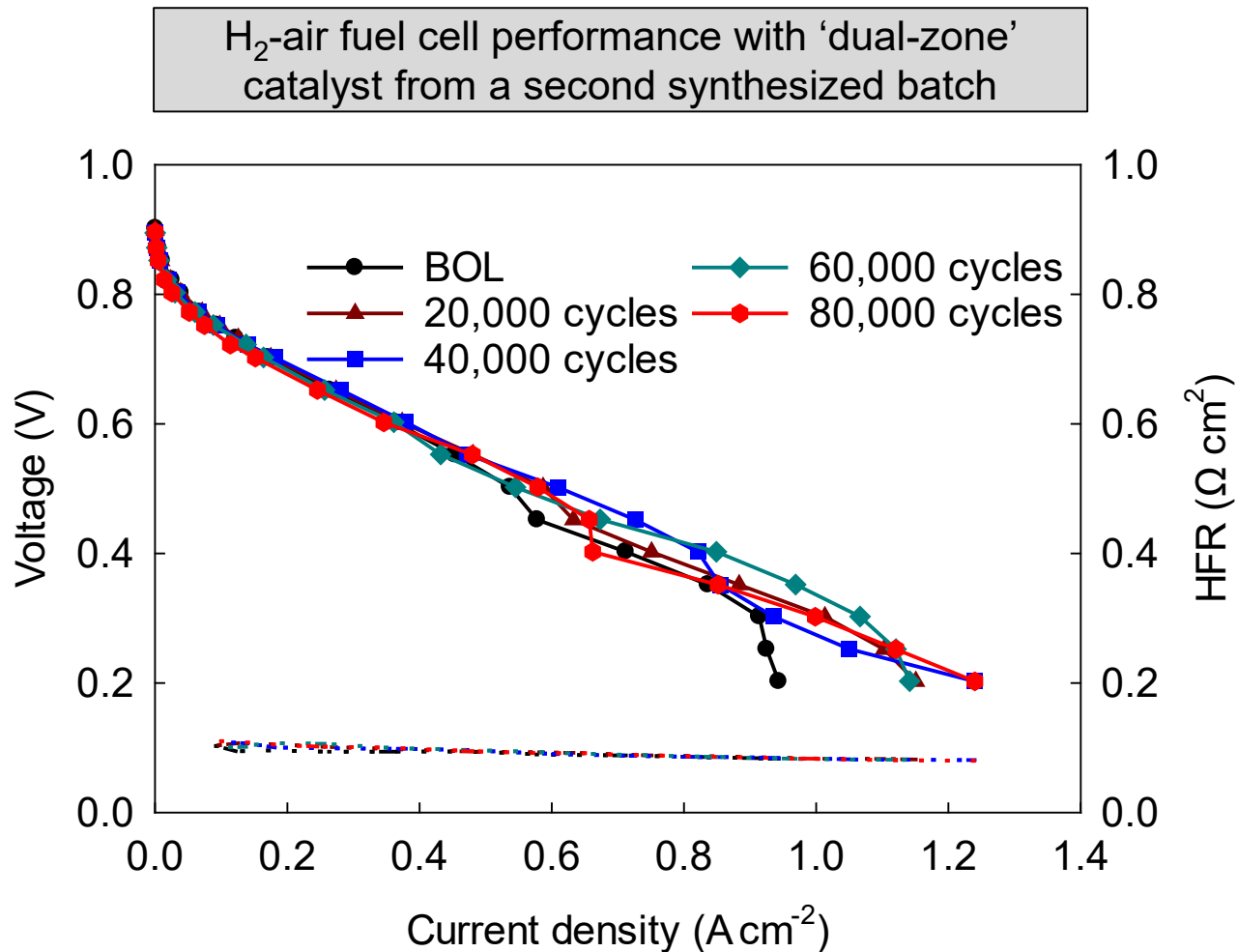
Cycling between 0.60 V and OCV (3 s at each voltage), air



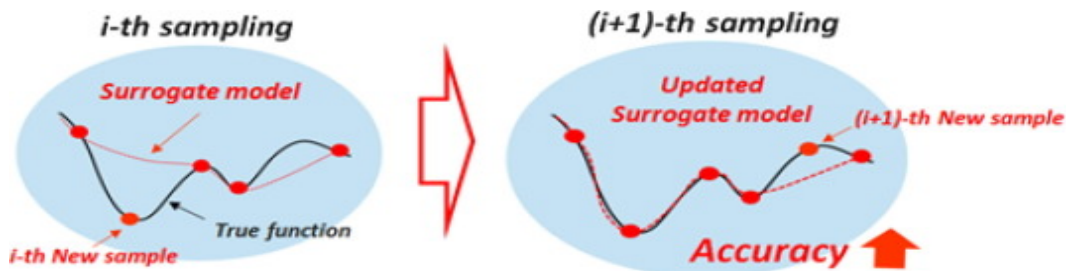
- No difference in durability of systems utilizing Nafion™ 211 and Nafion™ XL (ceria-stabilized) membranes
- Ceria content in the membrane likely too low for successful mitigation of catalyst performance loss in the thick PGM-free cathode

Major Progress in Durability: 'Dual-Zone' Catalyst Performance (Second Batch)

Anode: Pt/C, 0.1 mg_{Pt}/cm²; H₂: 1.0 bar partial pressure, 700 sccm; 100% RH. **Cathode:** 'Dual-zone' catalysts, 4 mg/cm²; Air: 1.0 bar partial pressure, 1700 sccm; 100% RH. **Membrane:** Nafion®-211. **Cell:** Differential cell, 5 cm² electrode area. **Cell temperature:** 80 °C.

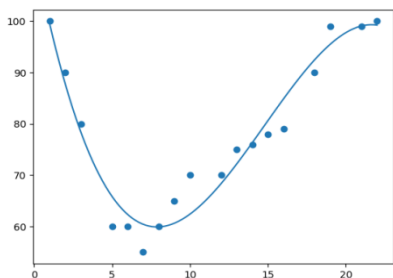


Machine Learning: ML-based Regression to Build Surrogate Models

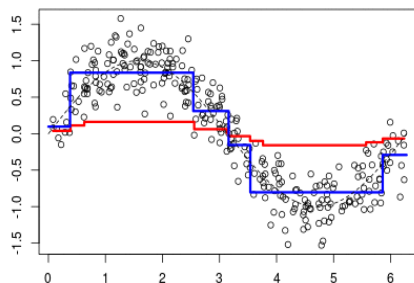


$$y = f(x)$$

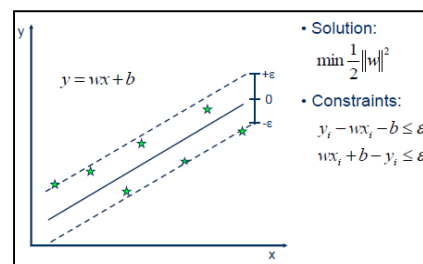
Polynomial Regression:



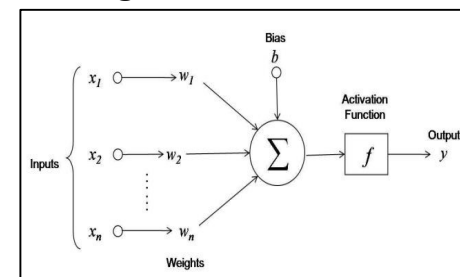
Gradient Boosting Regression:



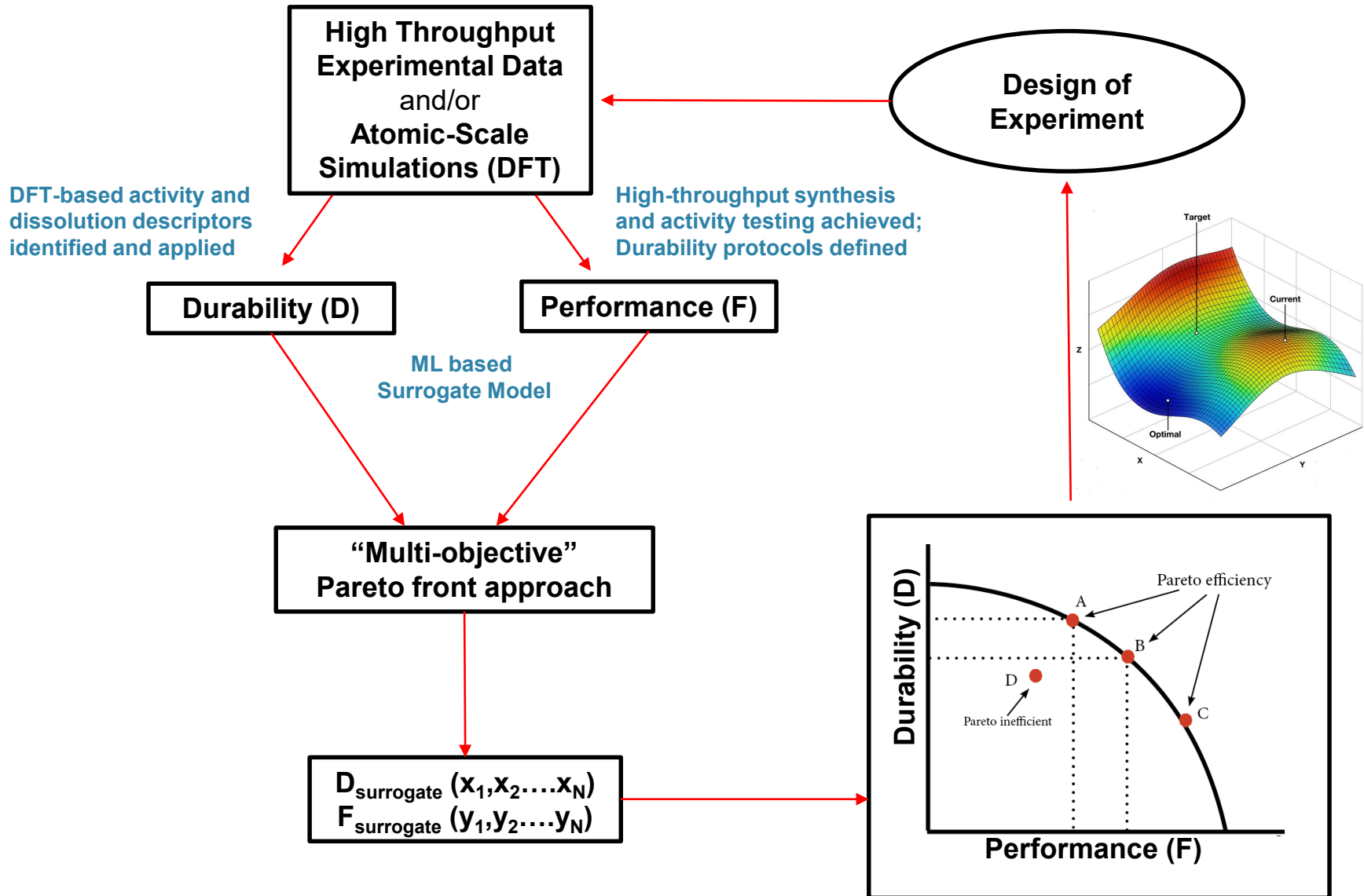
Support Vector Regression:



Neural Network Regression:



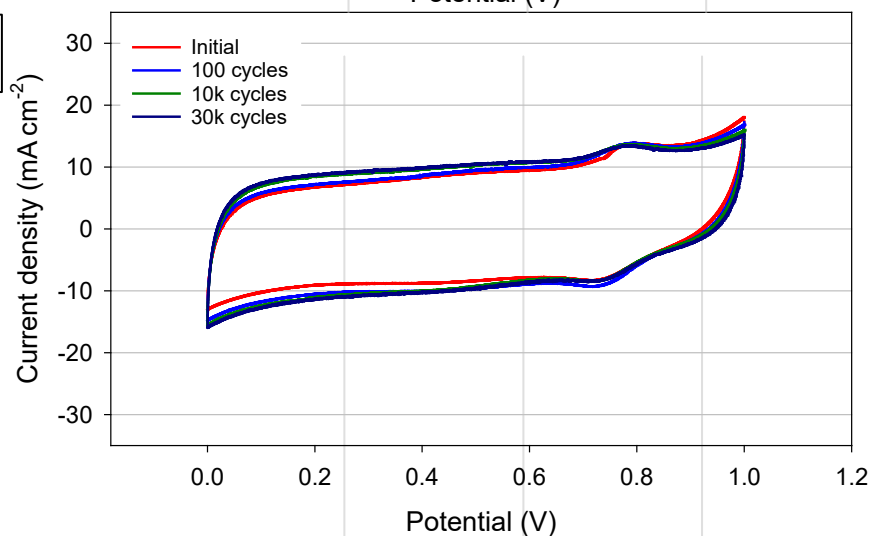
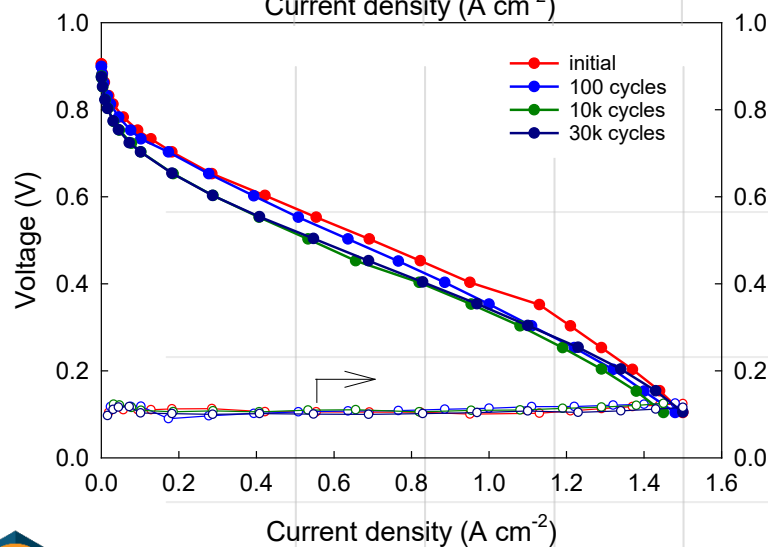
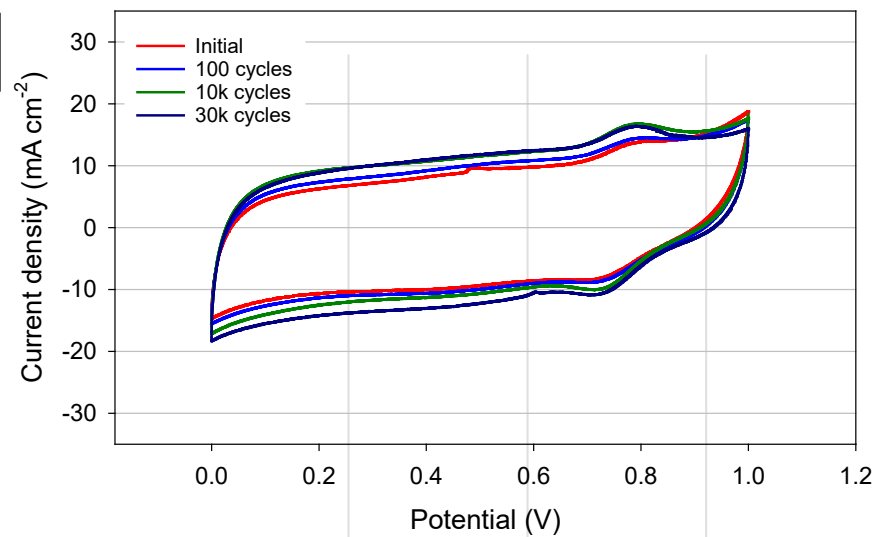
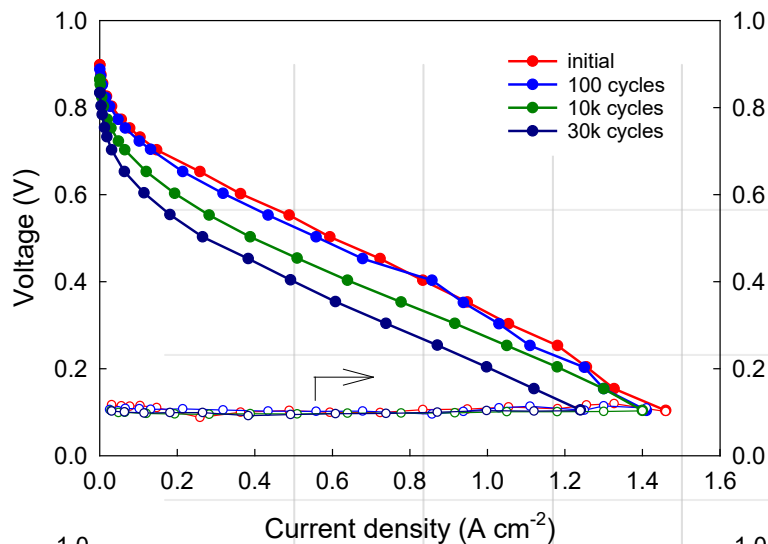
Machine Learning: Future Work – Active Learning Design of Experiment



AST Protocols & Round Robin: (AD)⁵⁷Fe_{1.5}-N-C Catalyst AST in Air and N₂

Anode: 0.2 mg_{Pt} cm⁻² Pt/C H₂, 1.0 bar partial pressure, 500 sccm, 100% RH **Cathode:** ~ 4 mg/cm² (AD)Fe_{1.5}-N-C catalyst, 1.0 bar partial pressure, 2000 sccm, 100% RH **Membrane:** Nafion®211 **Cell:** differential cell with 5 cm² electrode area, **Cell temperature:** 80 °C

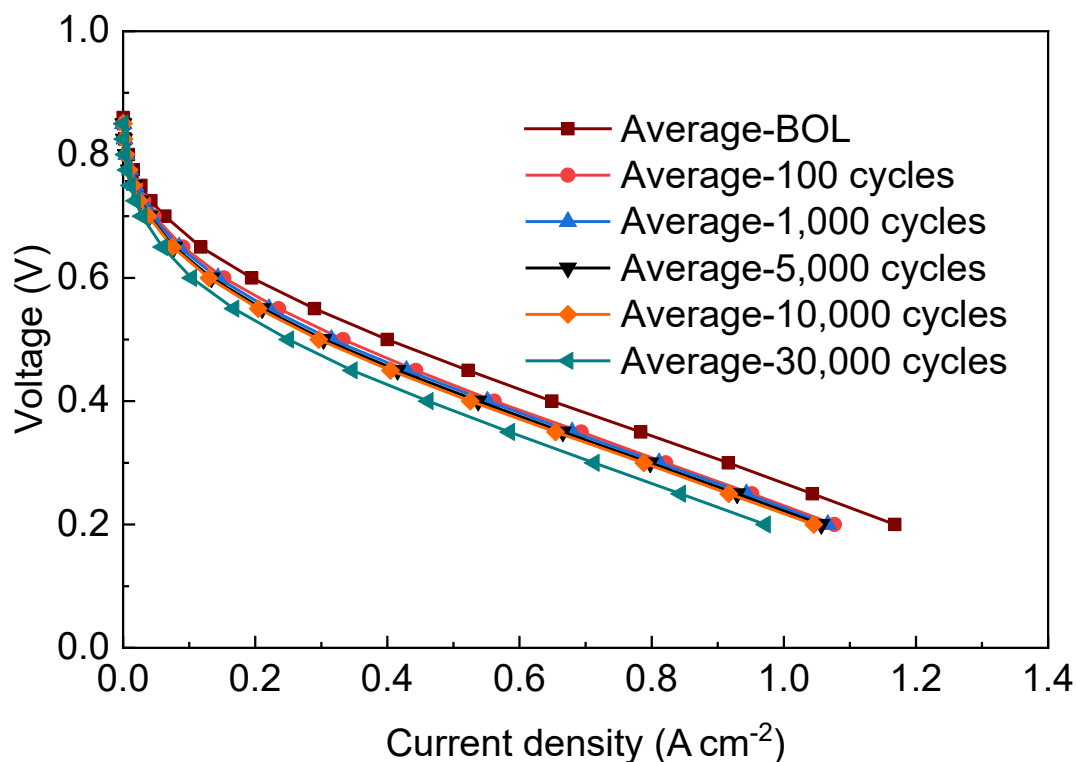
Cycling between 0.60 V and OCV (3 s at each voltage)



AST Protocols & Round Robin Testing: H₂-air Performance Recorded During AST

Anode: Pt/C, 0.1 mg_{Pt}/cm²; H₂: 1.0 bar partial pressure, 700 sccm; 100% RH. **Cathode:** Pajarito Powder's PGM-free catalysts, 4 mg/cm²; Air: 1.0 bar partial pressure, 1700 sccm; 100% RH. **Membrane:** Nafio®-211. **Cell:** Differential cell, 5 cm² electrode area. **Cell temperature:** 80 °C.

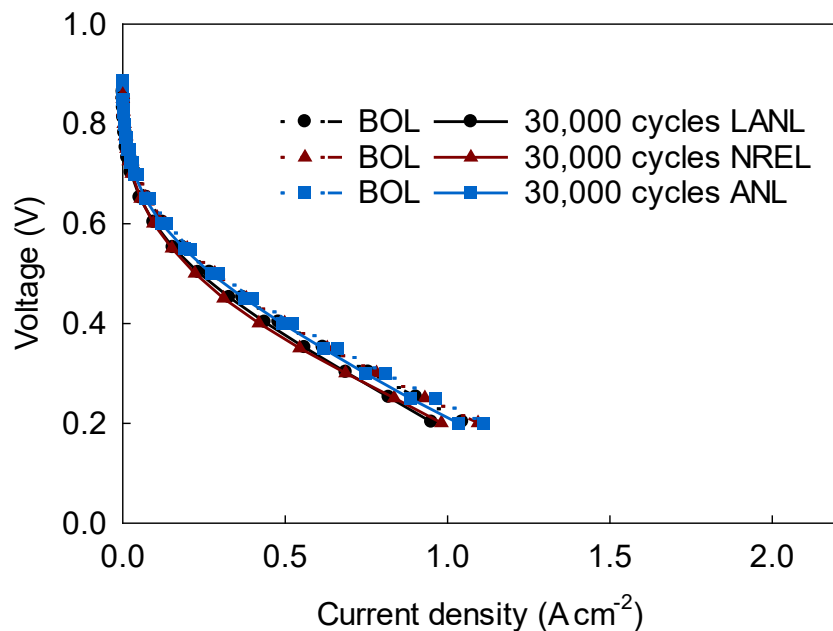
All H₂-air fuel cell performance recorded during accelerate stress testing for Pajarito Powder catalyst



AST Protocols & Round Robin Testing: Performance at 95 °C During ASTs

Anode: Pt/C, 0.1 mg_{pt}/cm²; H₂, 250 kPa total pressure, 700 sccm; 75% RH. **Cathode:** PGM-free catalysts, 4mg/cm²; Air, 250 kPa total pressure, 1700 sccm; 75% RH. **Membrane:** Nafion® 211. **Cell:** Differential cell, 5 cm² electrode area. **Cell temperature:** 95 °C.

H₂-air fuel cell performance with Pajarito Powder catalyst



H₂-air fuel cell performance with LANL catalyst

